THREE DIMENSIONAL FINITE ELEMENT ANALYSIS OF A NOVEL BRACING SYSTEM IN SMALL DEEP EXCAVATIONS

A THESIS SUBMITTED TO
THE GRADUATE SCHOOL OF NATURAL AND APPLIED SCIENCES
OF
MIDDLE EAST TECHNICAL UNIVERSITY

BY

PELİN ÖZLÜ

IN PARTIAL FULFILLMENT OF THE REQUIREMENTS
FOR
THE DEGREE OF MASTER OF SCIENCE
IN
CIVIL ENGINEERING

SEPTEMBER 2012

Approval of the thesis:

THREE DIMENSIONAL FINITE ELEMENT ANALYSIS OF A NOVEL BRACING SYSTEM IN SMALL DEEP EXCAVATIONS

submitted by **PELİN ÖZLÜ** in partial fulfillment of the requirements for the degree of **Master of Science in Civil Engineering Department, Middle East Technical University** by,

Prof. Dr. Canan Özgen ____________________
Dean, Graduate School of **Natural and Applied Sciences**

Prof. Dr. Güney Özcebe ____________________
Head of Department, **Civil Engineering**

Inst. Dr. N. Kartal Toker ____________________
Supervisor, **Civil Engineering Dept., METU**

Examining Committee Members:

Prof. Dr. Kemal Önder Çetin ____________________
Civil Engineering Dept., METU

Inst. Dr. N. Kartal Toker ____________________
Civil Engineering Dept., METU

Prof. Dr. Sadık Bakır ____________________
Civil Engineering Dept., METU

Dr. Onur Pekcan ____________________
Civil Engineering Dept., METU

M.Sc. Gökhan Yaman ____________________
TOKER Sondaj ve İnşaat Ltd. Şti.

Date: 14.09.2012

I hereby declare that all information in this document has been obtained and presented in accordance with academic rules and ethical conduct. I also declare that, as required by these rules and conduct, I have fully cited and referenced all material and results that are not original to this work.

Name, Last Name : PELİN ÖZLÜ

Signature :

ABSTRACT

THREE DIMENSIONAL FINITE ELEMENT ANALYSIS OF A NOVEL BRACING SYSTEM IN SMALL DEEP EXCAVATIONS

ÖZLÜ, Pelin

M.S., Department of Civil Engineering

Supervisor: Inst. Dr. N. Kartal Toker

September 2012, 124 pages

One of the most common retaining systems for deep excavations is by supporting a wall with multiple levels of anchors. In densely built urban areas, preventing soil movement with such a system can be very costly. Additionally, anchored walls are assumed and forced to act independently during design calculations, thus fail to take the advantage of the rigidity of the whole system at the corners of the excavation area. An alternative support system that uses the entire system is bracing of the walls with struts. But such a system greatly hinders construction space. In this research, a new type of supporting system has been investigated by performing a parametric study in finite element analyses program. New system is a single ring at each support level, supporting the system at several locations. A comparative study has been undertaken between the conventional systems and the new system in both 2D and 3D. PLAXIS finite element analysis software was used for the analyses. The primary aim was to investigate the structural and geotechnical performance of the arch supported system. The study revealed that the new system provides improvement for specific cases and can be considered as an alternatve support system for such cases.

Keywords: Deep Excavations, Struts, Anchors, Braced Cuts

ÖZ

KÜÇÜK DERİN KAZILARDA YENİ İKSA SİSTEMİNİN ÜÇ BOYUTLU SONLU ELEMANLAR YÖNTEMİ ANALİZİ

ÖZLÜ, Pelin

Yüksek Lisans, İnşaat Mühendisliği Bölümü

Tez Yöneticisi: Öğr. Gör. Dr. N. Kartal Toker

Eylül 2012, 124 sayfa

Derin kazılar için en yaygın iksa sistemlerinden biri perdeyi farklı yüksekliklerdeki ankrajlarla desteklemektir. Kalabalık kentsel bölgelerde, zemin hareketini böyle bir sistemle engellemek oldukça pahalı olabilir. Ayrıca, ankrajlı perdelerin bağımsız hareket ettiği kabulü ile yapılan modeller tüm sistemin köşelerdeki rijitliğinden kaynaklanan desteği göz ardı eder. Alternatif bir iksa sistemi ise tüm sistemi birlikte destekleyen, perdenin payandalarla desteklendigi sistemdir. Fakat böyle bir sistem ise inşaat alanını daraltmaktadır. Bu araştırmada önerilen yeni sistem, sonlu elemanlar analizi yöntemi ile parametrik çalışmak yapılarak incelenmiştir. Yeni sistem, her destek seviyesinde kazıyı destekleyen bir yük taşıyıcı halkadan oluşmaktadır. Karşılaştırmalı bir çalışma yürütülerek konvansiyonel sistem ile yeni sistem 2 ve 3 boyutlu analizler yapılarak çalışılmıştır. PLAXIS sonlu elemanlar analiz programı kullanılmıştır. Çalışmanın birincil amacı kemer destekli sistemin yapısal ve geoteknik performansını araştırmaktır. Araştırma, yeni sistemin belirli durumlarda iyileşme sağladığını ve bu tür durumlar için alternatif destek sistemi olarak kabul edilebilir olduğunu göstermiştir.

Anahtar Kelimeler: Derin Kazılar, Kazı Payandaları, Zemin Ankrajları, Destekli Kazılar

ACKNOWLEDGEMENTS

I would like to express my special thanks to my dear supervisor, Inst. Dr. N.Kartal Toker, his assistance, support and guidance throughout this study.

I would like to express my gratitude to my family; my lovely mother, Nigar, my father Orhan, my brother, Berk and my husband, Emrah.

Sincere thanks to my friends for their precious friendship and continuous support.

TABLE OF CONTENTS

LIST OF FIGURES

FIGURES

LIST OF TABLES

TABLES

CHAPTER 1

INTRODUCTION

In urban environments, where land is scarce, basements, car parking facilities and transportation structures are generally constructed below ground level. As such, in densely populated cities, ground deformation around deep excavations is a major concern, since excessive movements can damage adjacent buildings and utilities. Therefore, retaining wall support system design should be carefully taken into consideration in order to provide appropriate lateral support for the soil around the excavation.

The most common retaining structures in Turkish geotechnical practice are walls supported with multiple levels of anchors. However, for many deep excavations, which are often 15-20 m deep, anchored systems are very costly. An alternative support system to anchored walls is to use struts in order to support retaining walls, but this solution is not always applicable to the geometry of the excavation, and usually restricts the construction space a lot. This study presents a new concept for supporting deep excavations, with the aim of improved overall behavior, which may eventually lead to more economical designs.

1.1 Research Goals

The first objective of this study is to propose a new support system specifically for excavations that are equidimensional in plan. This new support system is in loop shape, which can also be regarded as four arches, each supporting one of the excavation walls; the proposed support concept aims to take the advantage of arch geometry that is often used in structural engineering to eliminate tensile and shear stresses. Using arch shaped supports also leaves the center of the excavation free for the works, and in theory considerable spans can be crossed using arch-structures. Second aim of this study is to compare and highlight the differences in the performance of the proposed retaining system with respect to conventional designs by finite element analysis. Last objective of the research is to propose suitable application cases and application rules for the system.

1.2 Scope of Work

This study includes modeling and design of retaining structures for various hypothetical excavation cases supported entirely by anchors, struts or arches. Two and three-dimensional finite element analyses are performed with varying excavation area, support spacing, surface loading conditions and soil stiffness applied to dry sand and drained clay. Early in the work, the analysis of anchor-supported walls was found to take longer time and result in inferior behavior (i.e. greater deformations, larger moments in the wall etc). Hence, the analyses were focused on the comparison of retaining walls supported by struts and arches from that point on.

Comparisons are done between analysis results of strut-supported and arch-supported excavations with same soil type and support spacing for hypothetical cases. In addition, horizontal wall movements and dimensions of beam sections are tabulated in order to see the compatibility and feasibility of each case.

1.3 Outline of the Thesis

The remainder of this thesis is divided into four chapters. The contents of respective chapters are as follows;

Chapter 2 provides literature review on the various aspects of deep excavation support systems including earth pressures, deformation characteristics and other factors relevant to the performance of excavation system. Design considerations and finite element case studies are also discussed in this chapter.

Chapter 3 explains the criteria adopted for design with different retaining support systems, and presents the sequence of parametric study followed through the research. The input data of parametric studies used in this research are also introduced in this chapter.

Chapter 4 consists of the results of parametric study from three-dimensional finite element analysis and the comparison between retaining structures supported by anchorages, struts and arches. Moreover, the general conclusions and recommendations based on results of parametric study are also represented in this part.

Chapter 5 concludes summary of parametric study results and presents recommendations for future studies.

CHAPTER 2

LITERATURE REVIEW

Lateral support should be provided for the soil around an excavation to minimize the movement of the surrounding soil. Without proper lateral support, lateral movements, settlements and failure of the adjacent soil will certainly be caused by the excavation. Therefore, a suitable retaining system should be installed in the soil prior to excavation in order not to affect in situ stress conditions significantly.

2.1 Deep Excavation Support Systems

2.1.1 Earth Pressures

Correct estimation of earth pressures on the retaining wall is key to correct retaining system. Terzaghi and Peck (1967) suggested pressure diagram mainly applied for cuts in stiff clay. (Figure 2.1) Peck (1969) defined deep excavations to be excavations with vertical sides that require lateral support. He reanalyzed the pressure diagram proposed by Terzaghi and Peck (1967) and generated earth pressure diagrams in order to monitor closer results of actual lateral loads measured on deep-braced excavations in Chicago and Boston. (Figure 2.2) By using earth pressure diagrams, braced excavation design can be done on earth pressures. Watanabe (1980) compared the pressure distribution diagrams prepared from various sites in Japan by using the data of grouped into one sandy and two cohesive soil types (soft and firm) (Figure 2.3)

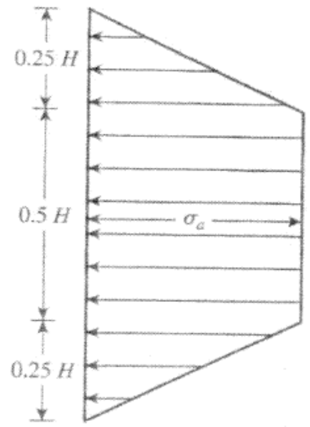

$\sigma_a = 0.2 \cdot \gamma \cdot H_e \ \ to \ \ 0.4 \cdot \gamma \cdot H_e$

where γ is unit weight of excavated soil and H_e is excavation depth.

Figure 2.1 Apparent pressure diagrams suggested for stiff clay (Terzaghi and Peck, 1967)

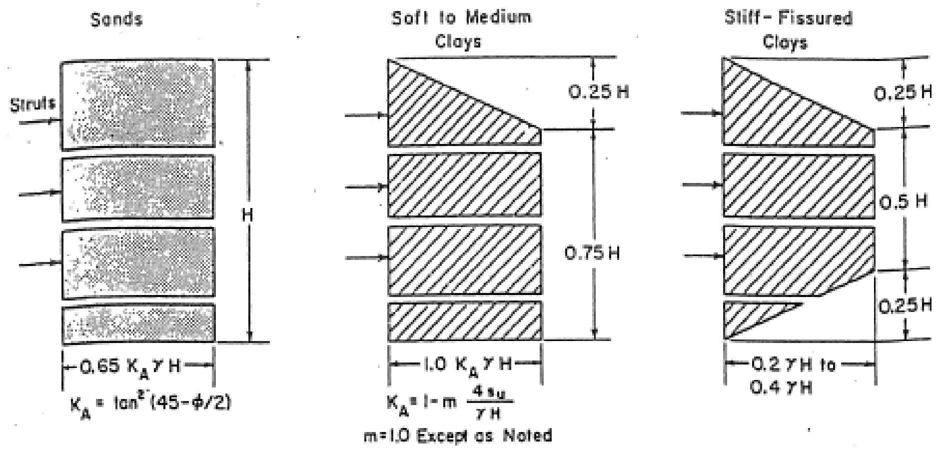

Figure 2.2 Apparent pressure diagrams suggested for computing strut loads in braced cuts (1969)

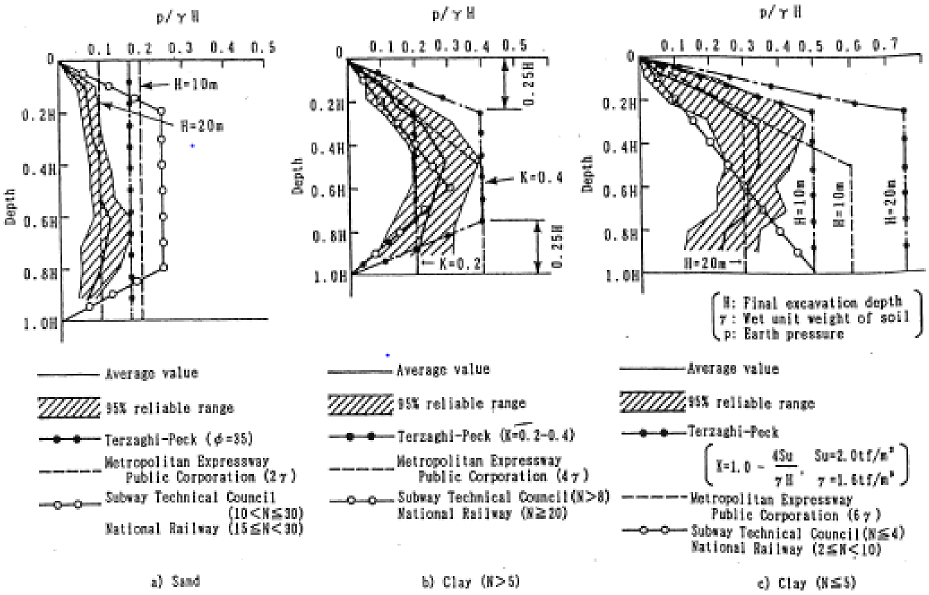

Figure 2.3 Comparison of pressure distribution diagrams proposed by various institutions (Watanabe 1980)

Katsura et. al. (1994) prepared a table of retained side lateral pressure envelopes of the walls from various studies.(Figure 2.4) For sandy soils earth and water pressures calculations are made separately while for cohesive soils total stress is used to calculate lateral pressure. So, lateral pressure is calculated by groundwater level for sands, and by SPT N values for cohesive soils.

Wong et. al. (1997) summarized the maximum earth pressure for excavations with five types of walls in a mixed soil profile which consists of layers of soft soils overlying stiff soils in Singapore.(Figure 2.5)

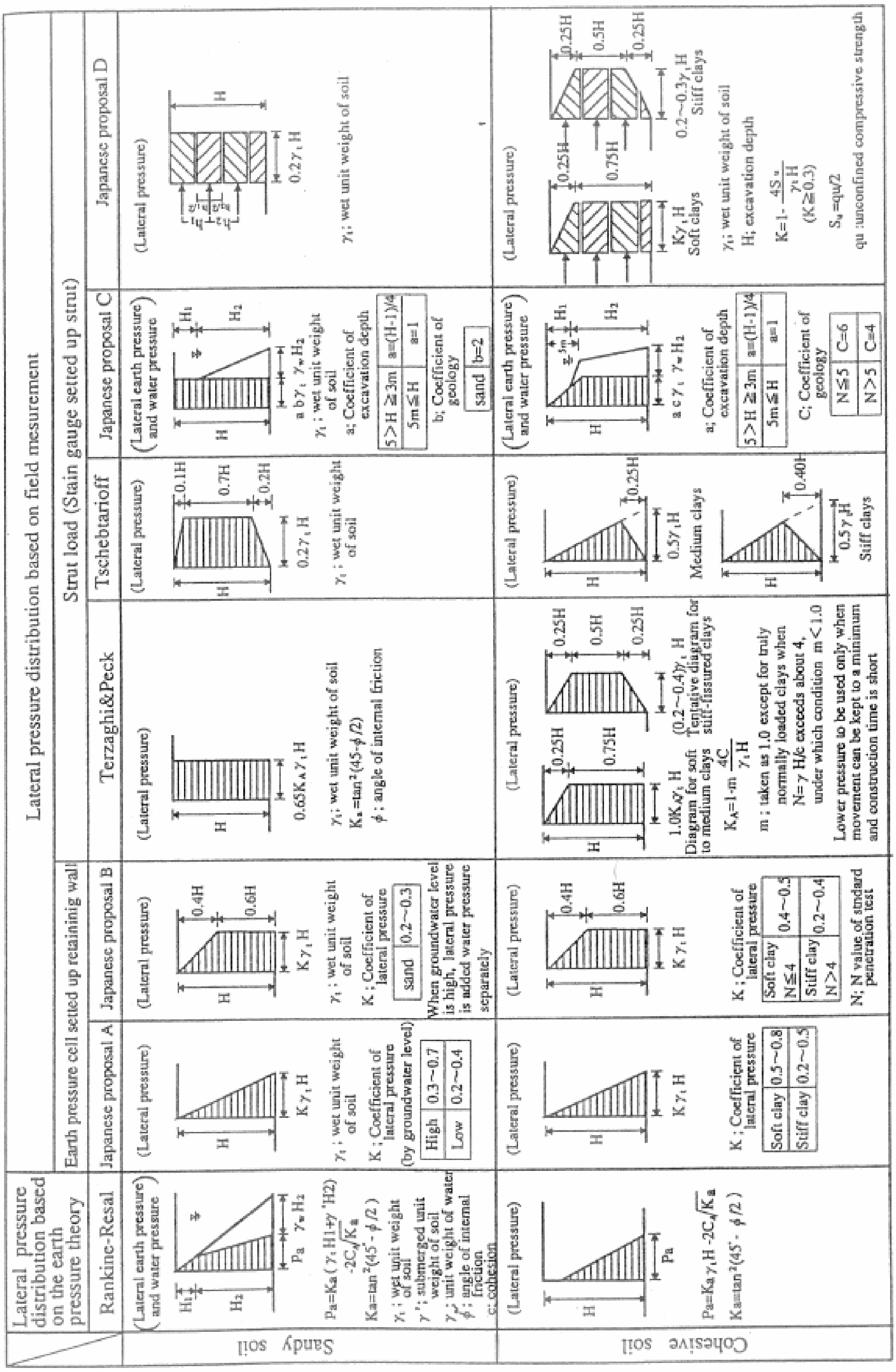

Figure 2.4 Lateral Pressure distribution diagrams (retained side) for design of earth retaining systems (Katsura et.al., 1994)

For h<0.9 H

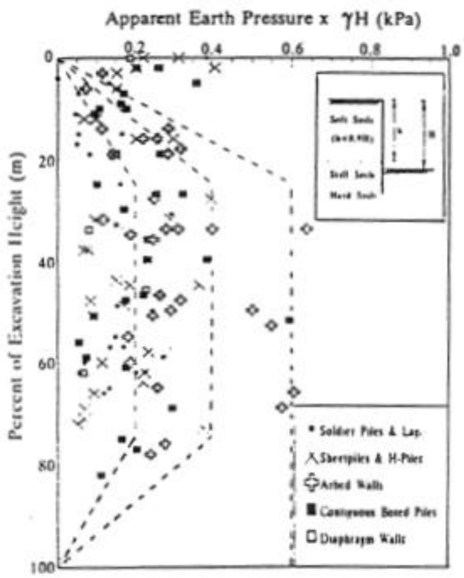

For h<0.8 H

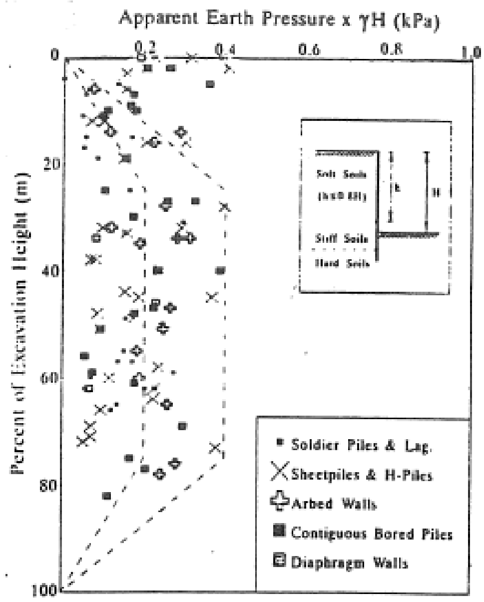

For h<0.6 H

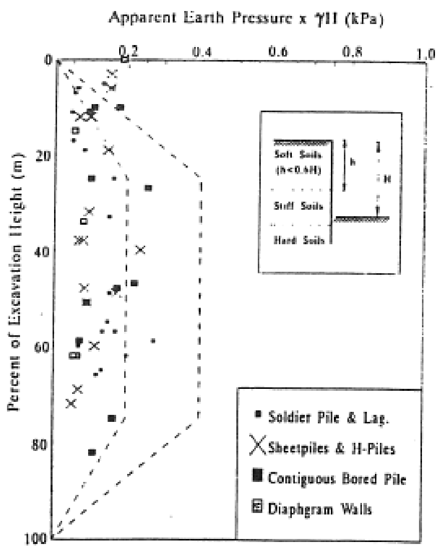

Figure 2.5 Apparent earth pressure diagram for excavation supported by four types of walls in stiff soil profiles (Wong et. al., 1997))

2.1.2 Deformations

In previous studies Terzaghi & Peck (1967), Lambe (1970), Goldberg et al.(1976), O'Rourke (1981), Mana and Clough (1981), Wong and Broms (1989), Clough and O'Rourke (1990), Ou et al.(1993) and Wong et al. (1997) made significant reviews of performance of deep excavations.

Peck (1969) discussed lateral movements, ground settlements next to excavations, base failure because of heave, methods of reducing ground settlements next to excavation and earth pressure diagrams for deep excavations. Soil type, depth of excavation and workmanship are the three major themes discussed by Peck. The summarized information from case histories showed that settlements around deep excavations correlate to soil type. Figure 2.6 summarizes the settlement history information of various case histories. The settlement profiles based on soil conditions and workmanship are divided into three "zones" as shown in figure.

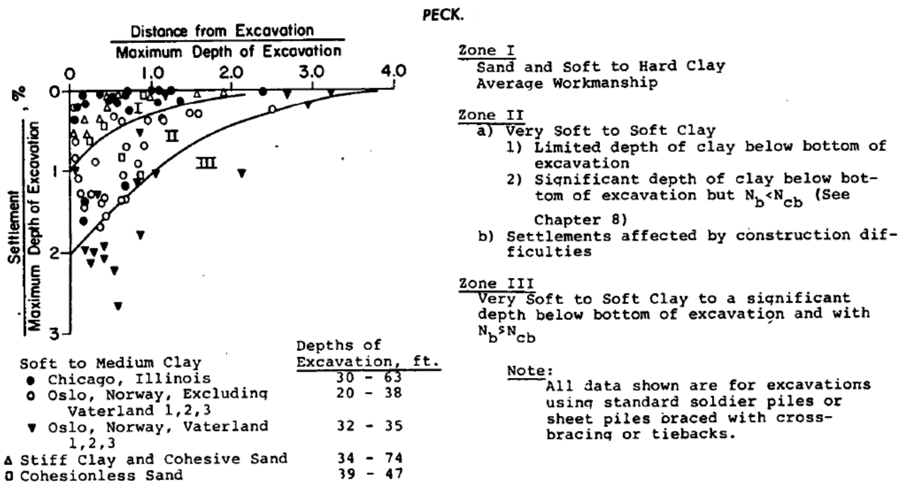

Figure 2.6 Summary of settlements adjacent to open cuts in various soils, as function of distance from edge of excavation (Peck,1969)

Another important point noted by Peck (1969) is that decreasing the spacing of bracing could reduce lateral movements considerably. Therefore in this study support spacing is used as a controlling parameter while comparing strut supported and arch supported system. Lambe (1970), Goldberg et al.(1976), O'Rourke (1981), Clough and O'Rourke (1990) also made similar observations.

Lambe (1970) focused on design and analysis of braced excavations. He analyzed factors affecting the soil movements and support systems of deep excavations for the subway in Boston. He figured out that support system loads and ground movements could not be predicted with confidence from solely the comparison of predictions to measured performance of case histories. He concluded combined usage of finite element method and published case histories were the most effective ways for gaining an understanding of deep excavation performance.

Maximum horizontal wall movement is another important design consideration while designing excavation support systems. Goldberg et al. (1976) used 63 case histories to estimate maximum horizontal wall movements, maximum ground settlements and deformed shape of the ground surface adjacent to excavation. He correlated his results depending on soil type and depth, and concluded that wall movements caused by deep excavations in sand/ gravel or very stiff to hard clay are usually less than 0.4 percent of the excavation depth. For excavations in soft soils wall movements can be around 1 percent of the excavation depth.

O’Rourke (1981) studied ground movements in braced excavations and focused on the importance of site preparation activities such as relocation or underpinning of utilities, dewatering, support wall construction and deep foundation installation. He examined the relation between the deflected shape of support wall and the ratio of horizontal and vertical deflection of ground surface by reviewing 7 case histories and find out that the ratio of horizontal to vertical deflection of ground surface is 1.6 for absolute cantilever deformation and 0.6 for absolute bulging deformation of the braced wall. O’Rourke also observed the effects of brace stiffness, pre-stressing of braces and brace placement timing and concluded that the effective stiffness of braces could be as low as %2 of ideal stiffness (AE/L) due to the effects of bending of braces and compression in connections.

Mana and Clough (1981) studied the relation between maximum ground settlements and lateral wall movements based on finite element analysis and pointed out the importance of safety factors against basal heave on lateral deflections. They pointed out that increasing the wall stiffness or decreasing the support spacing, or both, decreases the movements. And they concluded that movements are decreased by increasing strut stiffness and increased with respect to excavation width and depth to an underlying firm layer. Movements can be reduced by applying preloads in the struts although higher preloading has diminishing effect. The soil modulus has significant effects on movement levels. Higher modulus values show smaller movement results.

Lateral wall movements relative to width and depth of excavation is investigated by Wong and Broms (1989). As excavation proceeds deeper, the lateral movements increase as factor of safety against basal heave decreases.

Clough and O'Rourke (1990) studied movement information from case histories to aid in estimating maximum wall movements and settlement profiles of ground around the excavation. They point out that patterns of settlement adjacent to excavation due to excavation and bracing is affected by soil type. They proposed normalized settlement envelopes shown in Figure 2.7.

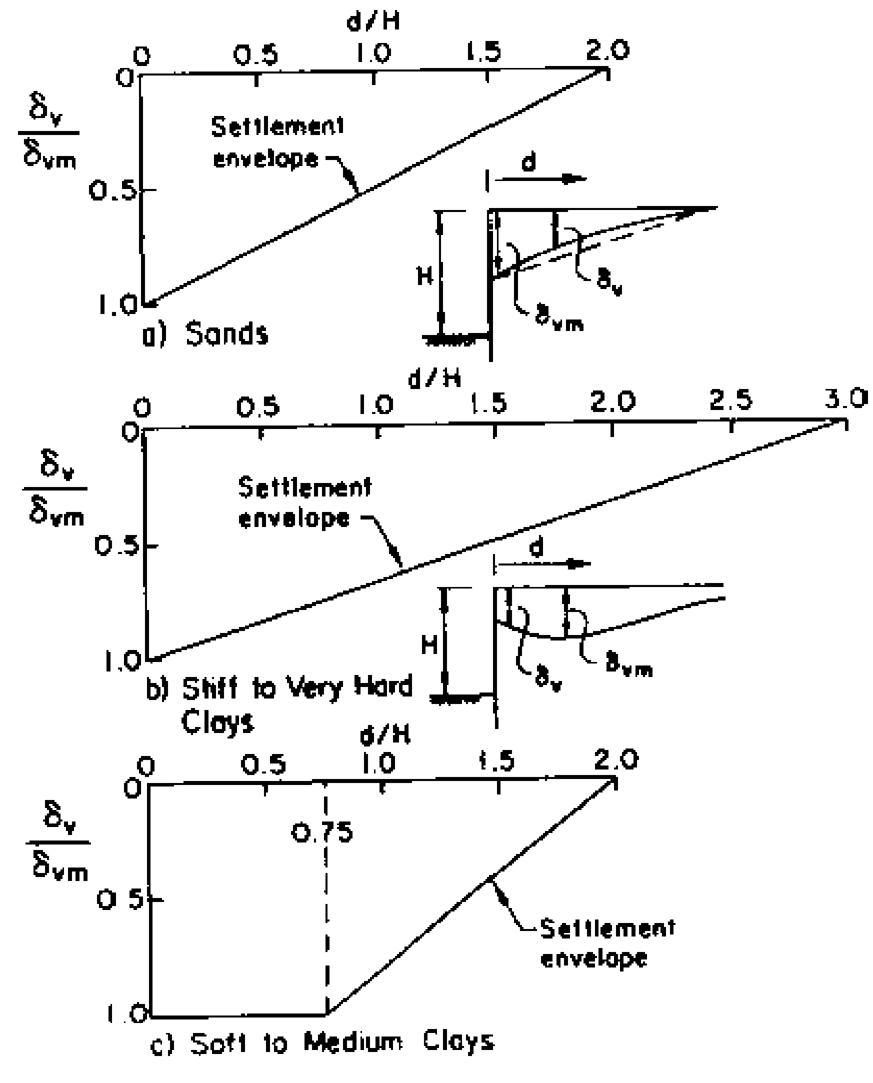

Figure 2.7 Dimensionless settlement profiles recommended for estimating the distribution of settlement adjacent to excavation in different soil types (Clough and O'Rourke, 1990)

Clough and O'Rourke illustrated the effects of support system stiffness on wall displacements in a chart (Figure 2.8) by considering effects of excavation base heave and system stiffness.

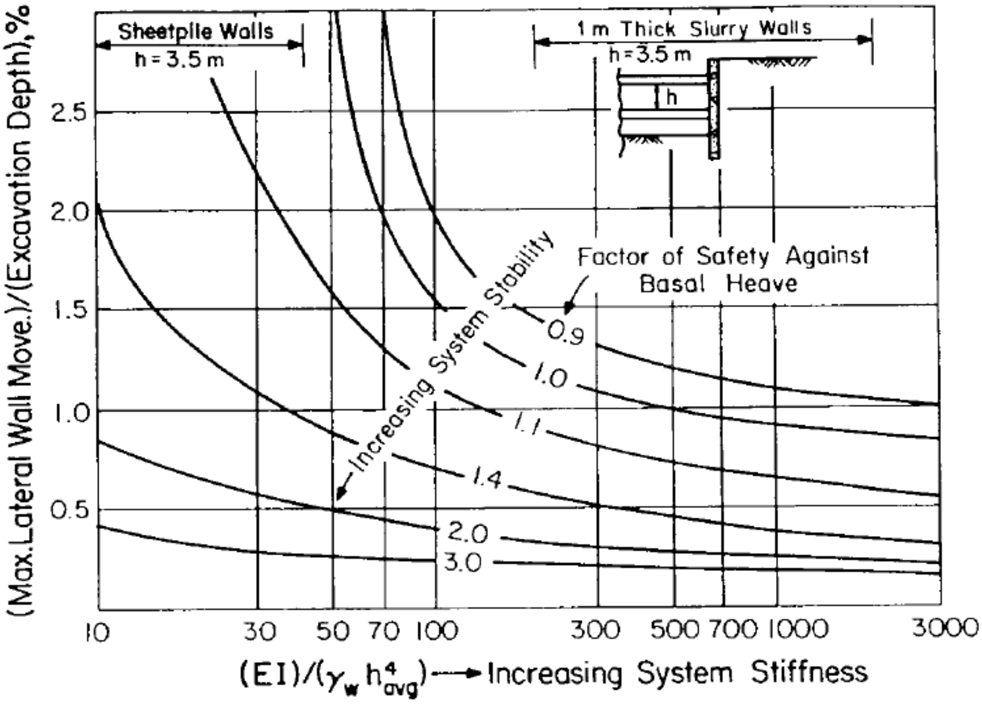

Figure 2.8 Chart for estimating maximum lateral wall movements and ground surface settlements in clays (Clough and O'Rourke, 1990)

Ou et al. (1993) studied ten finite element analysis cases of ground settlement and wall deflection caused just due to the soil mass removal under the condition of plane-strain. He observed that maximum lateral wall deflection occurs slightly above the excavation surface within the magnitude range 0.2%-0.5 % of excavation depth (Figure 2.9).

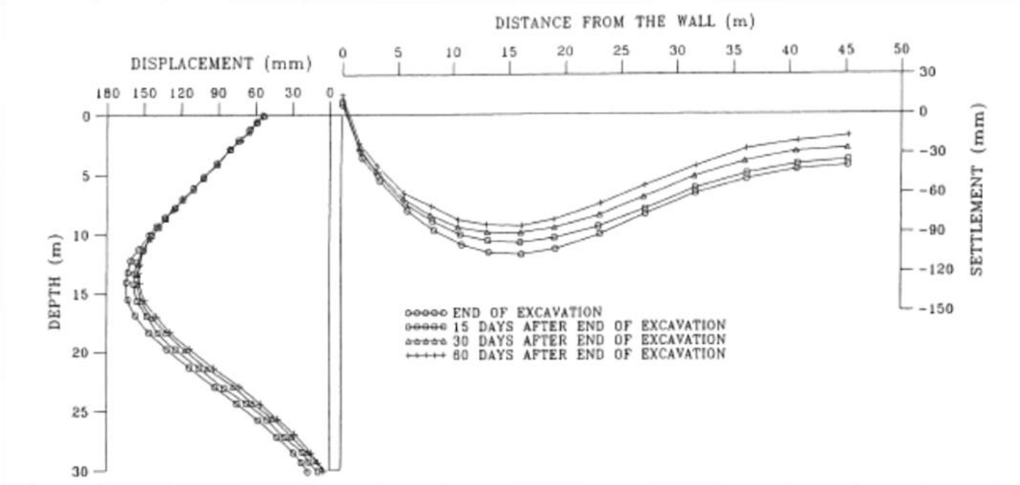

Figure 2.9 Relationship between maximum lateral wall deflection and excavation depth.(from Ou et al.,1993)

The performance of braced diaphragm walls embedded in Boston Blue clay is represented by Whittle and Hashash (1993) in their parametric studies. They focused on wall embedment depth and support spacing. Two wall lengths (L=20 m and L=40 m) is compared with the same support spacing (h=2.5 m) over the total excavation depth. (Figure 2.10). In the 20 m wall the maximum lateral deflection occurs at the bottom while in 40 m wall, it is observed in 8-10 m depth. They discovered that results the failure depth increases by 50 % as the wall length increases. The parametric studies also show that surface settlements are not affected by changes in wall length. The maximum lateral settlement takes place at the depth of 15-20 m behind the wall in both studies and it is nearly 0.5 % of the excavation depth. To understand the effect of support spacing on ground deflections, they compared well supported 60 m wall with poorly supported one. (Figure 2.11) For the well supported case, the wall movement occurred only below the excavation depth; on the other hand very large lateral movements observed all along the excavation depth in the poorly supported excavation.

Whittle and Hashash (1993) concluded that, support spacing have extreme effects on soil deformations. On the other hand, the length of embedment only affects stability of excavation. Therefore, to observe soil deformations better length of embedment is fixed and support spacing is a controlling parameter. In Figure 2.11, the maximum wall displacements are interpretable with respect to the depth of excavation (H), wall length (L) and support spacing (h).The figure 2.11 also shows that, for well supported excavations the ratio of maximum lateral displacement with respect to wall depth (δH_{max} / H) is more than 0.5%, whereas for poorly supported ones it is greater than 1.5-2 %. According to the authors, the most important design criterion for the walls is the ultimate bending moments.

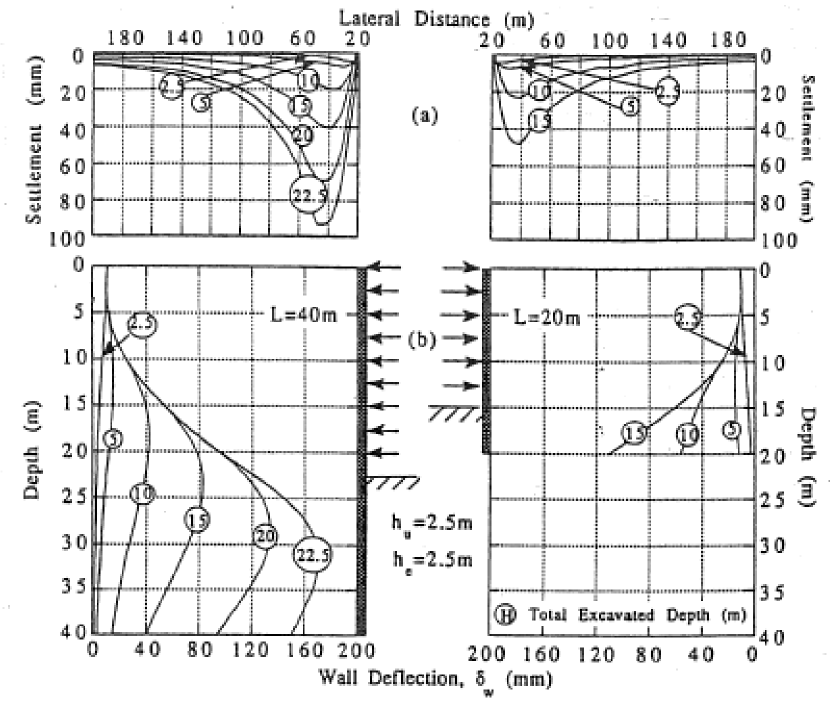

Figure 2.10 Effect of wall length on predicted ground movements (hu=unsupported excavation height; h=support spacing; he=Excavated soil height; Numbers in the circle indicate H=Total Excavated soil depth) (Whittle and Hashash, 1993)

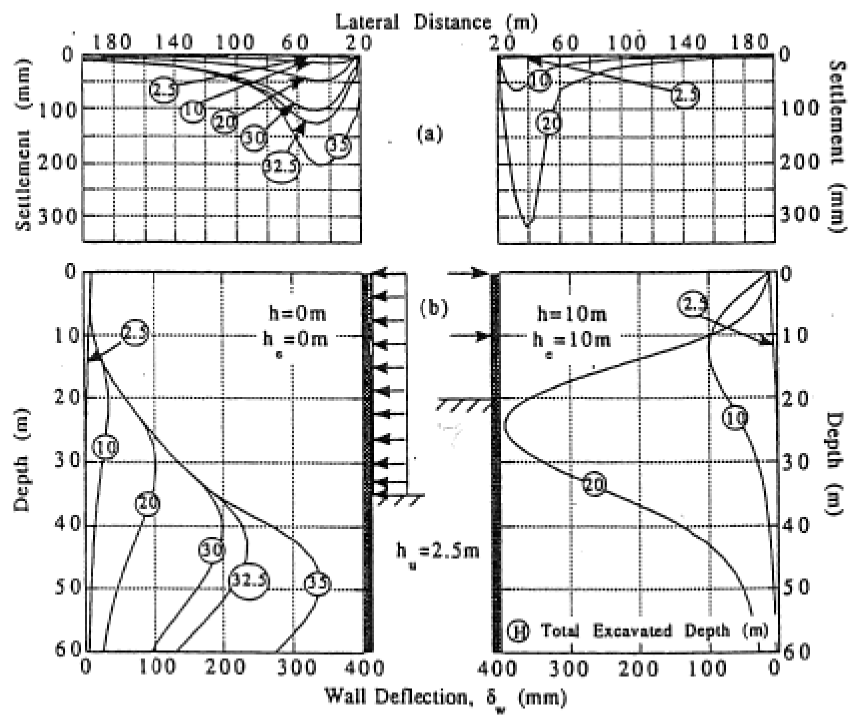

Figure 2.11 Effect of support spacing on predicted ground movements (hu=unsupported excavation height; h=support spacing; he=Excavated soil height; Numbers in the circle indicate H=Total Excavated soil depth) (Whittle and Hashash, 1993)

2.1.3 Design Considerations

2.1.3.1 Failure Modes

Failure modes are important in design considerations and in order to evaluate the loads on system. Variety of failure modes is checked for the selection of certain system parameters to prevent failure.

US Army Corps of Engineers (1994) divides failure modes into 3.First one is deep-seated failure which is a rotational failure of soil mass. This type of failure cannot be normalized with structural changes of wall/anchor. The geometry of retained material should be amended or soil should be improved in order to prevent this type of failure. (Figure 2.12)

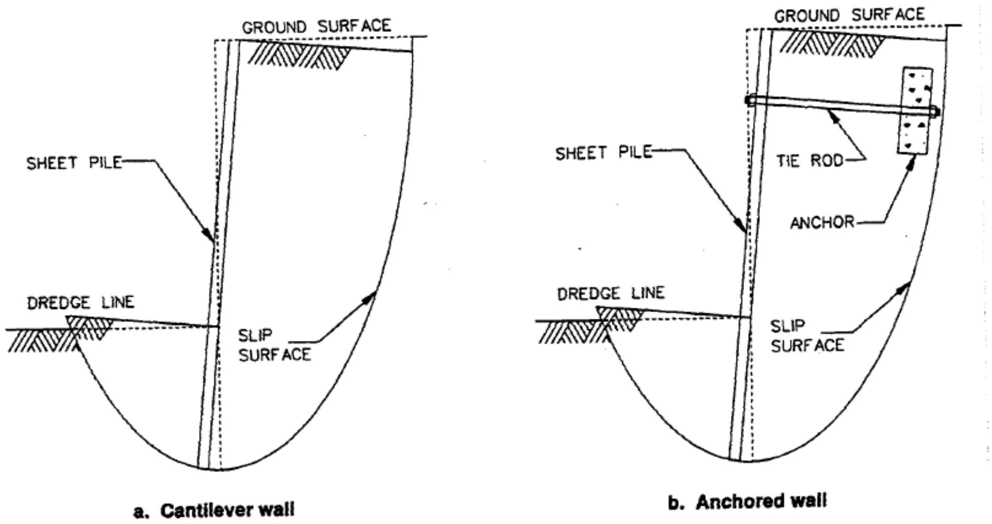

Figure 2.12 Deep-seated failure (US Army Corps of Engineers,1994)

Second failure mode is described as Rotational failure due to inadequate pile penetration. Because of the pressure applied by lateral soil and water behind the wall, rigid body rotation of wall can be observed. Penetration depth of piling and anchor positions should be checked for design considerations. (Figure 2.13)

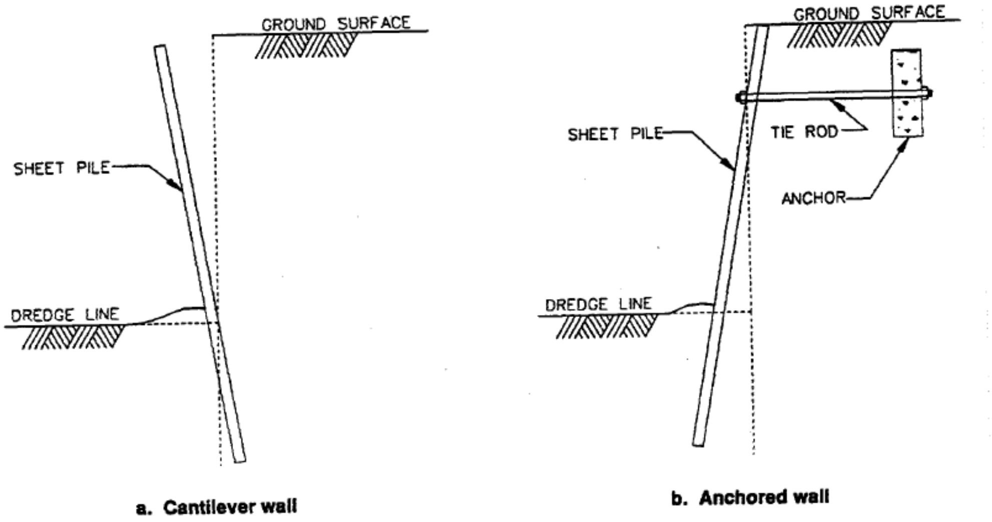

Figure 2.13 Rotational failure due to inadequate penetration (US Army Corps of Engineers, 1994)

The last failure mode is caused by overstressing of retaining system. The design of structural system should be checked in order to prevent this type of failure mode (See Figure 2.14 and 2.15). The failure modes of anchorages are illustrated in Figure 2.16 in TS EN 1997-1.

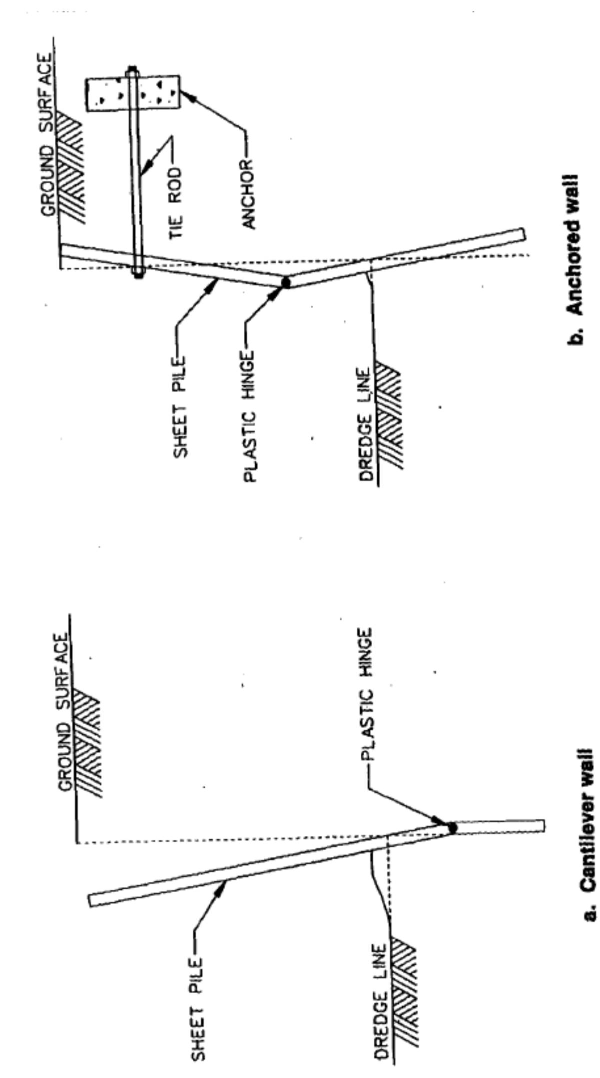

Figure 2.14 Rotational failure due to inadequate penetration (US Army Corps of Engineers, 1994)

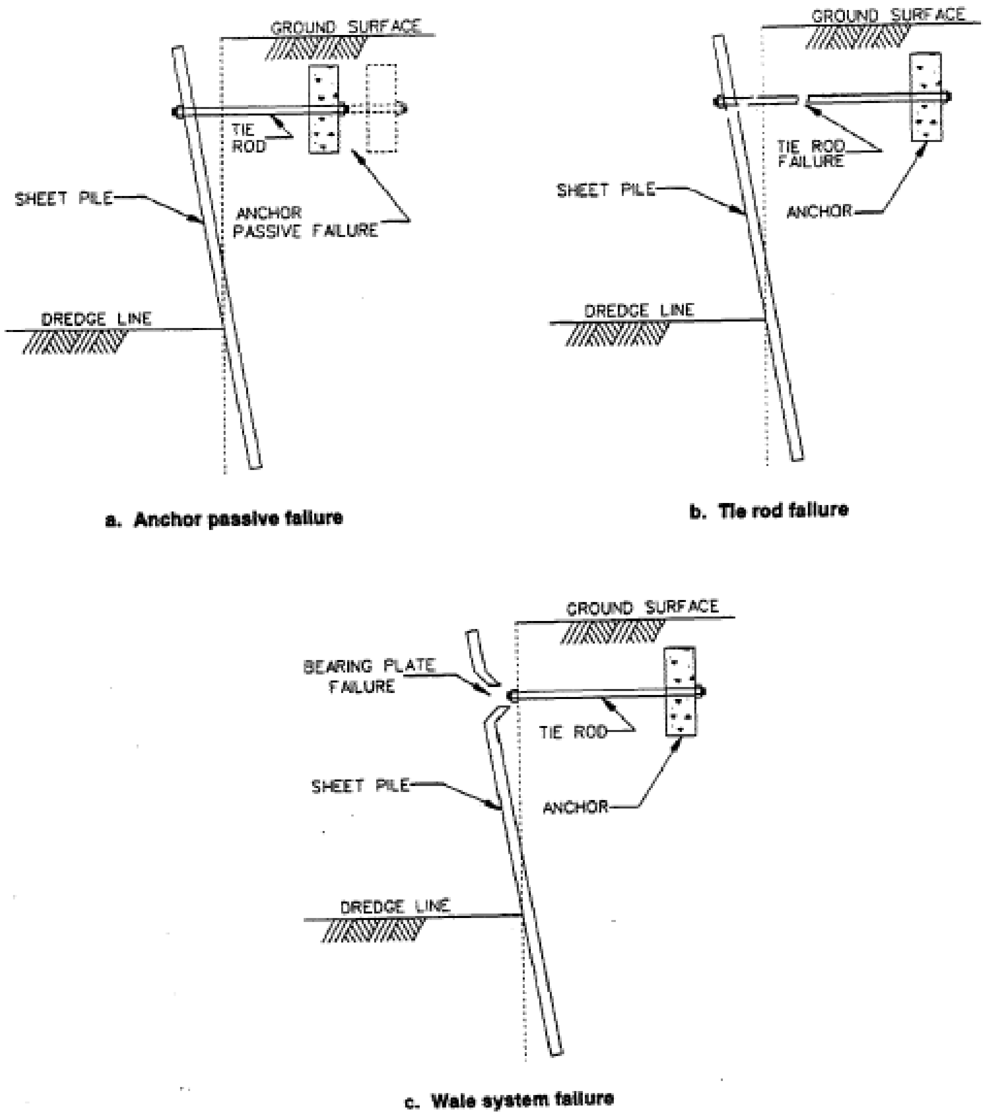

Figure 2.15 Anchorage failure (US Army Corps of Engineers, 1994)

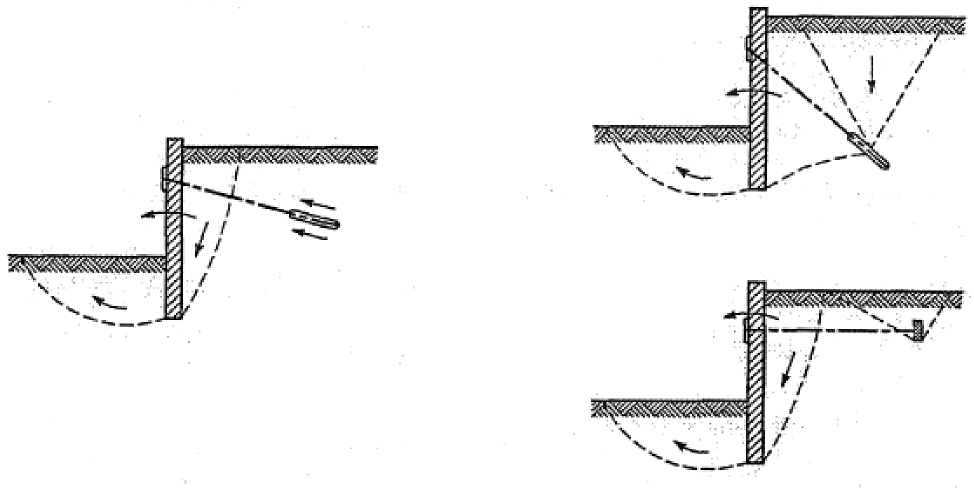

Figure 2.16 Failure modes of anchorages by pull-out force (TS EN 1997-1)

2.1.3.2 Ground Anchors

At Eurocode 7, anchor is defined as a tensile structure element composed of a tendon free length and a restraint which is provided by grout length bonded to the ground.

Limit states of performance of anchorages are listed below;

- The failure of anchor head, which is the part that transmit the restraining forces,
- The failure of the interface of grout,
- The instability of the supporting ground,
- The failure of anchor cables (tendons)

According to EN 1537, the necessary design calculations to design an individual anchor;

- Determination of internal anchor resistance,
- Determination of external anchor resistance,
- Determination of serviceability and durability of the anchor,
- Verification of free anchor length,
- Calculation of lock-off load of the anchor.

The internal anchor resistance, R_{ik} which is the load capacity of the tendon is calculated by the formula below;

$R_{ik}=P_{ik}=A_t f_{tk}$..E.q.6

Where; A_t is the cross section of tendon and f_{tk} is the tensile strength of the tendon.

The external anchor resistance (R_{α}) is the grout-ground interface withstanding of the anchor. According to EN 1537, R_{α} is equal to the load of continuous displacement of the fixed anchor length and being evaluated from load tests results. If no test data is available it can be calculated by using E.q.7.

And while making design, the characteristic external anchor resistance is generally assumed to be equal to or higher than the characteristic internal anchor resistance ($R_{\alpha k} \geq R_{ik}$).

And Eurocode 7 defines the characteristic pull-out resistance ($R_{\alpha,k}$) as the lowest of, external resistance (R_{α} or $R_{a,k}$),internal resistance (R_{ik}),tensile capacity of tendon (f_{tk}) or the capacity of anchor head. (Figure 2.17)

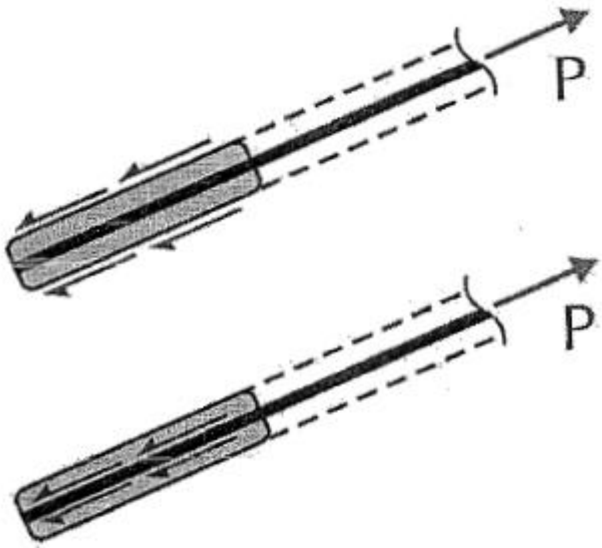

Figure 2.17 Internal and external anchorage resistance

The design pull-out resistance ($R_{\alpha,d}$) is formulated as below in Eurocode 7;

$R_{\alpha,d}=R_{\alpha,k}/\gamma_{\alpha}$..E.q.7

Where, $R_{\alpha,k}$ is the characteristic pull-out resistance and γ_{α} is the partial factor. The partial factor values are tabulated below;

Table 2.1 Partial Factors of pre-stressed anchorages

Reference	Anchorage		Partial factor			
ENV 1997-1[14]	Temporary	γ_m	1.25			
	Permanent	γ_m	1.5			
EN 1537[15]	(all)	γ_R	1.35			
EN 1997-1	*Partial factor set*		*R1*	*R2*	*R3*	*R4*
	Temporary	$\gamma_{a,t}$	1.1	1.1	1.0	1.1
	Permanent	$\gamma_{a,p}$	1.1	1.1	1.0	1.1
	Design Approach		*1-1*	*2*	*3*	*1-2*

The minimum free anchor length and lock-off load of an anchor is determined from the design of support system. According to EN1537, the anchor lock-off load (P_0) is calculated by using below relations;

$R_{\alpha,d} \leq ,65R_{\alpha,k}$..E.q.7

Where $R_{\alpha,d}$ is the anchor load and $R_{\alpha,k}$ is the load capacity of tendon,

And $R_{ik} \leq 0,6R_{\alpha,k}$..E.q.8

The design resistance R_d of the anchor in limit state mode is;

$R_d=R_k/\gamma_R$...E.q.9

Where, R_k is the lower value of anchor resistance (internal and external) and γ_R is the partial factor which should be greater than 1,35.

At serviceability limit design ,the main concerns are the limit values of allowable displacement and deformations of the structure ,deflections of the ground around the anchored structure and the tolerance of supported structure due to displacement and distortion.

2.2 Finite Element Analysis

Finite element analysis divides a continuum into many smaller parts in order to obtain an approximate solution of each part. The results from each part are conjoined to get the solution of whole domain. Plane-strain and three dimensional finite element analysis are studied in order to predict behavior of deep excavations by many researchers. In these studies lateral wall movement of the excavation and surface settlements are observed by using different computer programs such as SSFEAX,REWARD,PLAXIS,FLAC,CUT3D, etc. Plaxis V.8 and Plaxis 3D is used in this study in order to perform two and three dimensional finite element analysis.

Plaxis 3D is a geotechnical finite element analysis program which has 3D pre-processor and is further worked up within geotechnical context. The accuracy of the program depends on the expertise of the user about problem modeling, the understanding of soil models and their limitations, the model parameters selection, and ability to evaluate the reliability of the computed results.

In Plaxis, deep excavation case is simulated by ‘staged construction’ by activating or deactivating the structural elements to simulate the excavation or construction sequence. This procedure provides a realistic assessment of stresses and displacements.

2.2.1 Soil Models

There are several soil models available in Plaxis, as well as the ability to employ user-defined soil models. This study uses only Mohr-Coulomb elasto-plastic model. In finite element modeling, the behavior of soil is mostly modeled as elasto-plastic, just like in Mohr-Coulomb model, which is modeled as linearly elastic perfectly plastic model. A perfectly plastic model is a constitutive model with a fixed continuous surface. In Figure 2.18 basic idea of an elastic perfectly plastic model is presented.

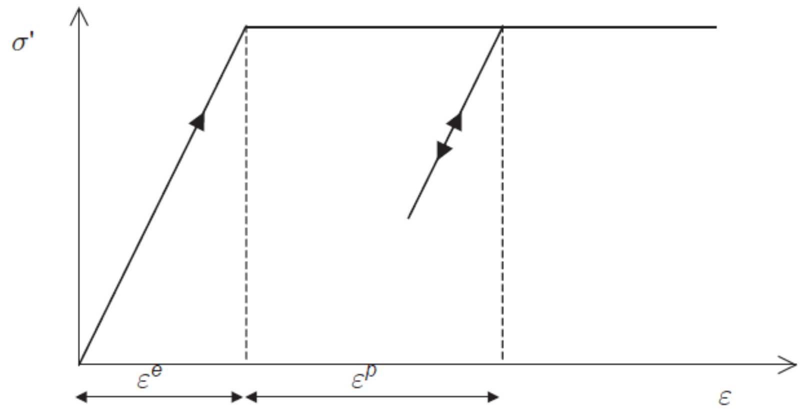

Figure 2.18 Basic idea of an elastic perfectly plastic model

Mohr-Coulomb model is selected because it gives realistic results of bearing capacities and footings collapse loads and cases where collapse load plays a dominant role. The user can also distinguish between drained and undrained behavior. Total stress parameters (cu, Øu, Eu and υ) is adopted for the drained study case.

2.2.2 Examples of 2D and 3D FEM Analyses of Deep Excavations

Plaxis is commonly used in design and analysis of deep excavations in plane-strain. Çalışan (2005) studied an excavation for the construction of a hotel in Gaziosmanpaşa/ Ankara. Plane-strain analyses are performed by using software programs REWARD and PLAXIS and compared field observations and plane-strain analysis.

There are buildings and roads adjacent to the construction area. For the excavation sides which are neighbor to adjacent buildings, Ø80 cm piles are used with 100 cm spacing, and for the remaining sides, Ø65 cm piles are used with 120 cm spacing. The excavation is 27 m depth and cross-sectional view of the in-situ wall presenting the anchor length, tilt angle and anchor spacing is shown in Figure 2.19.

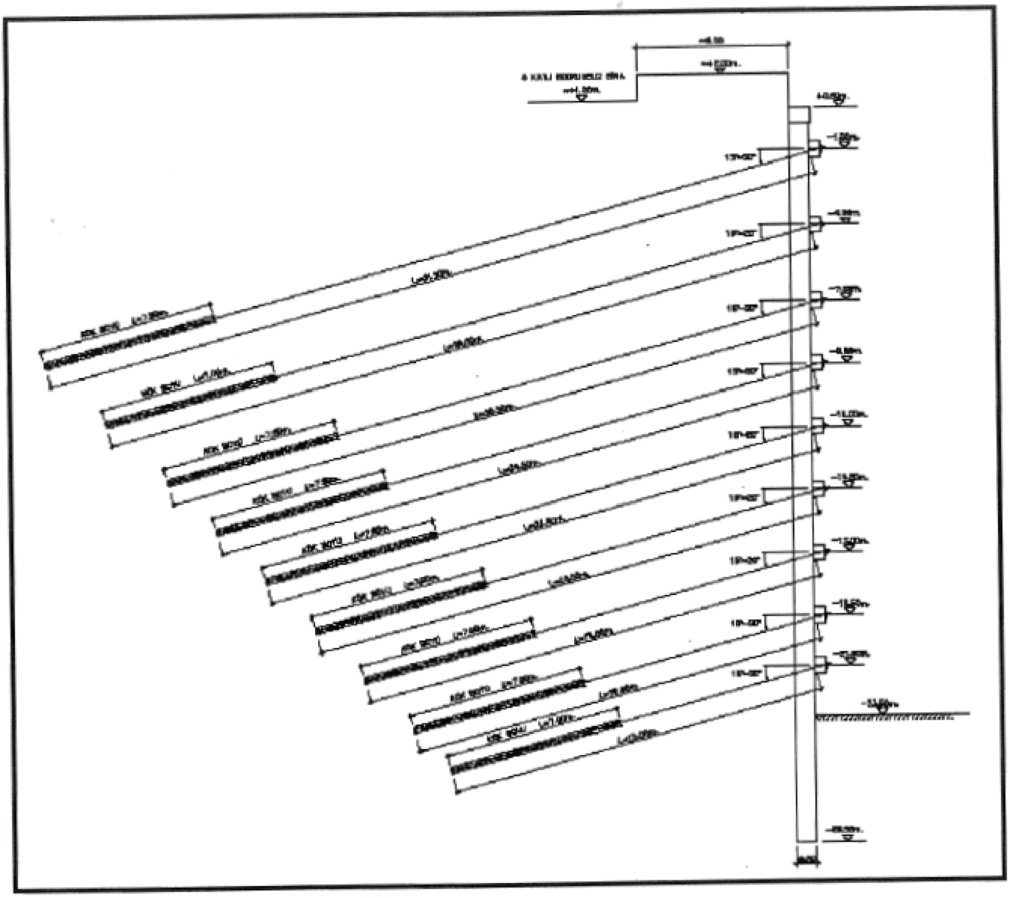

Figure 2.19 Cross- section view of the excavation (Çalışan, 2005)

His observations and results (Table 2.2) showed that the results of PLAXIS analyses are reasonably higher than field observations, since plane stress analysis does not take corner effect into account, which can only be studied by 3D analysis.

Table 2.2 Estimated and Observed Deflections (Çalışan, 2005)

Side	Excavation Depth (m)	Estimated Deflections (mm)		Observed Maximum Deflection (mm)	δ/H (%)		
		Plaxis	Reward		Plaxis	Reward	Observed
A-B	29,5	108,5	88	20	0,36	0,29	0,07
B-C	23	-	76	35	-	0,33	0,15
C-D	25	-	76	17	-	0,3	0,07
D-A	26,5	-	81	29	-	0,31	0,11

Ou, et. al. (1996) defined excavations as three dimensional problems and studied three dimensional finite element procedure. They performed different mesh alternatives and found out that, the meshes should be dense behind and in the excavated area. The mesh they proposed is illustrated in Figure 2.20.

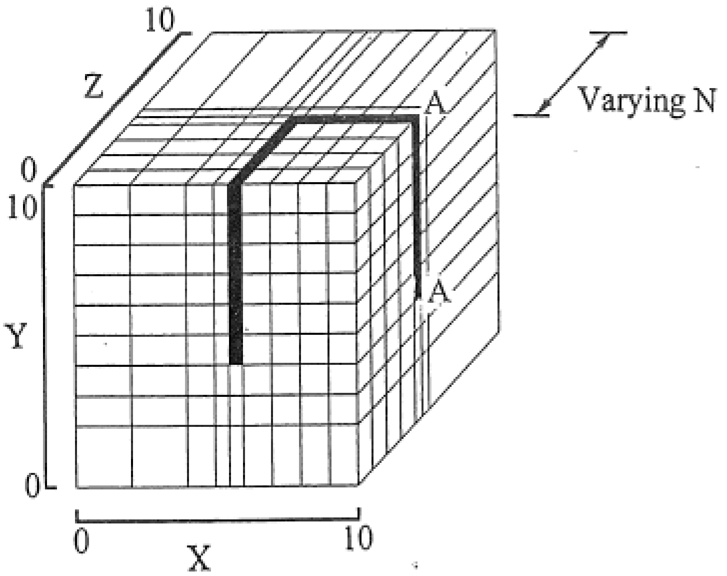

Figure 2.20 Suggested Mesh Number Behind and at the Excavated Area (Ou et.al., 1996)

The excavation case is assumed to be done with low to medium plasticity of silty clayey soil profile in order to study the three-dimensional characteristic of the excavation in Taipei. Top-down construction method is used in three stages for the 16 m depth excavation. And 70 cm thick by 32 m length diaphragm wall is assumed as support structure.

Ou, et.al. (1996) studied the primary wall length effect on wall deflection by making analysis with constant complementary wall length, only changing primary wall length. The varying primary and complementary wall length combinations are shown in Figure 2.21.

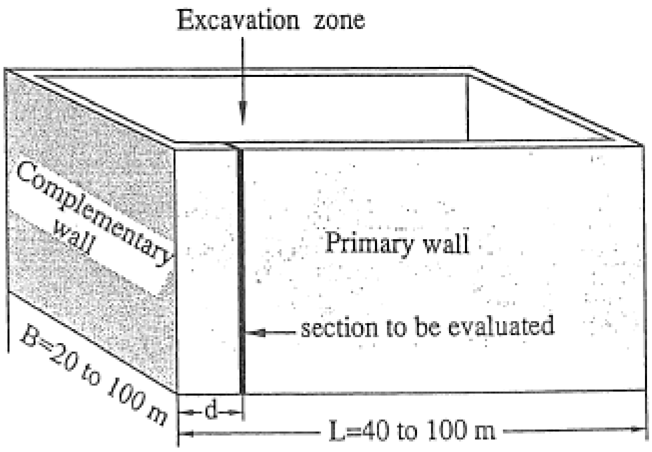

Figure 2.21 Suggested Mesh Number Behind and at the Excavated Area (Ouet.al.,1996)

For various primary wall lengths, the maximum displacement remains same of the wall with small complementary wall length.(L=20 m) For 40,60 and 100 m complementary wall lengths, the maximum displacement of walls reduces for smaller primary wall lengths. It should also be noted that, as primary wall length increases, three dimensional analysis results approaches plane-strain analysis results and the maximum displacements near the corners are smaller than sides.

In order to define the deflection behavior of a wall section, plane-strain ratio (PSR), which is the ratio of maximum wall displacement (δ) to maximum wall displacement of the section (δ_{ps}) with same excavation width should be examined. As plane-strain ratio gets higher, the corner effect decreases, and for PSR value is equal to 1, the section come around to plane-strain condition.

Based on the relations above, the relation between PSR value, length ratio of complementary wall with respect to primary wall (B/L) and corner distance to a section is plotted in Figure 2.22.

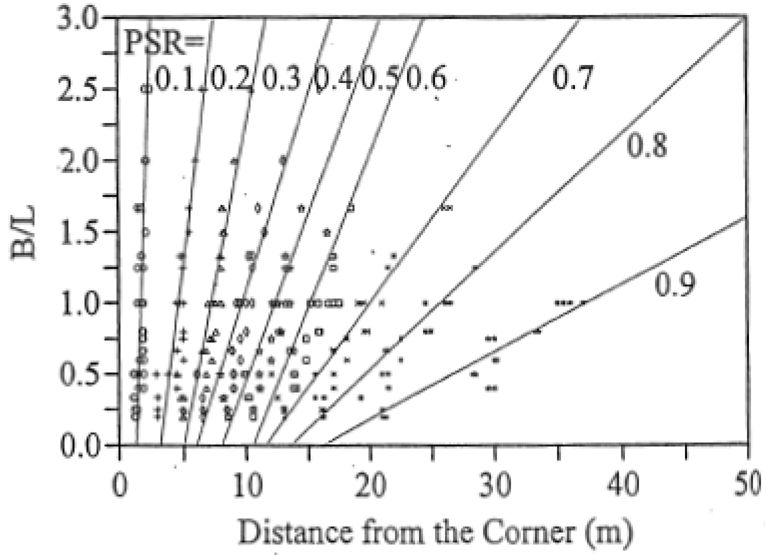

Figure 2.22 Relation of B/L Ratio and Corner Distance for Various PSR Values (Ou et.al., 1996)

The deflection attitude of a wall during excavation depends on sequence of excavation, excavation method, method of wall support, depth of excavation, penetrated depth of excavation wall, the geometry of excavation, wall stiffness, soil strength etc. Therefore, it is very important to calculate relationship between wall length and PSR value in every case. This is possible but time consuming since great numbers of analyses required. As a first order approximation, the ratio of three dimensional analyses to plane-strain analyses can be considered alike.

Ou, et.al. (1996) studied PSR method by convergence studies from the excavation case of Hai-Hua building in Taipeicity. The excavation is 20.3 m depth, supported with 110 cm thick and 42 m length diaphragm wall. And there exist 7 excavation stages to apply top-down construction method. Both plane-strain and three dimensional analyses are performed, and wall deformations are monitored along the excavation.

Three dimensional analysis results were quite close to field observations, on the other hand, plane-strain analysis shows conservative results. (Figure 2.23 and 2.24) The maximum deflections of the wall are predicted by multiplying PSR values with plane-strain results. Figure 2.25 shows, the maximum wall deflection results of inclinometer I4 and I5 of three dimensional analyses, plane-strain analysis and field measurements. It can easily be observed from the figure 2.25 that, maximum wall deflections of finite element analysis and field measurements were very close to each other.

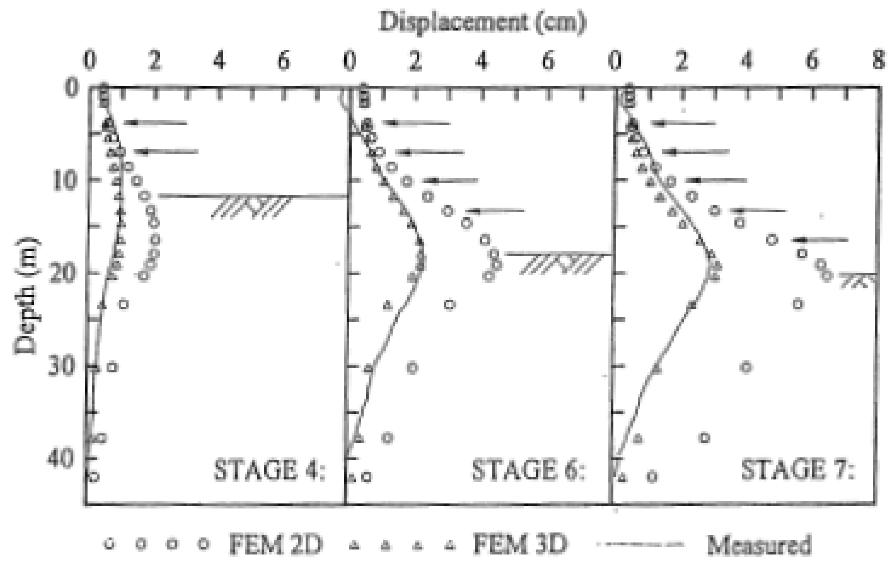

Figure 2.23 Measured and predicted Wall Displacements for Corner excavation Sections (I4) (Ou et.al, 1996)

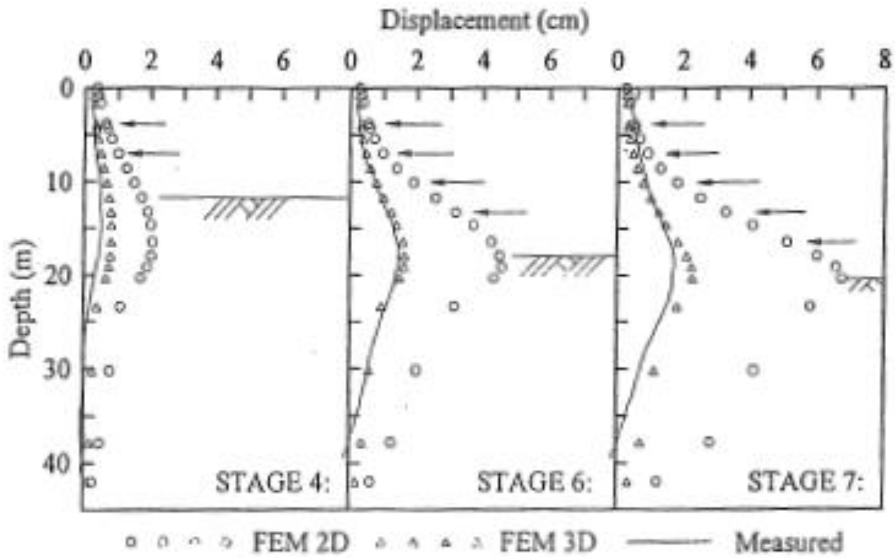

Figure 2.24 Measured and predicted Wall Displacements for Corner excavation Sections (I5) (Ou et.al, 1996)

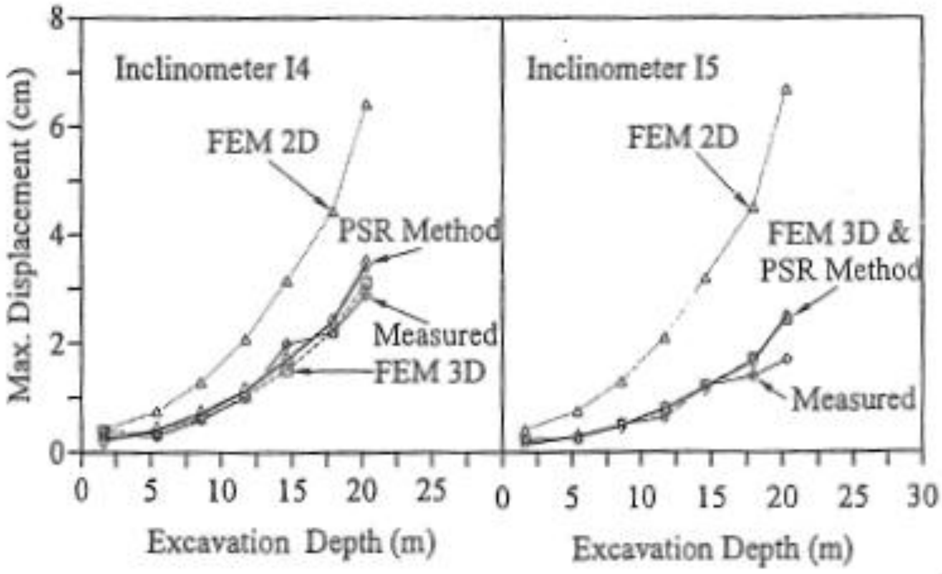

Figure 2.25 Comparison of Measured and Calculated Maximum Wall Deflections from PSR Method (Ou et.al, 1996)

Ou et al.,(2000) studied three dimensional analysis of Taipei National Enterprice Center (TNEC) in order to measure diaphragm wall deformations and ground surface settlements. The TNEC is an 18 storey building with 5 basement levels. In order to construct 19.7 m depth basement, top-down construction method is used. The structural bracing system is composed of 90 cm thick and 35 m deep diaphragm wall which is supported by concrete floor slabs and temporary steel struts. A dense array of inclinometers was installed to take measurements during and after the construction stages as shown in construction site demonstration

The excavation is performed in site composed of five layers of silty clay and silty sand deposits over a thick layer of gravel formation which is 46 m below ground surface.

Figure 2.26 shows the results of longitudinal and latitudinal wall deformations during and after all excavation stages. The Figure 2.26 (a) shows that the ratio of maximum longitudinal wall deformation with respect to excavation depth are between 0.0043-0.0057. These ratios are higher than previous observed studies, since wall deformations normally increase as construction period gets longer. According to the results of latitudinal measurements, I-1 tends to move toward west, while I-3 tends to move toward east. According these observations, the soil not in the center of the site has tendency to deflect toward the excavation center.

Ou et al., (2000) also indicated that the value of maximum ground surface settlements are decreased with decreasing the distance to the southeast corner.

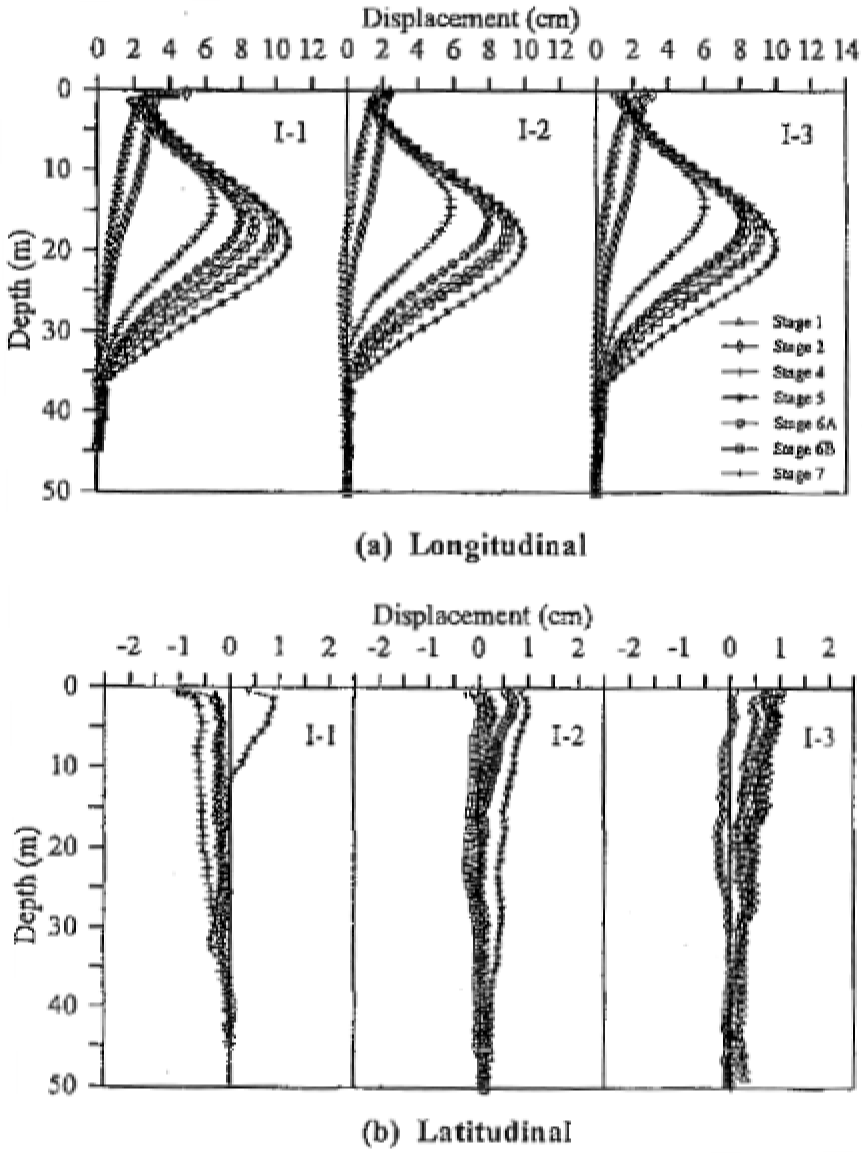

Figure 2.26 Longitudinal and Latitudinal Wall Deformations at I-1, I-2 and I-3 (Ou, Shiau, Wang, 2000)

Ünlü, (2008), performed parametric study by varying soil stiffness in in-situ walls supported at one, two and four levels both with plane-strain and 3D finite element analysis. In order to monitor corner effect, comparative studies were made due to deflection, moment, anchor loads and effective lateral earth pressures of retaining walls. According to Ünlü, (2008), corner effect is observed up to 20 m distance from corner and anchor loads increase until 10-15m distance from corner. Additionally her studies show that, corner effect decrease as the stiffness of support system and elastic modulus increase. Moreover, calibration of models was made by using inclinometer data of two actual deep excavation cases. According to findings of these case studies, modeling perpendicular pile wall as a strut in plane-strain analysis gives quite similar results of cantilever systems in 3D analysis.

CHAPTER 3

METHODOLOGY

The problem was first studied in plane-strain and parametric study started with an excavation case supported with anchorages. Then, same excavation case was studied with strut supported system, again in 2D. Since proposed supporting system is a three dimensional problem, it needed to be analyzed and compared with conventional supporting systems in 3D. Therefore second step of the analysis study started with three dimensional modeling.

Firstly 2D designs were repeated with same parameters in 3D in order to compare the results with those of the new support system. After seeing that anchored walls give less efficient results than strut-supported excavations, the third round of the comparisons began between arch-supported excavation and strut-supported system. Several analyses performed with varying excavation width, soil type, surcharge, tie bar connection angle etc., in order to compare proposed supporting system in terms of efficiency.

Throughout finite element modeling, the excavation sequence is composed of several construction stages. Firstly, retaining wall and pile cap are activated. Then soil is removed till first excavation level. After that walers and supporting elements (struts or anchors) are activated. This procedure is repeated for each support level up to excavation depth.

3.1 Parametric study

Two soil profiles were used in the analyses: Uniform Ankara Clay and uniform dry sand. The excavation depth (H) was 20 m, the excavation width (B) was varying between 20-30-50 m, the embedment depth of the wall was 5 m.

In all cases 80 cm bored piles were modeled with 1 m center to center spacing as supporting wall and 50cmx50 cm walers were simulated at each support level and 80x80 cm cap walers were placed at ground level.

Three types of wall supporting system (anchored walls, walls with struts and arch supports) were calculated in this study for the 20 m deep excavation. Main variable parameters were support type, excavation width, support spacing, surcharge loads applied all over the soil surface and soil type. The variables of the parametric study are listed in Table 3.1. Beyond these major variables, wall support without pile cap, shape of arch support (round vs. parabolic), tie bar angle, and cancelled anchors at corners were secondary variables of this parametric study.

Table 3.1 Variables of the parametric study

Support Type	**Excavation Width,B**	**Support Spacing**	**Surcharge**	**Soil Type**
Anchor Strut Arch Support	20x20 m 30x30 m 50x50 m	Varying between 3-5 m intervals	No Surcharge 100 kPa 200 kPa	Ankara Clay Dry Sand

3.2 Design Criteria

Lateral loads take place at deep excavations due to soil pressures behind walls. For the analysis of bracing system, below subjects were taken into consideration as design criteria;

a) Lateral deflection criteria of walls which was taken as 0.5% of wall height (H/200) due to observed values of past studies performed by Whittle and Hashash (1993) and Ou et al.(1993).Excavation depth was 20 m in all through the study therefore lateral deflection criteria was taken as 10 cm in this study.

b) Reinforcement ratio for the pile was taken as 0.025 which gives the maximum moment capacity under pure bending as 1260 kN.m. In the analyses, maximum bending moment in the piles occurred as 845 kN.m/m. Thus, the piles had a minimum factor of safety of 1.50.

c) Yield strength of the struts was taken as 355 MPa. During the analyses, strut sections were optimized by checking the yield stress resulting from both axial force and bending moment.

d) Overall stability of the system was checked by using PLAXIS.

3.3 Material Properties

3.3.1 Soil Parameters

Linearly elastic perfectly plastic material model was used for soil model. While modeling soil, several stress-strain behaviors were assumed. Material model requires five input parameters which are Young's modulus (E), Poisson's Ratio (ν), friction angle (φ), cohesion (c) and dilatancy angle (ψ) which can be obtained from tests of soil samples. Cohesion, friction angle and dilatancy angle control the plastic behavior while Young's modulus and Poisson's Ratio control elastic behavior.

Parametric studies were performed for Ankara clay and dry sand. During analyses, water flow was not taken into consideration. Sand was assumed as dry and clay as drained. Constant elastic modulus, cohesion, internal friction angle, unit weight, Poisson's ratio and interface reduction factor were taken in the calculations. Soil parameters used are tabulated in Table 3.2 below.

Table 3.2 Soil Parameters Used in Parametric Studies

PARAMETER	SYMBOL	UNIT	ANKARA CLAY	DRY SAND
Material Model	-	-	Mohr-Coulomb	Mohr-Coulomb
Unsaturated Soil Weight	γ_{unsat}	kN/m^3	19	19
Saturated Soil Weight	γ_{sat}	kN/m^3	20	19
Elastic Modulus	E	kN/m^2	31.500	31.500
Poisson's Ratio	μ	-	0.3	0.3
Cohesion	c_{ref}	kN/m^2	20	0
Friction Angle	φ	°	25	32
Dilatancy Angle	ψ	°	0	0
Interface Reduction Factor	R_{inter}	-	1	1

3.3.2 Support System Parameters

Anchored support system for three-dimensional analyses includes wall, anchors and walers which basically transfer the earth pressure from the wall to anchors. For strut-supported retaining systems, the only difference is the supporting element.

When simulating cases in three dimensional analyses, care must be taken in defining the stiffness parameters of the structural elements, because of the additional z axis. Three-dimensional analysis requires three stiffness parameters to represent the axes instead of one input.

E_1 and E_2 denote the Young's modulus in first and second axial direction respectively for the wall component. G_{12} implies the in-plane shear modulus. G_{13} and G_{12} imply out of-plane shear modulus related to shear deformation over first and second axes, respectively. The wall's local system is represented in Figure 3.1.

The elastic behavior of an anchor element is represented only with the relation between axial force (N) and displacement (u) of the form (N= EAu/L).The stiffness of the anchor (EA) is represented by material stiffness and cross section (A).

For the beam component, beam stiffness involves the input of Young's Modulus and three moments of Inertia: I_2, I_3 and I_{23}. I_2 and I_3 show the moments of inertia against bending around second and third axes, respectively and always perpendicular to the beam axis. I_{23} shows the moment of inertia for oblique bending, and it is equal to zero for symmetric beam elements. The local system of axes is represented in Figure 3.2 below.

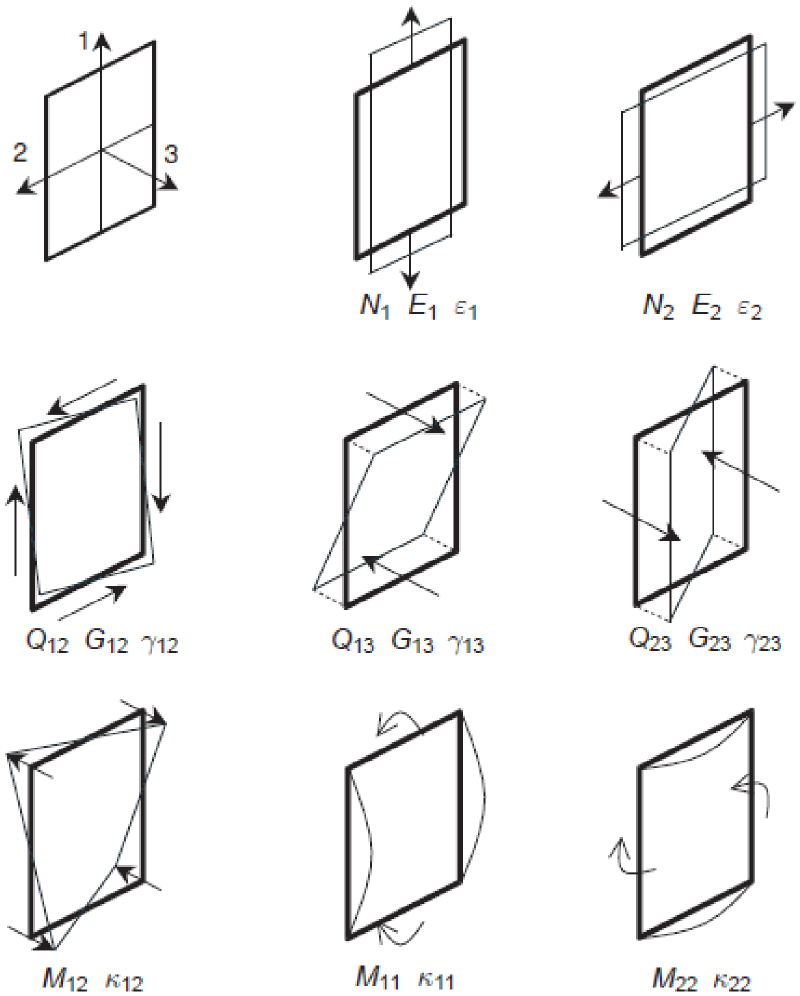

Figure 3.1 Definition of a Wall's Local System Axes and Positive Normal Forces, Shear Forces and Bending Moments

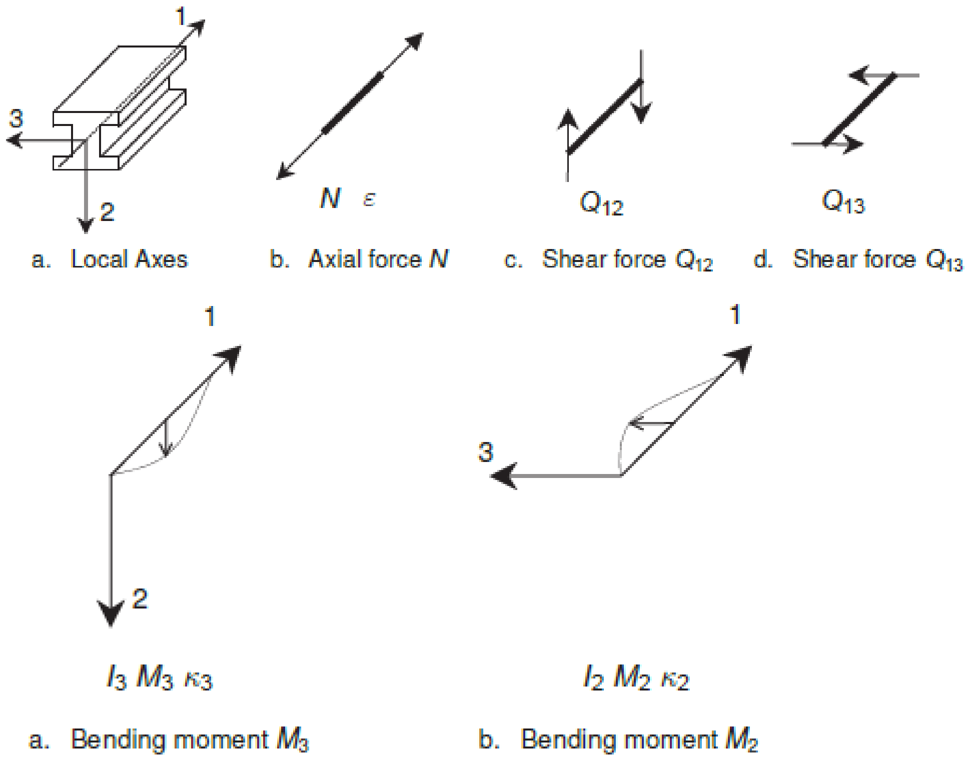

Figure 3.2 Definition of a Beam's Local System Axes and Positive Normal Forces, Shear Forces and Bending Moments

In the model, bored piles were defined as equivalent plate elements by selecting appropriate stiffness values. Plate elements were assumed to be plates with a rectangular cross-section in PLAXIS.

For the axial stiffness in the major direction, bored piles were considered as made up of C25 class concrete having a young modulus of 30.000 MPa. For the horizontal stiffness of plate 0.001 times the major stiffness was used in order to reflect a realistic behavior. For shear stiffness values of the piles, PLAXIS tutorials were used.

D=0.8 m and S=1.0 m where, “D” is the pile diameter and “S” is center to center spacing between adjacent piles. The formulations given below were taken from the manuals of PLAXIS. In which, d_{eq} represents the equivalent depth of the plate calculated by considering the ratio between axial and flexural stiffness of the original pile and plate element, E_1 represents the major axial stiffness calculated by considering the ratio between flexural rigidities of original pile and equivalent plate, E_2 represents the horizontal axial stiffness (minor stiffness) calculated as mentioned above and G_{12}, G_{13}, G_{23} represent the shear modulus values taken from PLAXIS tutorials as sheet pile wall assumptions since they are not in primary concern for the analyses. Equivalent plate parameters were calculated as below;

$$d_{eq} = \sqrt{\frac{3 \cdot D^2}{4}} \Big/ S \qquad d_{eq} = 0,693\ m$$

$$I_{pile} = \pi \cdot r^4 / 4 \qquad I_{pile} = 0,0201 m^4$$

$$E_1 = E_{beam} \cdot I_{pile} \cdot I_{eq} \qquad E_1 = 21,75 \cdot 10^6\ kN/m^2$$

$$E_2 = E_1 / 1000 \qquad E_2 = 21,75 \cdot 10^3\ kN/m^2$$

$$G_{12} = 6 \cdot E_{wall} \cdot I_{pile} \Big/ 10 \cdot {d_{eq}}^3 \qquad G_{12} = 1,087 \cdot 10^6\ kN/m^2$$

$$G_{23} = {E_{wall} \cdot A_{pile}} \big/ {20 \cdot d_{eq}} \qquad G_{23} = 1{,}088 \cdot 10^6 \ kN/m^2$$

$$G_{13} = {E_{wall} \cdot A_{pile}} \big/ {6 \cdot d_{eq}} \qquad G_{13} = 3{,}627 \cdot 10^6 \ kN/m^2$$

$$\gamma = \left({\pi \cdot r^2} \big/ {d_{eq}} \right) \cdot \ \gamma_{concrete} \qquad \gamma = 17{,}4 \ kN/m^3$$

The parameters used for support wall, anchors and struts as stiffness values and material properties are shown in Tables 3.3, 3.4 and 3.5, respectively.

Table 3.3 Wall Stiffness Parameters for Three-Dimensional Analysis

PARAMETER	**NAME**	**UNIT**	**WALL PARAMETERS**
Young's Modulus (*)	E_1	kN/m^2	21.750
	E_2		21.750.000
Shear Modulus (*)	G_{12}	kN/m^2	1.087.000
	G_{13}		1.088.000
	G_{23}		3.627.000
Poisson's Ratio	n	-	0
Plate Thickness	d	m	0,693
Unit Weight	γ	kN/m^3	17,4

(*)Direction 1:horizontal along the wall
Direction 2: vertical through the wall
Direction 3: normal to the wall

Table 3.4 Anchor Parameters for Three-Dimensional Analysis

PARAMETER	NAME	UNIT	ANCHOR	GROUT
Stiffness of Anchor	EA	kN	101.000	-
Shear Modulus	S	kN/m^2	-	21.000.000
Unit Weight	γ	kN/m^3	-	10
Diameter	-	m	-	0,15
$T_{top,max}$	-	kN/m	-	200
$T_{bot,max}$	-	kN/m	-	200

Table 3.5 Strut and Waler Parameters for Three-Dimensional Analysis

PARAMETER	NAME	UNIT	STRUT	SECONDARY STRUT	WALER	TOP WALER
Beam Area	A	m^2	0,22(*)	3,65x 10^{-3}	0,25	0,64
Young's Modulus	E	kN/m^2	210x10^6	210x10^6	30x10^6	30x10^6
Unit Weight	γ	kN/m^3	78,5	78,5	24	24
Moment of Inertia	I_3	m^4	0,958x10^{-3}(*)	0,0172x10^3	5,200x10^{-3}	0,03413
Moment of Inertia	I_2	m^4	0,958x10^{-3}(*)	0,0172x10^3	5,200x10^{-3}	0,03413

(*) Beam area and moment of inertia were varying throughout the study. Sample value of one section is inserted in table above.

3.4 Methodology of 2D Analysis

Initially, the conventional support systems were modeled as plane-strain problems with PLAXIS Version 8 two dimensional finite element program. Since the geometry was symmetric, only half of the excavation was considered in the analyses. The piles and walers were modeled by means of “plate” elements. While calculating EI and EA values both pile and waler dimensions were taken into consideration.

The boundary condition of soil mass was selected as free in each direction which is a prescribed force equal to zero and a free displacement. And 80 m wide and 50 m deep soil was selected as boundary geometry for plane-strain analysis.

Coarse mesh generation was selected and a geometry contour was created near the structure in order to provide a finer area close to excavation.

For each case of excavation, several designs were analyzed during the parametric study in order to satisfy the design criteria.

3.4.1 Design with Anchors

According to soil pressure distribution behind the retaining wall, as suggested by Terzaghi and Peck (1969) five anchor support points were determined as an initial trial case. Support spacing was assumed as 5 m in the vertical, throughout the depth. Effective anchor lengths were calculated according to Rankine’s Earth Pressure theory. The unstable wedge behind the wall was drawn from 1.1-1.5 H below ground level making an angle of 45° + φ/2 with the horizontal axis. Therefore, effective anchor lengths are decreasing with depth at each level. On the other hand, anchor root length was assumed as 7 m at all anchor levels.

Anchor effective lengths, supporting levels and lateral anchor spacing varied during design. The most efficient case was determined regarding the lateral deformation criterion.

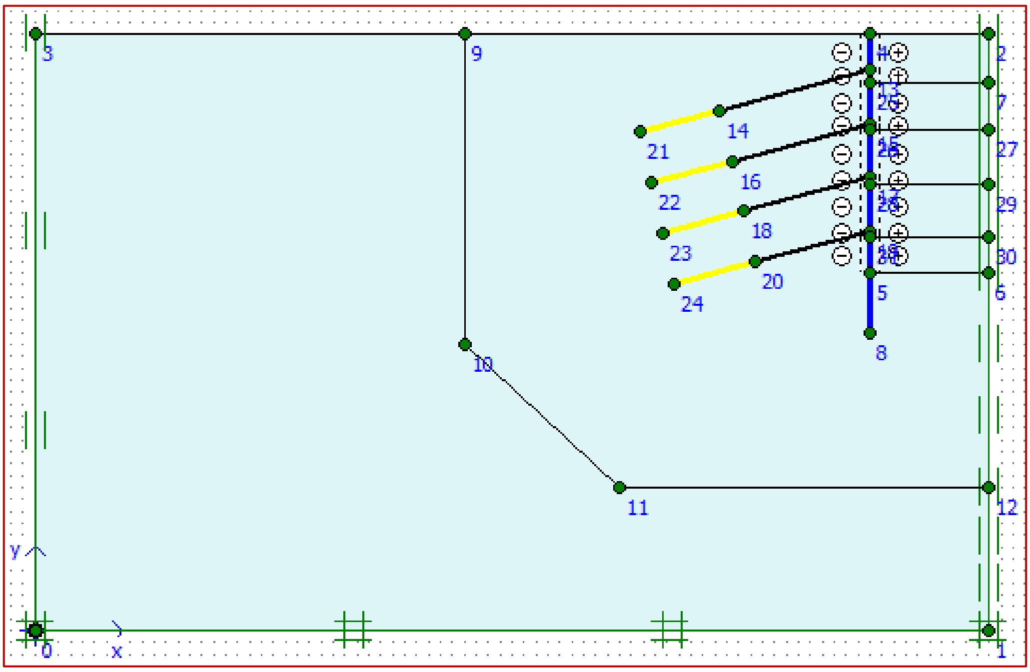

Figure 3.3 Anchor Model in Plaxis 2D

3.4.2 Design with Struts

Same case is repeated with four strut support points. Struts are modeled with fixed-end geometry. Since in actual geometry struts are positioned crosswise from one side of support wall to the other, effective stiffness of the struts were entered in the model as half of the actual axial stiffness of the beam element. Related modification was done according to the transformation of the local axial stiffness to global stiffness with an angle of 45° (real orientation of the corner strut makes that angle with the normal of the supporting wall). Since the transformation is done by multiplying the stiffness value by $\cos^2\alpha$, modification constant used is 0.5 in the problem.

Lateral strut spacing and beam cross-sections were changed during the design calculations. After making trial and error analyses, optimum case was determined which gives nearest lateral deformation criteria to anchored case.

Arch-support could not be modeled in 2D finite element program since arch shaped struts are three dimensional.

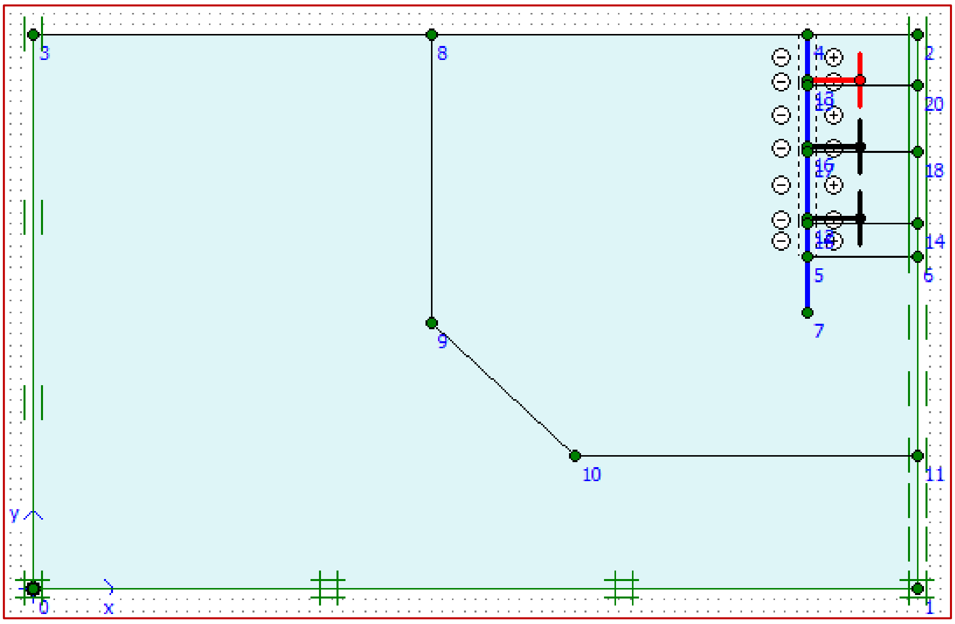

Figure 3.4 Strut Model in Plaxis 2D

3.5 Methodology of 3D Analysis

While many cases can be defined as plane-strain analysis, to increase the reality of some problems, three-dimensional analysis are used. Moreover in our case study, the geometry of new type of retaining system does not allow simulation in two dimensional sections. In this analysis, instead of modeling two-dimensional section of the original geometry, the whole geometry was considered.

Since all three dimensional parts are taken into account in the analysis, three-dimensional analysis involves relatively more elements, nodes, and run time as compared to plane-strain analysis.

Three-dimensional analyses were performed using PLAXIS 3D 2010.10-node tetrahedral elements were used for basic soil elements; moreover 3- node line elements as beam elements, 6-node plate elements as piles and 12-node interface elements for soil-structure interaction behavior are used. In three dimensional analyses it is an important point to model walers as separate geometric item since load distribution cannot be achieved without them.

By taking into consideration of symmetric conditions of both axes, only quarter of the problem was modeled (as opposed to modeling half of the problem as it was done in the 2D analyses). Boundary of soil mass were taken as 50x50x50 m for 20x20 m wide, 80x80x50 m for 30x30 m wide and 100x100x50 m for 50x50 m wide excavation. Mesh generation is done with global coarseness set to “coarse”. Figure 3.5 illustrates the typical three-dimensional mesh.

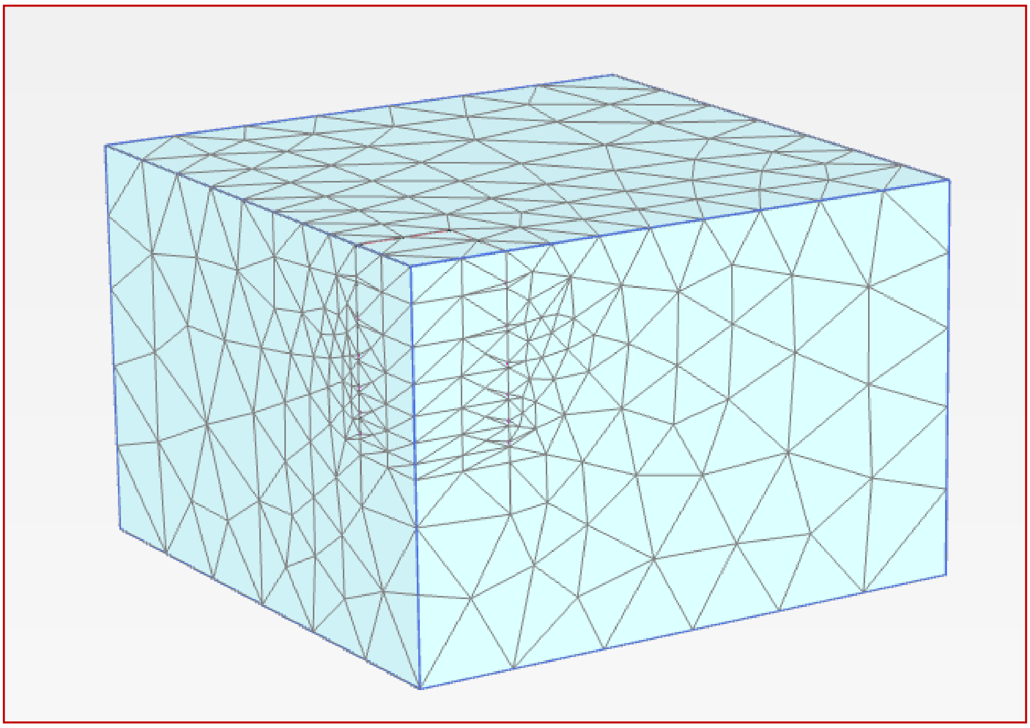

Figure 3.5 Typical Three-Dimensional Mesh

3.5.1 Design with Anchors

Our optimum solution of 2D analysis was replicated in 3D model as an initial trial. After that, making the use of corner effect, anchors near the corners are deleted. In figure 3.6 a view is shown from three dimensional anchored case.

Different from 2D analysis, number of anchors can be varied in every particular level. By the help of this property the model was optimized with varying anchor quantity in each row. The design analyses were repeated using sand as soil type for each case.

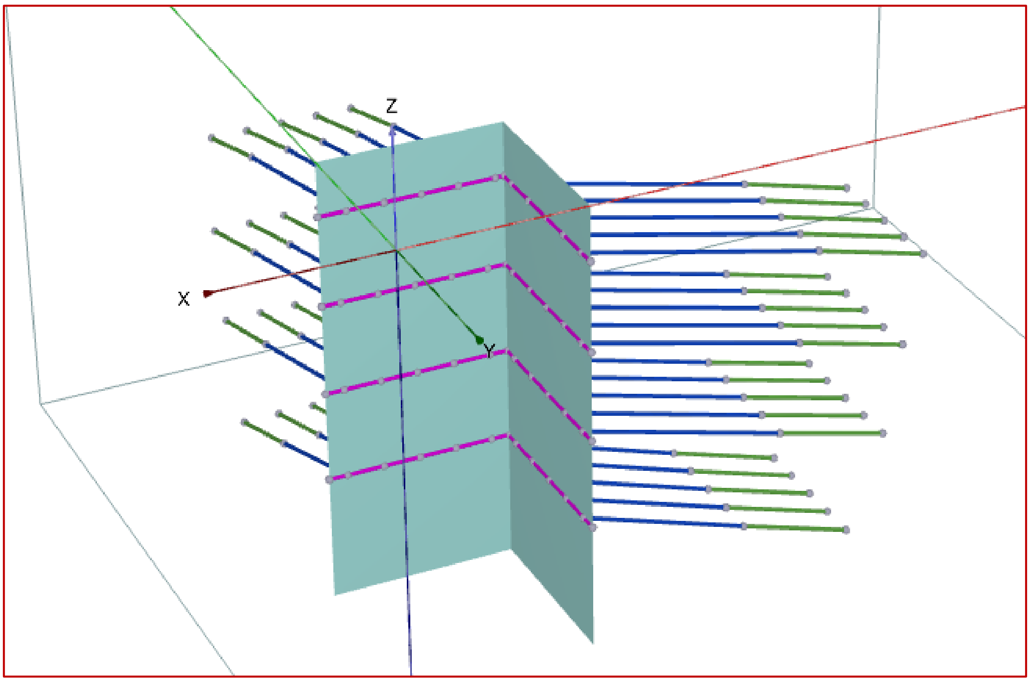

Figure 3.6 Three Dimensional Anchored Case

3.5.2 Design with Struts

Just as anchors, best 2D solution was repeated first. Then loads (100 kPa and 200 kPa) were applied as surface loads on all soil surfaces. Strut cross-sectional dimensions had to be increased after applying surface loads. The other parameter that was changed while making trial and error was the strut spacing and lateral support quantity. Three dimensional strut-supported case is illustrated in Figure 3.7.

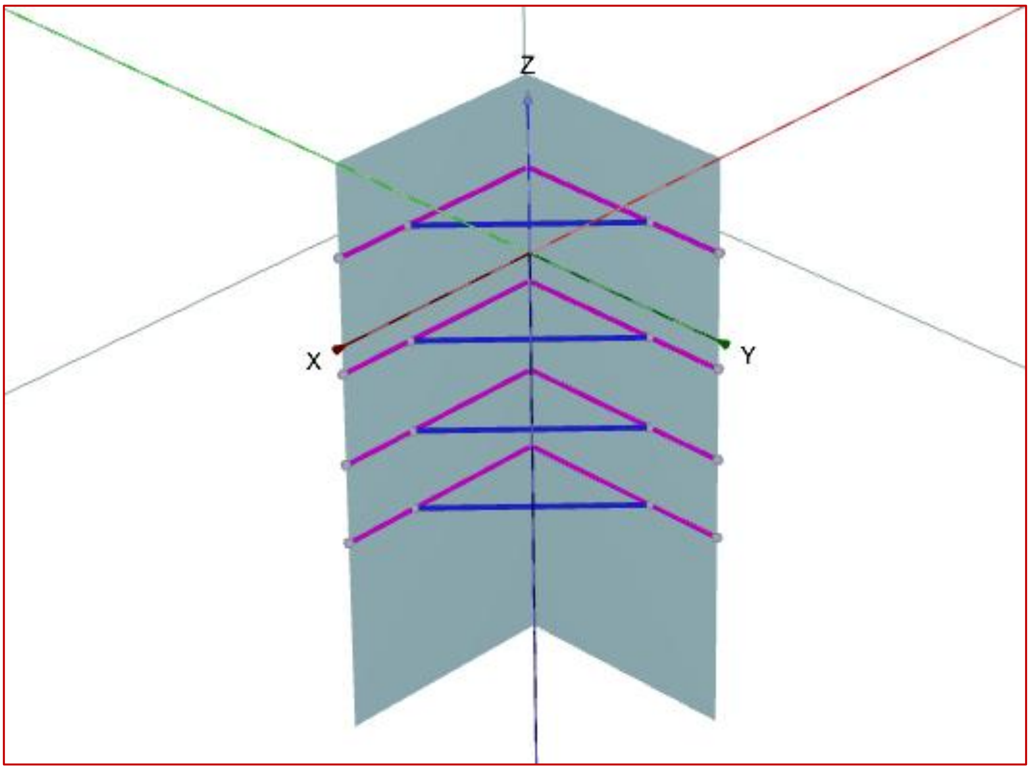

Figure 3.7 Three Dimensional Strut-Supported Case for the 20x20 m and 30x30 m Excavation Width.

In further analyses, width of the excavation was increased to 30 and 50 m keeping excavation depth same. In cases with 50m excavation depth, another crosswise strut beam was placed parallel to existing beam in order to share arising loads as shown in Figure 3.8. All excavation support combinations were replicated for sand.

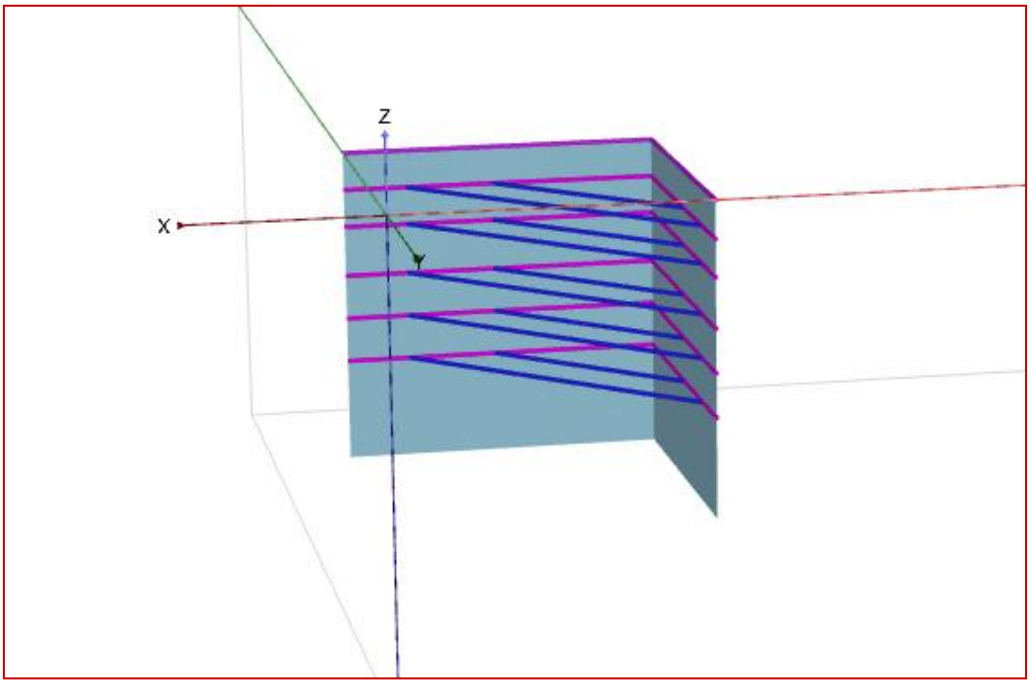

Figure 3.8 Three Dimensional Strut-Supported Case for the 50x50m Excavation Width

3.5.3 Design with Arch Support

Following the initial set of analysis, it was clear that anchor supported system allows greater deformations and wall moments, compared to strut and arch supported systems. Arch supported models were created for each strut-supported case with same properties in terms of surface loads (100 kPa and 200 kPa), support spacing, excavation width and soil type. Arch shaped beams are constituted by using pieces of small beam elements welded to each other with an angle. From each connection point to walers, there are secondary beam elements as shown in figure 3.9

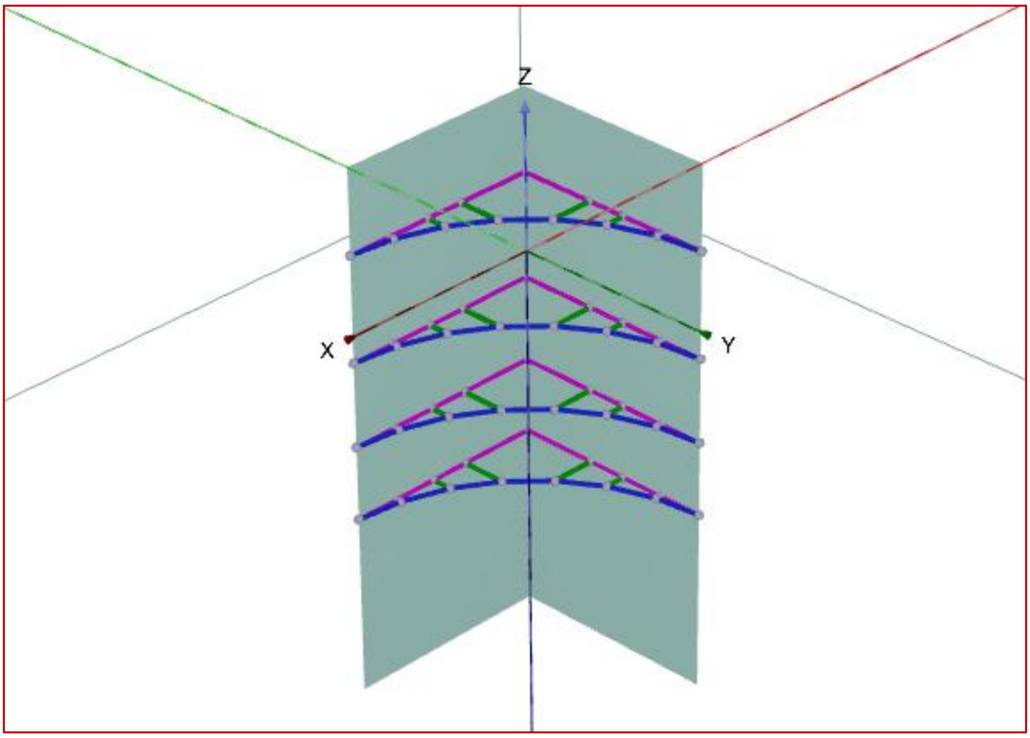

Figure 3.9 Arch-Support and Secondary Beam elements

3.6 Evaluation of Arch Support

3.6.1 Arch Geometry

Since it is not applicable to form the arch shape with single piece of beam, arch geometry is made up with small pieces of welded pipe sections. For some of the analytical analyses, arch shape was modeled with equal length of beam sections in the form of polygonal section as shown in figure 3.10. The number of pieces that comprises beam section was changed in order to identify the effect.

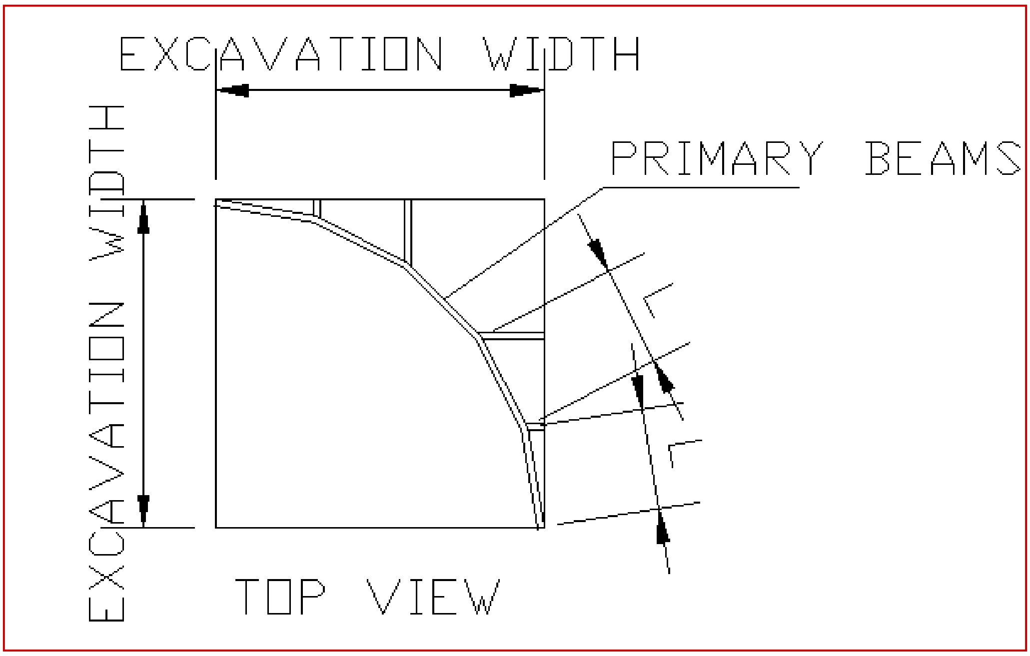

Figure 3.10 Round Shaped Arch Support

A parabolic geometry was modeled, after arch-support was laid out in a circular shape. Parabolic equation used in the model was selected as a second degree polynomial $Ax^2+Bx+C=y$. Origin of the reference axes was assumed as the center of the excavation area (Figure 3.11). Equation constants A, B and C were determined by considering two main criteria. These criteria are defined below;

- The slope is 0 at $x = 0$ and $y = B/2$
- $x = y$ where the slope is -1

Where, B is the excavation width.

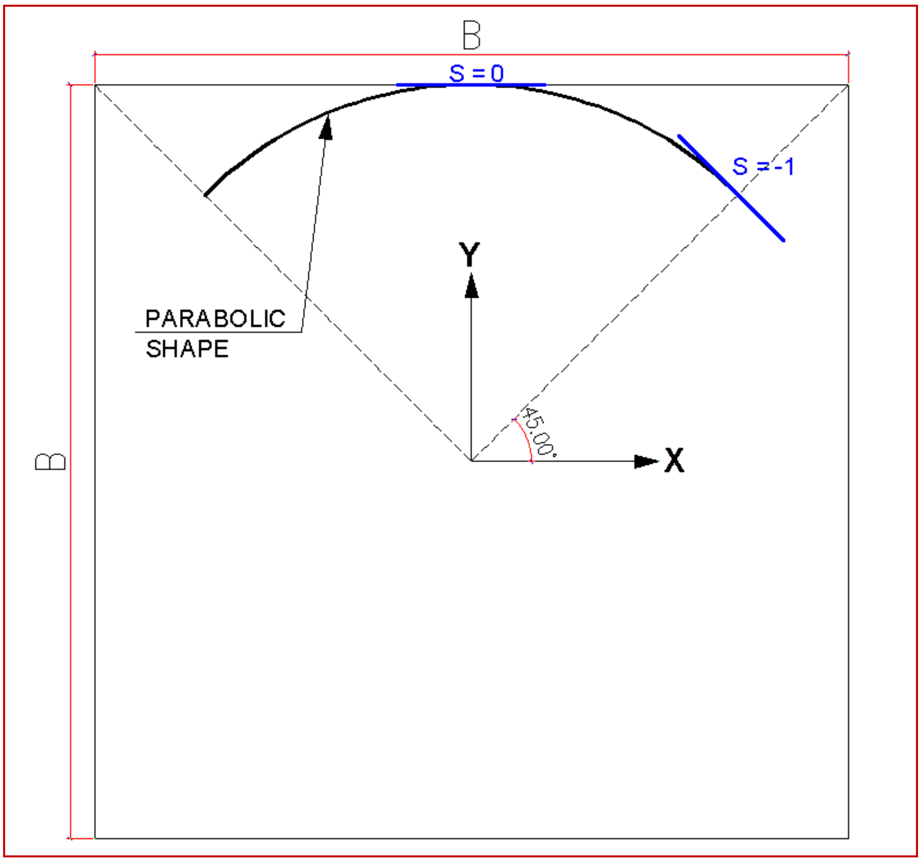

Figure 3.11 Layout Parameters of the Parabolic Strut Shape

After the calculation of the constants, parabolic equation was formed as below.

$y(x) = -\frac{3}{B} \cdot x^2 + \frac{B}{2}$ Where; B is the excavation width

Various arch shapes were formed according to the formula given above. Typical arch beam modeled is shown in Figure 3.12. It was observed that parabolic shaped beams furnish more efficient results than circular ones.

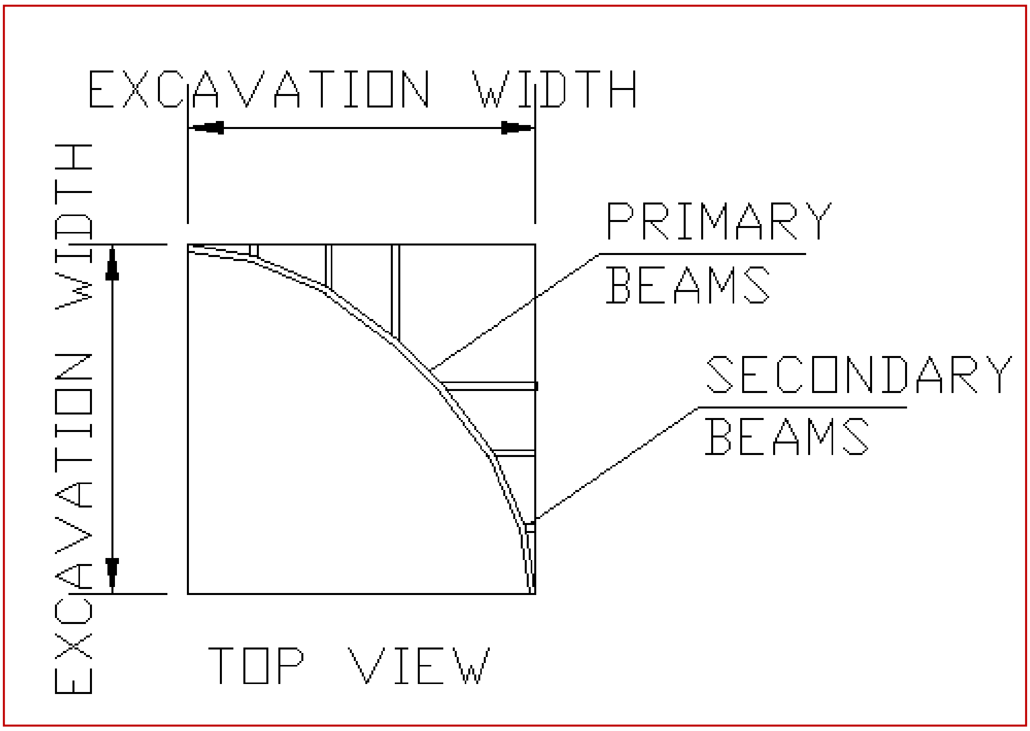

Figure 3.12 Parabolic Shaped Arch Support

3.6.2 Tie Bars

Arch-Support system was developed with tie bars connecting the conjunction point of primary beam segments to walers. The tie bar system was built up as secondary supports in order to distribute loads to walers and walls as explained before.

The tie bars were making ninety degrees with the walls at the beginning of parametric studies. And it was observed that this connection support disposition causes too much axial loads on the beam section nearest to the corner. In order to decrease that axial load, the angle of secondary beams changed making ninety degrees angle with the arch elements as shown in

Figure 3.13 below. This issue will be discussed in section 4.3.3 in greater detail.

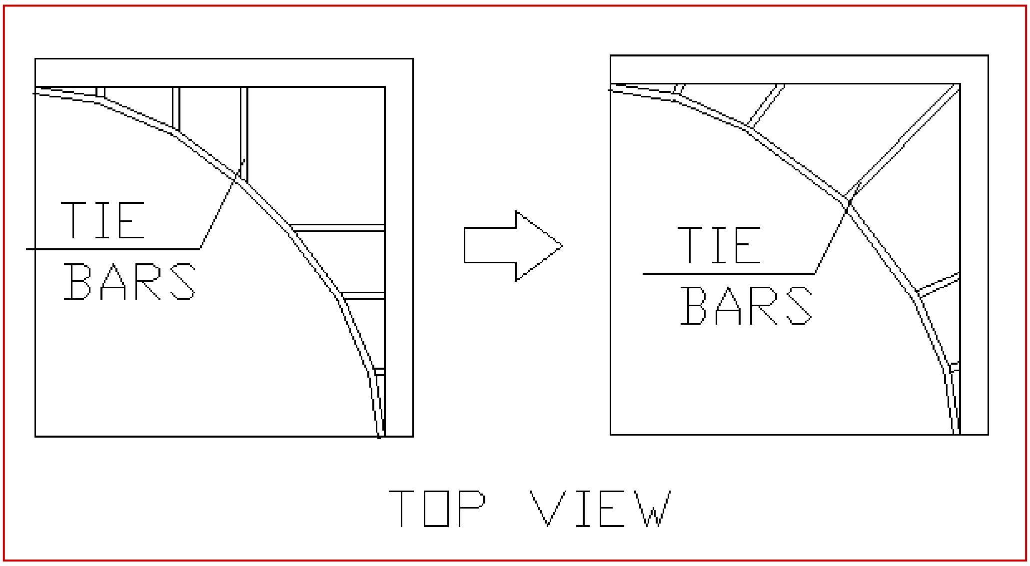

Figure 3.13 Modification Made on Tie Bar Connection Angle to Strut-Supports

3.6.3 Comparison with Conventional Supports

Early in the analyses it was observed that anchor supported excavations were giving inferior results with respect to strut-supported excavations which was explained in detail in section 4.3. Therefore, comparative studies were focused on analyzing arch-supported and strut-supported excavations.

For the same cross-sectional dimensions of supporting beam, analyses were conducted and the results of wall lateral deflection values were compared. Pile lateral moments, support forces and stresses of supporting beams and lateral deflection of walls were compared for all three retaining systems.

Then, cross sectional dimensions of beam sections were varied for strut and arch supported excavations, such that walls supported by the two types of supports exhibit the same maximum horizontal deflection values. Following this analysis, costs of the two support systems that result in the same horizontal deflection were calculated using 2012 unit prices.

CHAPTER 4

ANALYSES AND RESULTS

A parametric research was performed in order to investigate the performance of arch supports by using geotechnical software PLAXIS. Plane-strain and three dimensional analyses were conducted throughout the research program.

Plane-strain analyses were conducted to observe general behavior of supported excavations both with anchors and struts. After completion of pilot runs in 2D, three dimensional analyses were conducted by using PLAXIS 3D both for anchor-supported and braced excavations.

Investigation of the performance of arch-supported walls compared to strut supported ones was continued by selection of some major parameters which were discussed in section 3.1 before. Analyses and evaluation of results of each category will be explained briefly in this chapter.

4.1 2D Analyses

In all two dimensional analyses, 20x20 m excavation area was considered with an excavation depth of 20m. The analyses were performed both in Ankara clay and dry sand. Pile diameter was taken as 80 cm with center to center spacing of 1 m and pile length was fixed at 25 m.

4.1.1 2D Analyses with Anchors

In all analyses, root length of the anchorages and lateral anchor spacing were taken as 6.0 m and 2.0 m, respectively. Support depth and free length of the anchors are given in Figure 4.1.

	Anchor Location	Free Length
1	-3,00 m	13,50 m
2	-8,00 m	12,50 m
3	-13,00 m	11,50 m
4	-18,00 m	9,50 m

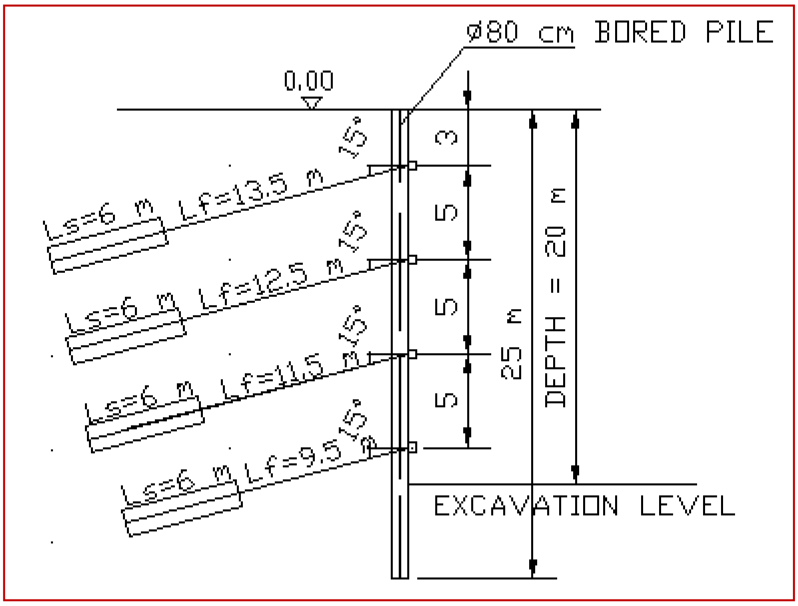

Figure 4.1 Cross sectional view of four level anchor-supported wall.

As a result of the analysis performed for Ankara clay, maximum lateral deflection of the wall is 77 mm which was below the deflection tolerance of 100 mm (H/200). The resultant deflected shape is shown in Figure 4.2.

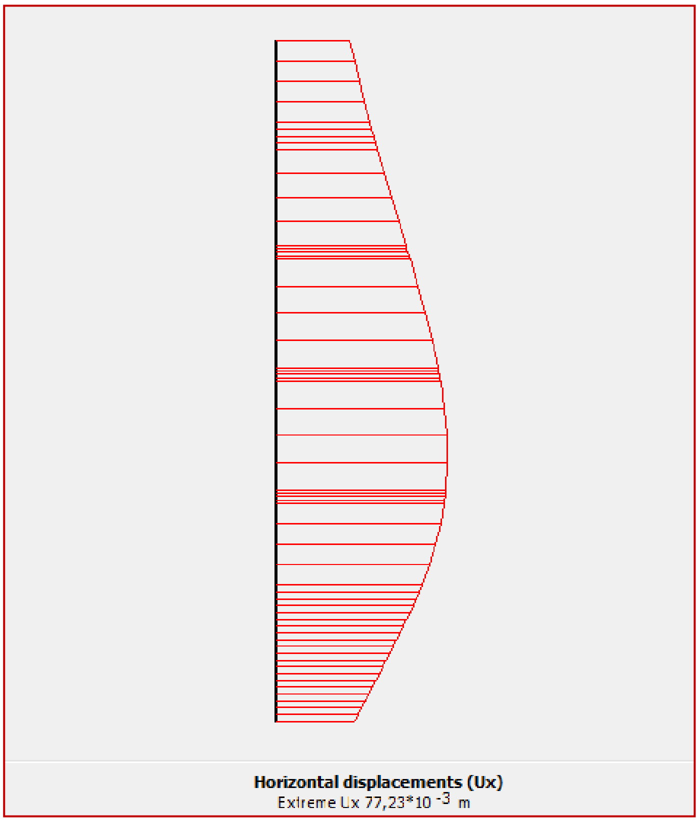

Figure 4.2 Deflected Shape of supporting wall with anchors in Ankara clay

As a result of the analysis performed in sand, maximum lateral deflection of the wall is 88 mm. The deflected shape of the wall was observed in sandy soil was similar to observed in clay analysis.(Appendix A.1)

4.1.2 2D Analyses with Struts

Pilot runs also continued for strut-supported excavations by using same parameters as in anchor supported excavation studies in terms of excavation area and depth. Steel hot-rolled pipe section with a diameter of 500mm and a thickness of 6mm was selected in order to model the strut beam. Since corner struts were considered in the analyses, lengths were calculated as hypotenuse of the corner dimensions. Thus, strut length spacing of each support level was defined in the model as 8.50m. Strut levels and length spacing are given below.

	Support Location	**Length Spacing**
1	-4,00 m	8,50 m
2	-10,00 m	8,50 m
3	-16,00 m	8,50 m

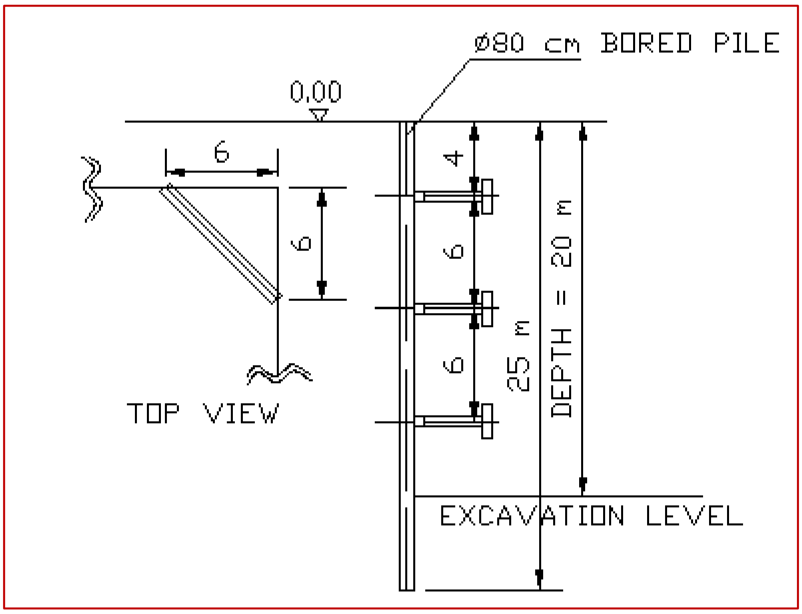

Figure 4.3 Cross-sectional view of three level strut-supported wall

As a result of the analyses performed in Ankara clay, maximum lateral deflection of the wall is 62 mm, which is below the deflection tolerance of H/200

As a result of the analyses performed in sand, maximum lateral deflection of the wall is 67 mm, which is inside deflection tolerance.

Comparison of the deflected shape of the wall gives similar results both for Ankara clay (Figure 4.4) and sand (Appendix A.2).

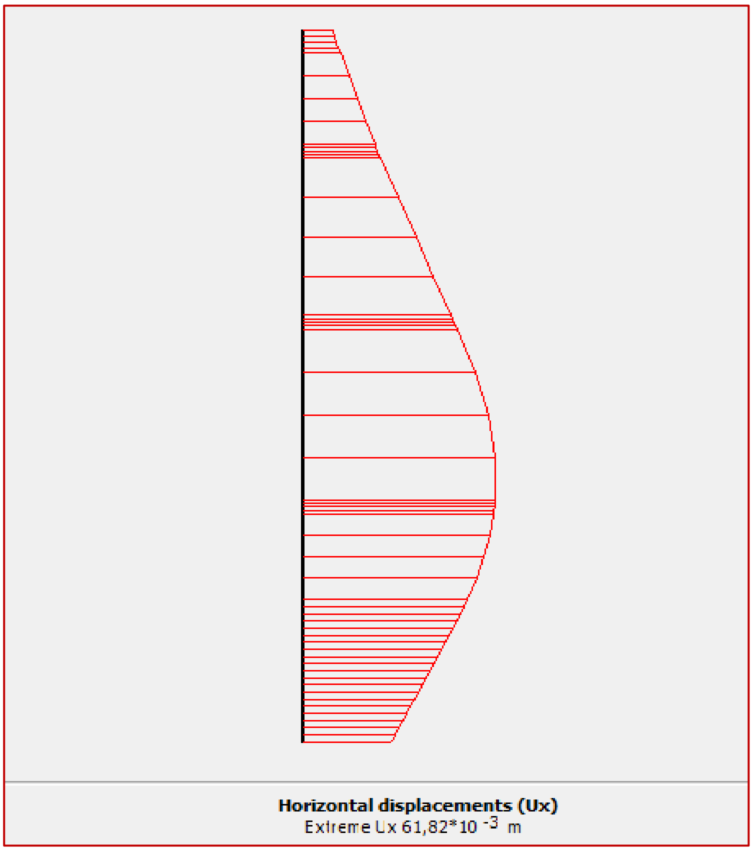

Figure 4.4 Deflected shape of supporting wall with struts in Ankara Clay

4.2 3D Analyses

As mentioned in the introduction of this chapter, three dimensional analyses were conducted in order to investigate the performance of proposed (arch-supported) bracing system. Since this research is based on parametric finite element analyses, a sequence was followed in the analyses. Therefore, primary runs were performed for anchor-supported excavations and then, braced excavations (strut and arch supported) were studied.

During analyses, axisymmetric boundary conditions were used in the models in order to reduce output data and save time.

4.2.1 Anchor-Supported Excavations

In three dimensional analyses, excavation area, excavation depth, vertical and horizontal anchor spacing, root length and free length values were taken same as plane-strain analyses in order to observe three dimensional behavior.

A total of six analyses were performed for anchor-supported cases. First set includes Ankara clay and sand soil types with the same parameters as in 2D. Other than 2D modeling, walers were defined in 3D models as beam elements working with bored pile walls which were defined as plate element.50x50 cm reinforced concrete walers were inserted at each support level and 80x80 cm pile cap were placed at ground level. Plane-strain analysis resulted in larger wall deflection and moment values than three dimensional analyses as shown in Figure 4.5 below. And as the width of excavation area increases, larger deflection and moment values were observed in three dimensional analyses. Deformation and moment vs. depth for 2D and 3D anchor-supported excavation can be seen in sandy soil in Appendix A.3.

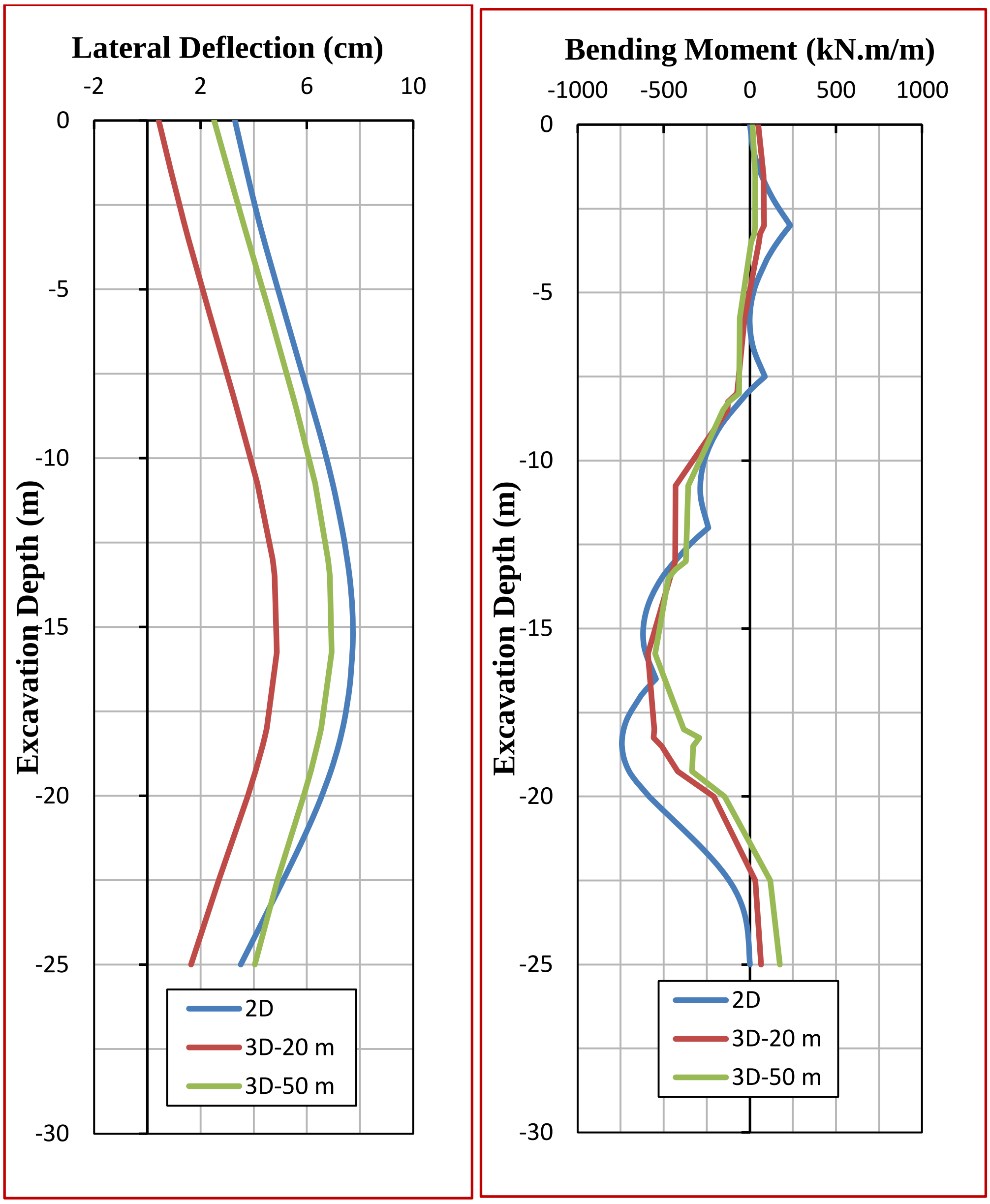

Figure 4.5 Deformation and moment vs. depth for 20x20 m width in 2D and 20x20 m and 50x50 m width in 3D anchor-supported excavation cases in clay

After completion of first anchor supported excavation case solution set, corner anchors of the two upper levels were removed in order to observe corner effect in 3D. Model views of the first set and second set are given in Figure 4.6 and Figure 4.7, respectively.

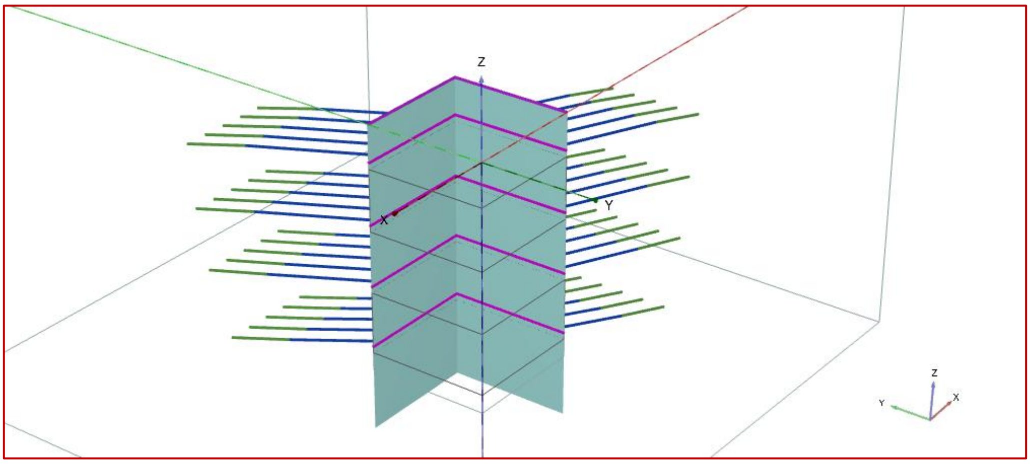

Figure 4.6 Model view of the first set of 3D anchor-supported analyses

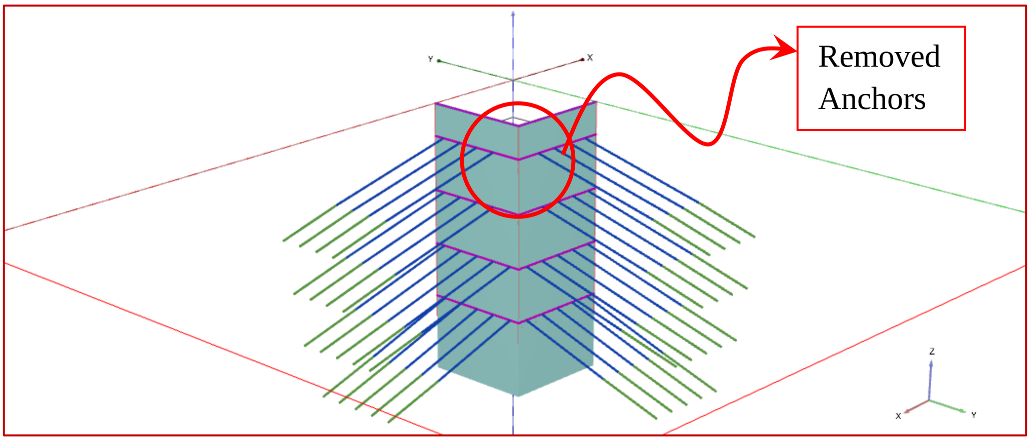

Figure 4.7 Model view of the second set of 3D anchor-supported analyses

Analyses were examined in terms of wall deformation and wall moment. Maximum lateral deflections and wall moments are given in Table 4.1. The effect of removed corner anchors is presented in the comparison diagram (Figure 4.8) of wall lateral deflection and moment with and without corner anchors both in clay and sand.

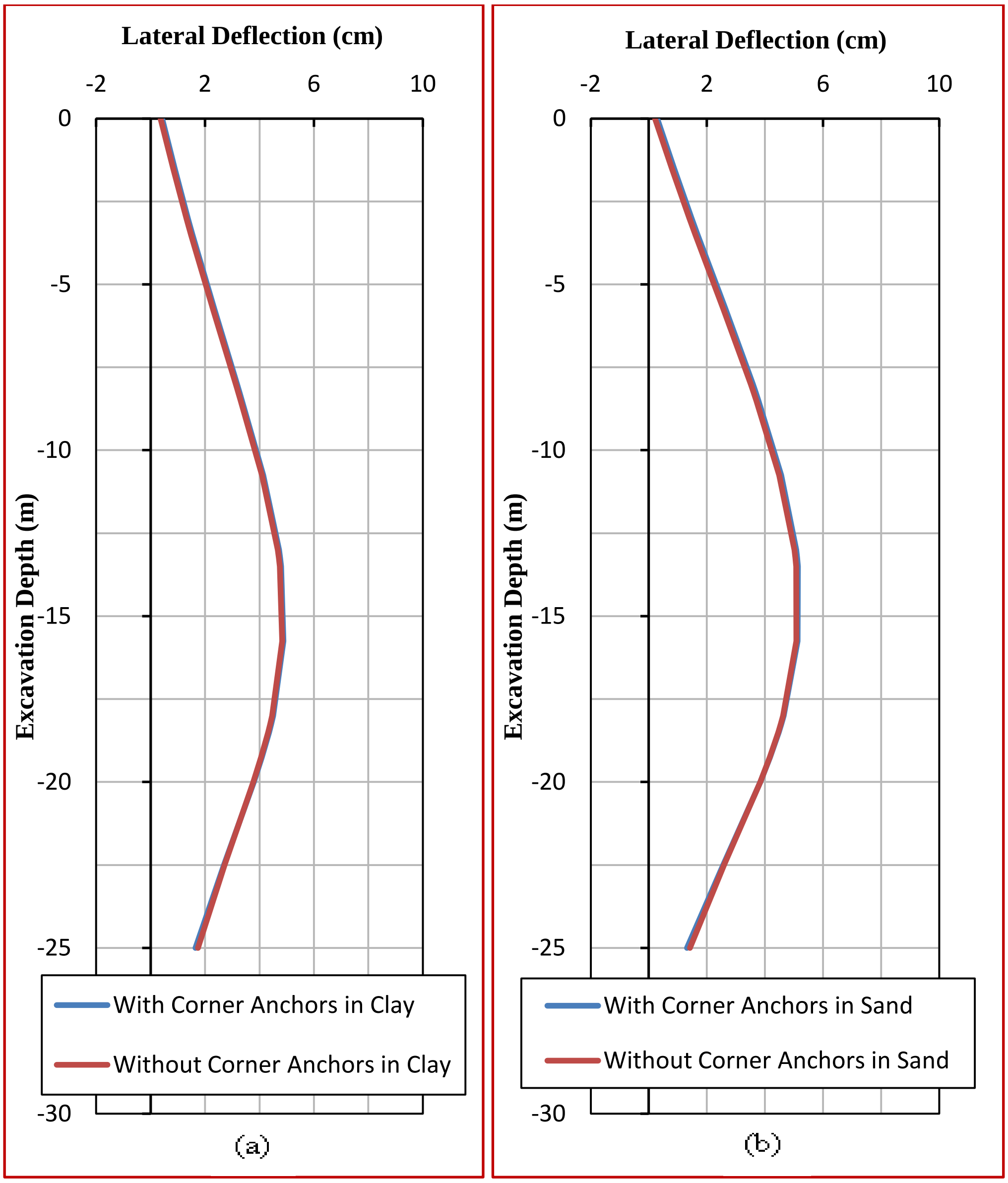

Figure 4.8 Deformation vs. depth graph for with and without corner anchor cases (a) in clay and (b) in sand.

For both soil conditions, the anchor-supported wall with and without corner anchors gives very similar conditions. Therefore, the stabilizing effect of the corner was observed on deflection and moment by these analyses results.

Table 4.1 Maximum Deflection and Maximum Moment For Anchor-supported Analyses

Soil Type		Maximum Deflection	Maximum Moment
Ankara Clay	With Full Anchors	48.77 mm	593.70 kN.m/m
	With Missing Anchors	48.33 mm	582.10 kN.m/m
Sand	With Full Anchors	51.38 mm	585.06 kN.m/m
	With Missing Anchors	50.78 mm	591.40 kN.m/m

As can be seen from Table 4.1 and Figure 4.8, the results are quite similar to each other. Maximum lateral deformation is 51.38mm for sand while the deformation is 48.77mm for clay. This shows that removal of the corner anchors did not have any significant effect.

4.2.2 Strut-Supported Excavations

After the completion of anchor-supported analyses, strut-supported models were constructed to investigate three dimensional behavior of braced excavations and to study the performance of arch-supported bracing.

In order to be able to compare the performance between strut and arch-supported bracings, excavation area in all models is selected as square shaped and normal type strut-supported beams were modeled as corner struts.

Throughout the study, some parametric variables were selected in order to perform several analyses with a purpose of observing behavior. A list of the analyzed cases is given in Table 4.2.

Table 4.2 Performed analyses for strut-supported excavations

CLAY		SAND	
(A) SUPPORT SPACING : 4/9/13/16.5 m			
EXC. WIDTH	**SURCHARGE**	**EXC. WIDTH**	**SURCHARGE**
20 m	-	20 m	-
20 m	100 kPa	20 m	100 kPa
20 m	200 kPa	20 m	200 kPa
30 m	-	30 m	-
(B)SUPPORT SPACING : 3.5/8/11.5/14.5/17 m			
EXC. WIDTH	**SURCHARGE**	**EXC. WIDTH**	**SURCHARGE**
30 m	-	30 m	-
30 m	100 kPa	30 m	100 kPa
30 m	200 kPa	30 m	200 kPa
(C)SUPPORT SPACING : 3.5/8/11.5/14.5/17 m			
EXC. WIDTH	**SURCHARGE**	**EXC. WIDTH**	**SURCHARGE**
30 m	-	30 m	-
30 m	100 kPa	30 m	100 kPa
30 m	200 kPa	30 m	200 kPa
50 m	-	50 m	-
50 m	100 kPa	50 m	100 kPa
50 m	200 kPa	50 m	200 kPa

As it can be seen from Table 4.2, half of the analyses were conducted for sandy soil condition while the rest of them were for clayey soil. Other parameters can be summarized as excavation width, support depth and presence of surcharge loading.

For clayey soil cases; the combination of 20x20m excavation width, support depth set of 2D analyses and the absence of surcharge loading will be used for the presentation of lateral wall deflection vs. depth and moment vs. depth responses. The comparison of plane-strain analyses results to 20x20m, 30x30m, and 50x50 m 3D strut-supported excavation models in clay can be seen in Figure 4.9

As can be seen from the results of analyses with variable (Figure 4.9), lateral wall deflection increases with increasing excavation width, on the other hand resultant wall moments were quite close to each other. On the other hand, such in results of anchor-supported excavation cases, in plane-strain analyses larger wall deflection and moment values were observed. Only clay results were illustrated here in Figure 4.9 but sandy soil gives similar results and can be examined in Appendix A.4.

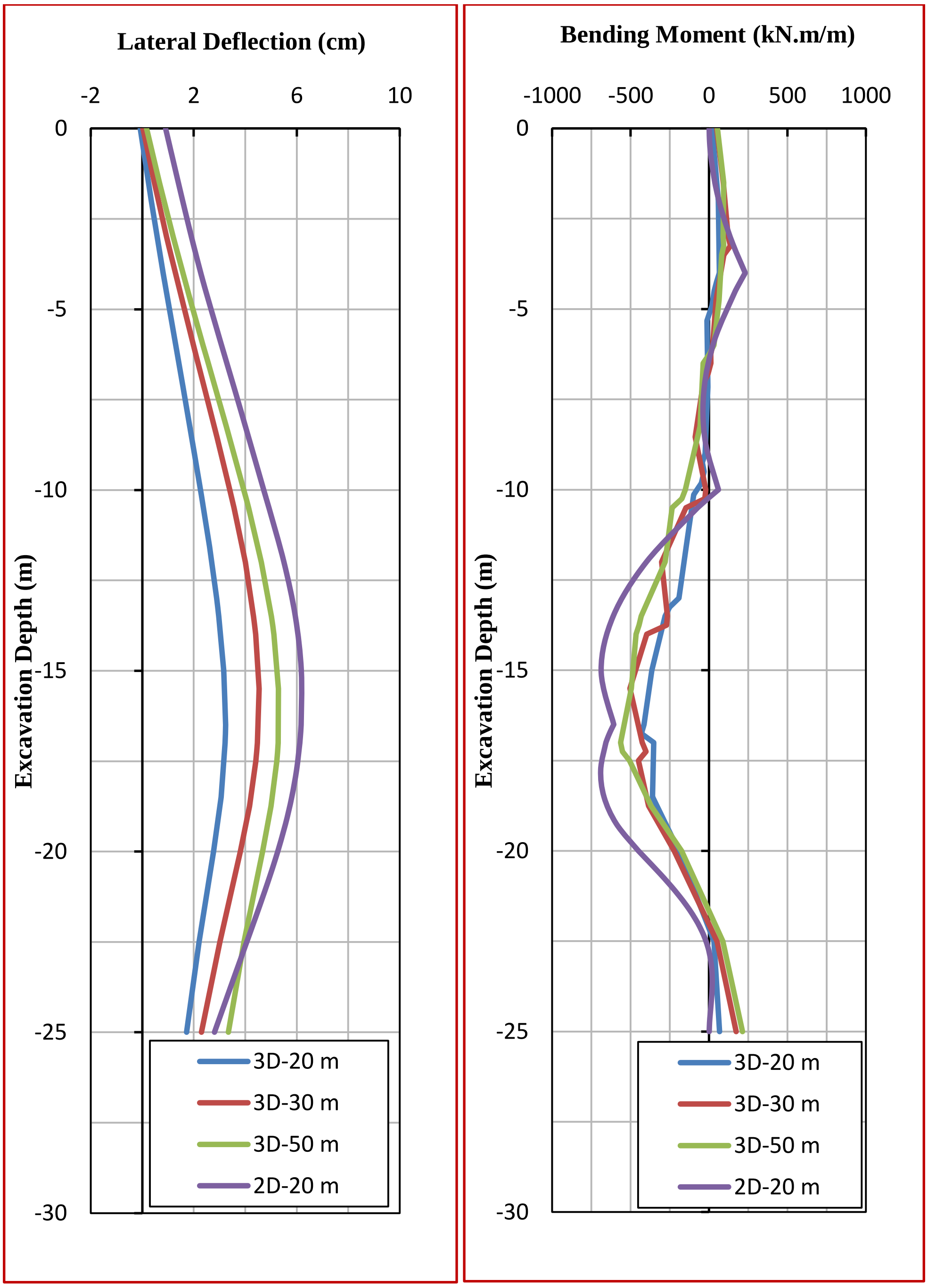

Figure 4.9 Wall deformation and moment vs. depth diagram of 20x20 m strut-supported excavation in plane-strain and 20x20 m, 30x30 m and 50x50 m in 3D analyses results with no surcharge in clay

Comparison of axial force values in the struts of the 20x20 m strut-supported excavation in plane-strain and 3D finite element analyses were shown in Figure 4.10. Axial force results are higher in plane-strain at first and second support point with respect to three dimensional analyses. But as the excavation depth increases, at third support point, the axial force of strut beam is almost equal in 2D and 3D results. The results of axial forces plane-strain vs. 3D in sand is shown in Appendix A.5.

Just like in three dimensional anchor-supported excavation models, 50x50 cm reinforced concrete walers were defined as beam elements. Three dimensional models with pile cap provide smaller deflection around ground level in 3D solutions. In order to monitor the effect of pile cap better on wall deflection results, the analyses with and without 80x80 cm pile cap were performed in 3D models. In Figure 4.11 deflection vs. depth graphs were shown for the pile cap variable both for no surcharge and 200 kPa surcharge applied cases. The presence of pile cap was not important cases with no surcharge as shown in Figure 4.11a. Lateral wall deflections results taken from models with pile cap were similar to ones with without pile cap. But, as can be observed from the Figure 4.11b, presence of pile cap in cases with surcharge has great effect on wall deflection. Smaller deflection values were observed in analysis with pile cap till half of the excavation depth in analysis performed with 200kPa surface loading. Similar results were observed in analyses repeated in sandy soil. (Appendix A.6)

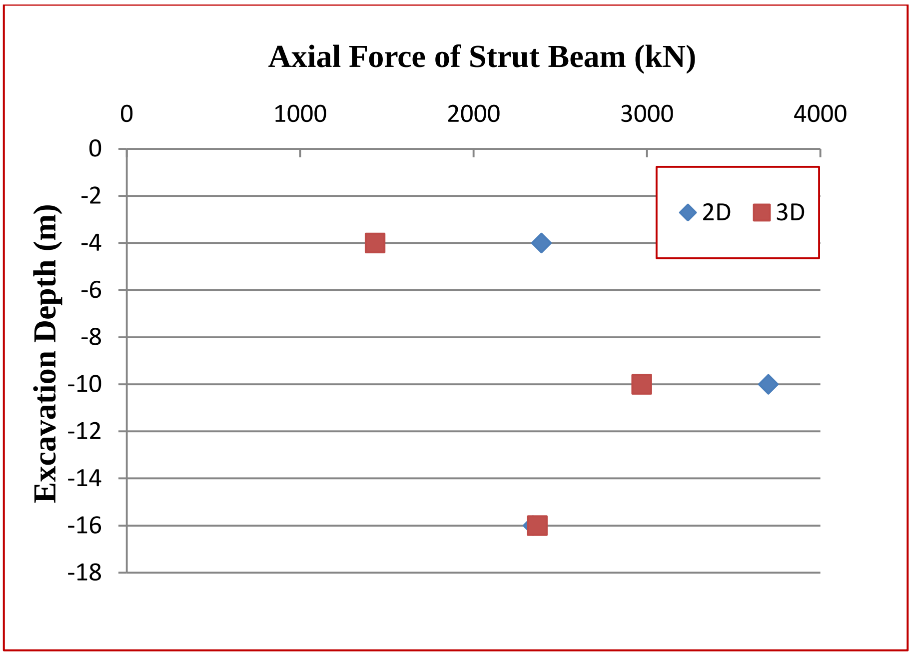

Figure 4.10 Results of axial force of strut-supported beam in plane-strain and 3D analysis for 20x20 m excavation in clay

Three different surcharge loadings were performed with different support location alternatives for 20 m, 30 m and 50 m excavation width. The comparative lateral wall deflection and moment results of different surcharge loading in 30x30 m width rut-supported excavation can be observed in Figure 4.12.

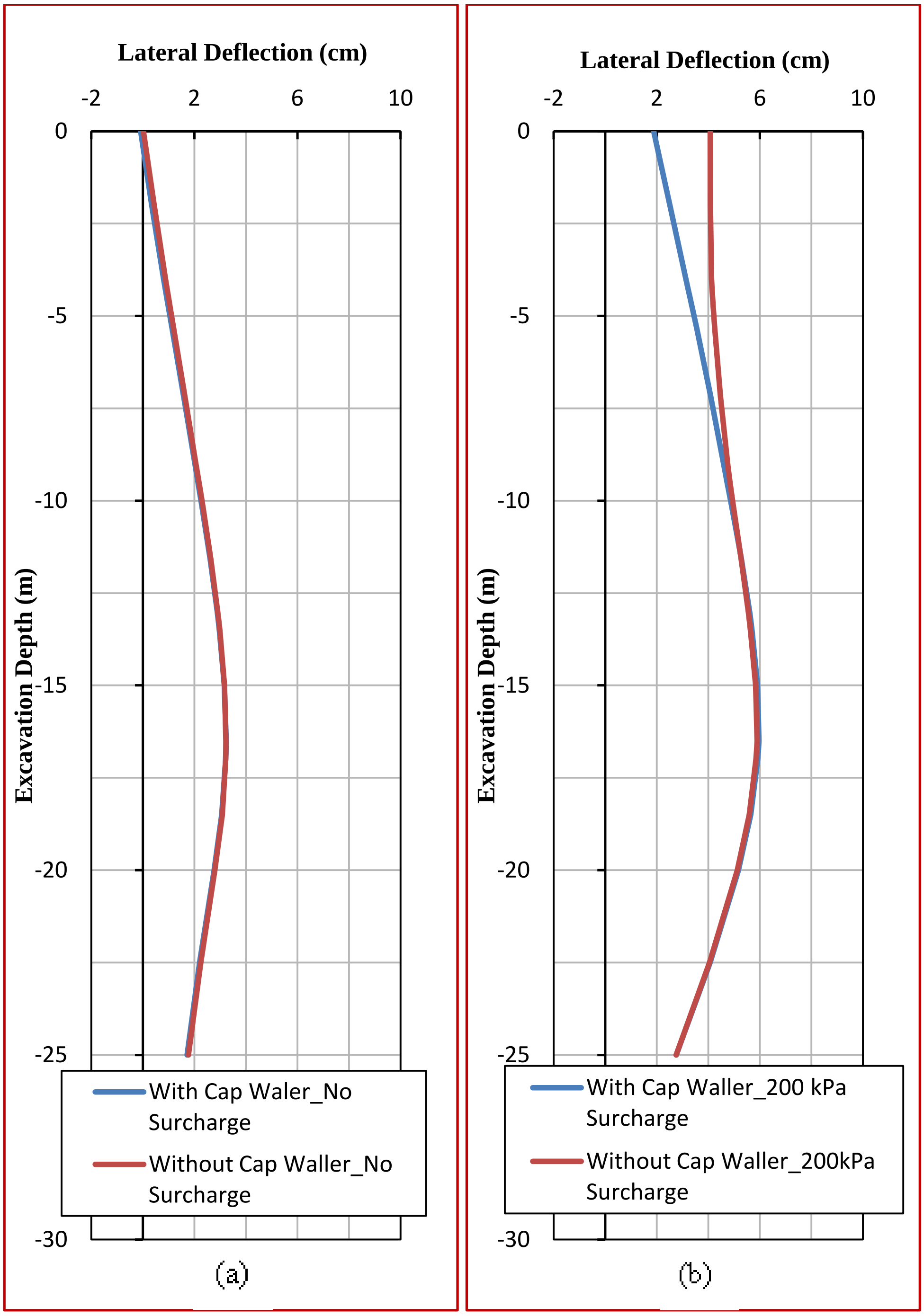

Figure 4.11 The effect of presence of pile cap on strut-supported excavation with no surcharge and 200kPa Surcharge for 20x20 m excavation in clay

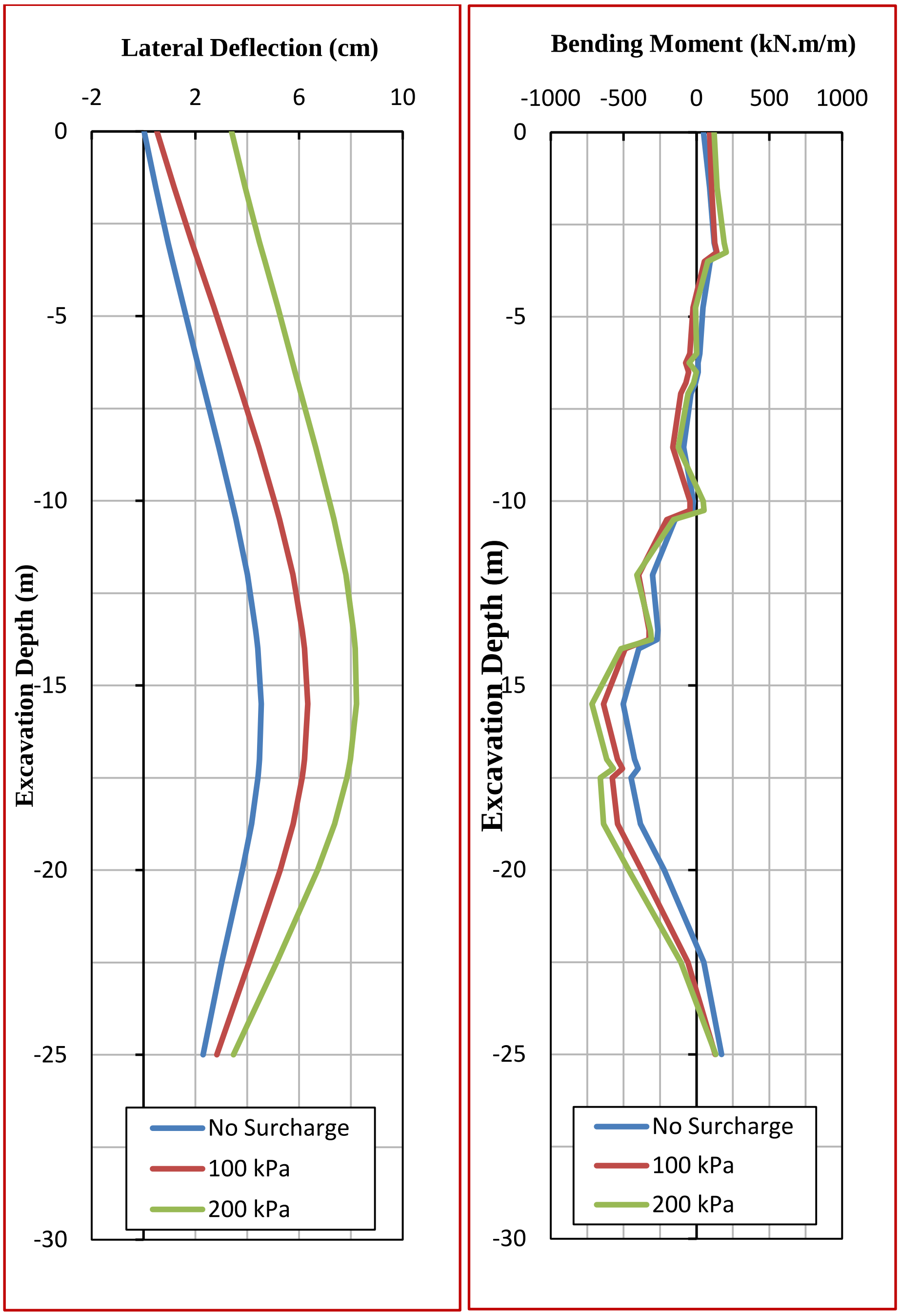

Figure 4.12 Wall deformation and moment vs. depth diagram of 30x30 m (B) strut-supported excavation with surcharge variable in clay

It was observed from Figure 4.12 that, with increasing surface loading, the supporting wall logically displays larger lateral deflection and moment values. Same is true for 30x30 m width excavation in sand with surcharge variable.(Appendix A.7)

4.2.3 Arch-Supported Excavations

The primary objective of research is to investigate the performance of arch-shaped supports with respect to corner struts, on this account, parameters like excavation area and depth, soil type, support spacing and strut-supported beam section were taken same as strut-supported analyses.

All the analyses related to strut-supported excavations were also repeated for arch shaped struts in order to be able to monitor the performance differences.

Parameters that were varied during the parametric studies for arch-shaped supports are tabulated in Table 4.3. As shown, half of 36 analyses were performed in Ankara clay and the rest in sand.

Table 4.3 Performed Analyses For Arch Shaped Strut-supported Excavations

CLAY			**SAND**		
(A)SUPPORT SPACING : 4/9/13/16.5 m					
EXC. WIDTH	**SURCHARGE**	**ARC-SUPPORT TYPE**	**EXC. WIDTH**	**SURCHARGE**	**ARC-SUPPORT TYPE**
20 m	-	CIRCULAR (*)	20 m	-	ROUND
20 m	-	PARABOLIC(**)	20 m	-	PARABOLIC
20 m	-	TIE BAR MOD. (***)	20 m	-	TIE BAR
20 m	100 kPa	PARABOLIC	20 m	100 kPa	PARABOLIC
20 m	200 kPa	PARABOLIC	20 m	200 kPa	PARABOLIC
30 m	-	PARABOLIC	30 m	-	PARABOLIC
(B)SUPPORT SPACING : 3.5/8/11.5/14.5/17 m					
EXC. WIDTH	**SURCHARGE**	**ARC-SUPPORT TYPE**	**EXC. WIDTH**	**SURCHARGE**	**ARC-SUPPORT TYPE**
30 m	-	PARABOLIC	30 m	-	PARABOLIC
30 m	100 kPa	PARABOLIC	30 m	100 kPa	PARABOLIC
30 m	200 kPa	PARABOLIC	30 m	200 kPa	PARABOLIC
(C)SUPPORT SPACING : 3.5/8/11.5/14.5/17 m					
EXC. WIDTH	**SURCHARGE**	**ARC-SUPPORT TYPE**	**EXC. WIDTH**	**SURCHARGE**	**ARC-SUPPORT TYPE**
30 m	-	PARABOLIC	30 m	-	PARABOLIC
30 m	-	TIE BAR MOD.	30 m	-	TIE BAR MOD.
30 m	100 kPa	PARABOLIC	30 m	100 kPa	PARABOLIC
30 m	200 kPa	PARABOLIC	30 m	200 kPa	PARABOLIC
30 m	200 kPa	TIE BAR MOD.	30 m	200 kPa	TIE BAR MOD.
50 m	-	PARABOLIC	50 m	-	PARABOLIC
50 m	100 kPa	PARABOLIC	50 m	100 kPa	PARABOLIC
50 m	200 kPa	PARABOLIC	50 m	200 kPa	PARABOLIC
50 m	-	TIE BAR MOD.	50 m	-	TIE BAR MOD.

(*)Circular Arch shape developed by 5 pieces of equal length pipe sections like the quarter of 20-sided polygonal section.
(**)Parabolic Arch shape developed by $y= (3/B)x^2 + (B/2)$ parabola
(***) Tie bar connection angle is 90 degrees to each arc-shaped beam section

In first trial, arch shape is developed by five pieces of equal length pipe sections with same internal angle like the quarter of a 20-sided regular polygon. Then, in order to improve the results and to make better use of arch shape, a parabolic arch- shape was built up. Figure 4.13 shows the results taken from strut supported excavation vs. circular arch-supported and parabolic arch-supported excavation by 20x20 m width in Ankara clay. As can be seen from axial load vs. depth graphs, struts take less axial loads and moments than arch-supports. The axial support force vs. depth graph for strut, circular and parabolic arch support for 20 x20 m excavation in sand can be observed in Appendix A.8.

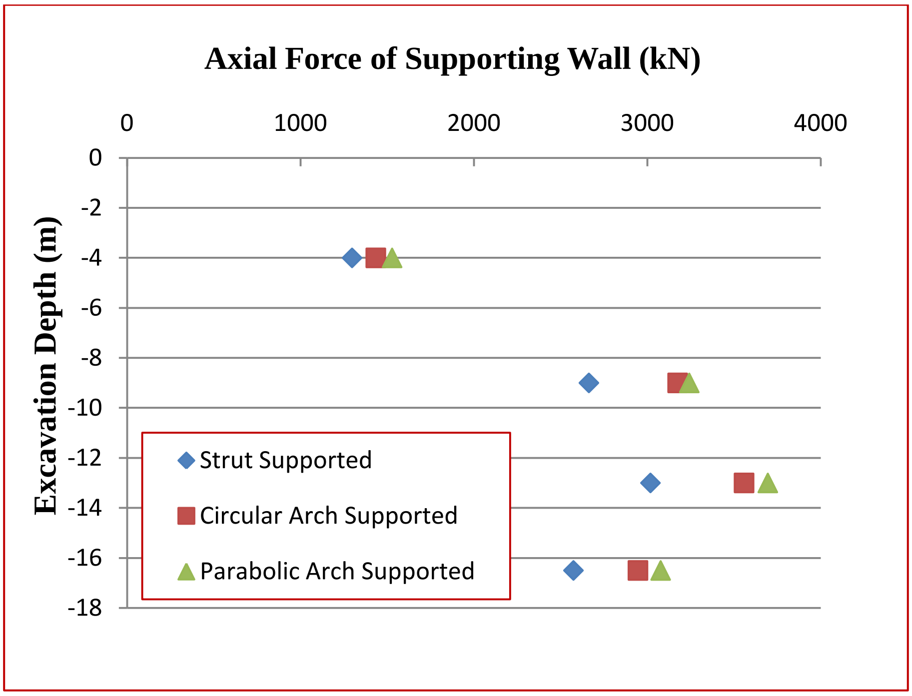

Figure 4.13 Axial support load vs. depth diagram of strut-supported, circular arch-supported and parabolic arch-supported 20x20 m excavation with no surcharge in clay

Parabolic and circular arch supports give similar axial loads, therefore in order to compare the performance of parabolic and circular arch supports, lateral wall deflection and moment vs. depth results were compared. (Figure 4.14) Since parabolic arch supports resulted in slightly better deflection and moment profiles, the remaining arch-supported models employ this parabolic shape. Similar findings were taken from the analysis performed in sand. (Appendix A.9)

Excavation width, support spacing, presence of surcharge loading, arch shape and change in connection angle of tie bar are other parameters which were taken into consideration. Just like in strut-supported analyses 20 m, 30 m and finally 50 m excavation width were considered. Lateral wall deflection and moment profiles of arch supported excavation with variable width and no surcharge were observed. (Figure 4.15) Therefore, as can be seen from Figure 4.15, as the width of the excavation increases, lateral wall deflection and moment values increases logically. Similar results were observed with analyses repeated in sandy soil. (Appendix A.10)

Different surface loading (no surcharge, 100kPa and 200 kPa) was another variable parameter that performed with different support location alternatives for 20x20 m, 30x30 m and 50x50 m excavation width. The lateral wall deflection and moment performance of 30x30 m width excavation along the excavation depth with different surcharge loading can be observed in Figure 4.16. Just like expected, lateral wall deflection and moment performance of 30x30 m width arch-supported excavation increases with increasing surface loading. 30x30 m excavation with different surface loading in sandy soil generated similar results. (Appendix A.11)

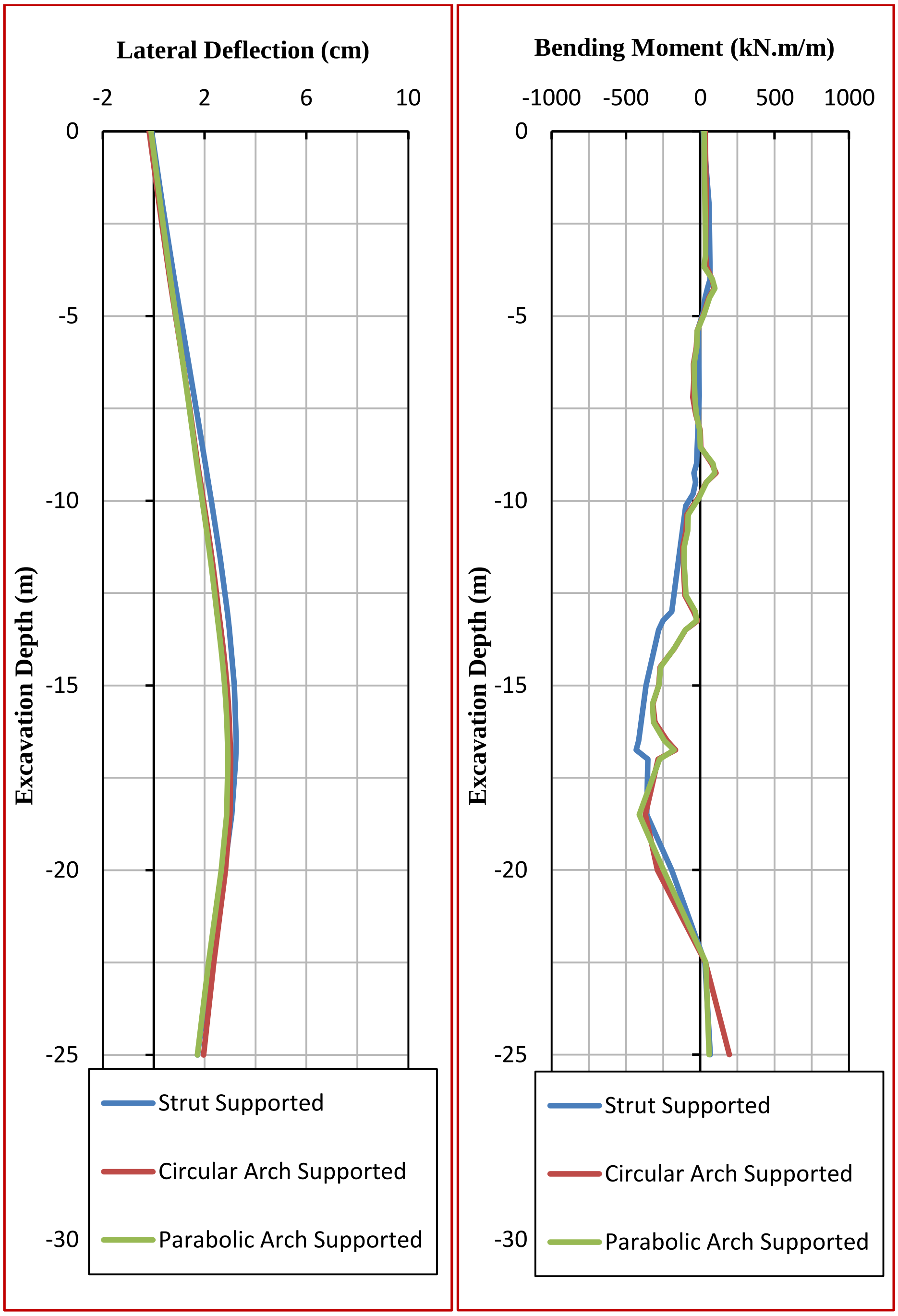

Figure 4.14 Wall deformation and moment vs. depth diagram of strut-supported, arch-supported and parabolic arch-supported 20x20 m excavation without surcharge in clay

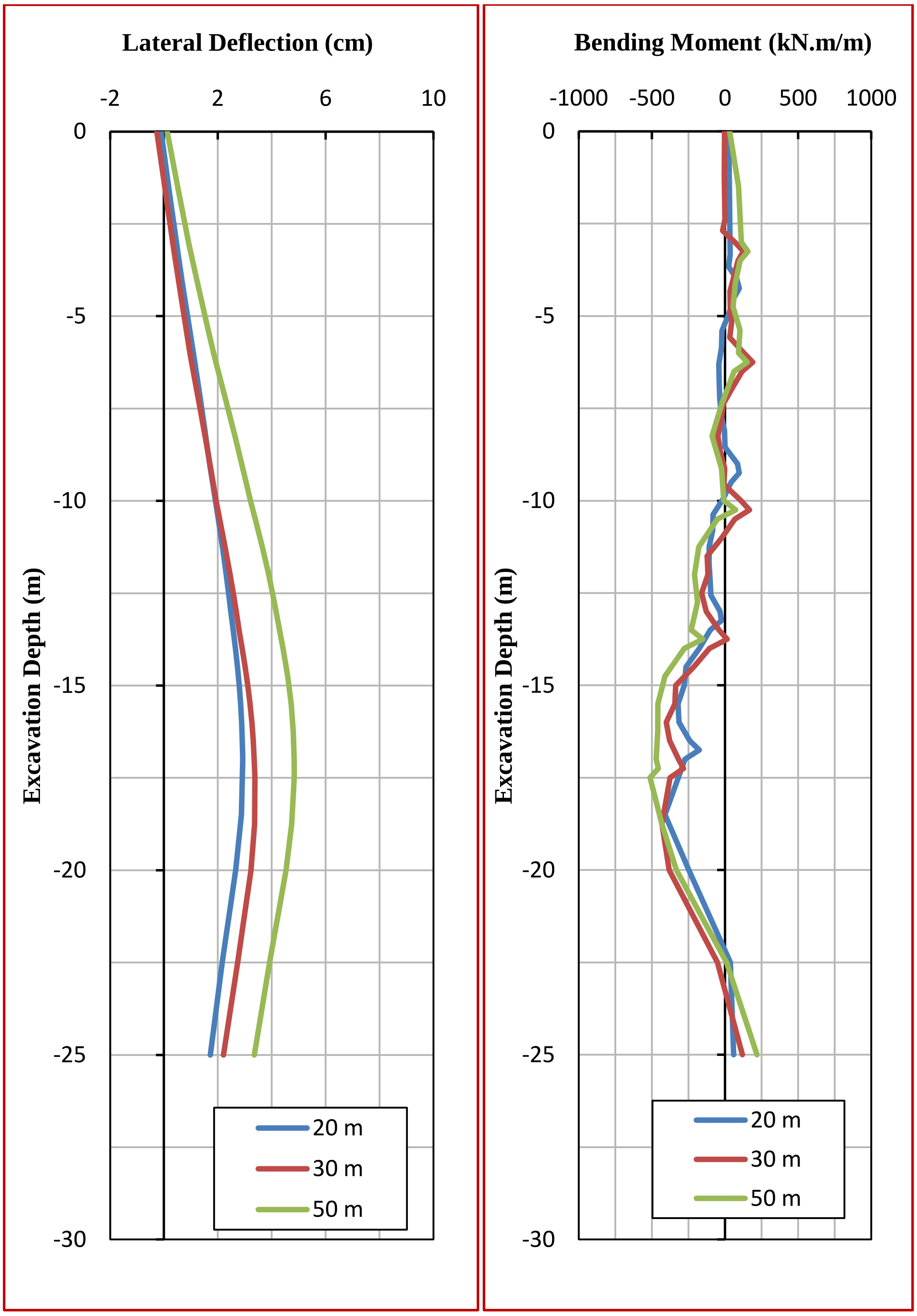

Figure 4.15 Wall deformation and moment vs. depth diagram of arch-supported excavation with varying width and no surcharge in clay

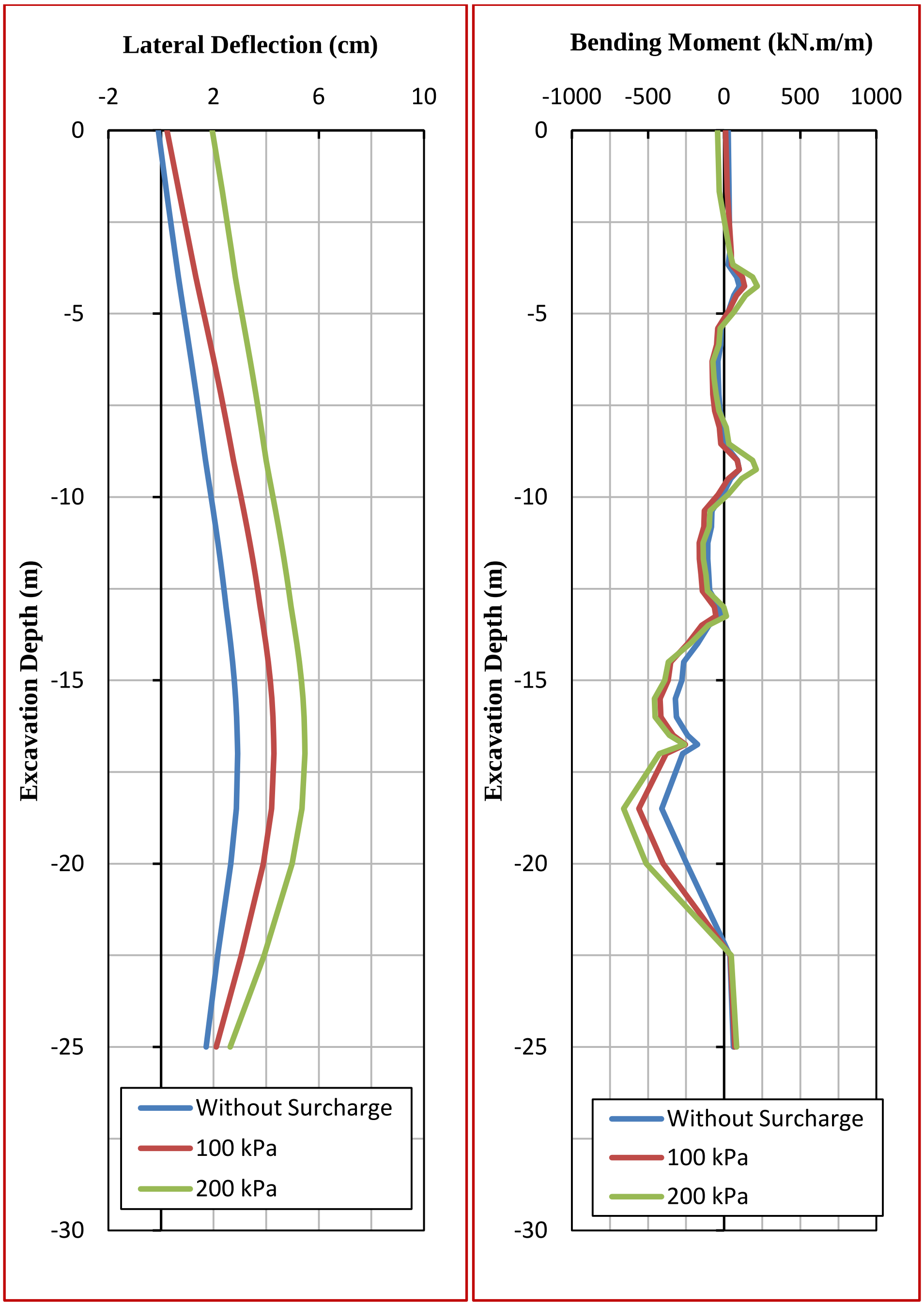

Figure 4.16 Wall deformation and moment vs. depth diagram of arch-supported 30x30 m excavation with surcharge variable in clay

While making analyses with varying excavation width and surcharge, it was observed that arch-supports take greater axial force than the strut cases. Moreover, excessive forces were formed at beam segments in the mid-length of arch. In order to decrease that load, the tie bar support connection angle was changed as described in section 3.6.2. Tie bars were initially connected to waler with an angle of ninety degrees, then connection angle of tie bars were changed with an angle perpendicular to adjacent support as illustrated in Figure 3.15. Due to this modification achieved at tie bar connection angle, the axial force of supports were decreased.(Figure 4.17) However, yield strength of tie bar connection perpendicular to the arch was greater than if they are perpendicular to waler as shown in because of the growing moment. (Figure 4.18) Identical tie bar connection angle modification was repeated in 50x50 m excavation with no surcharge in clay and sand and similar results were taken. The axial force vs. excavation depth and normalized yield stress vs. excavation depth results observed in sandy soil for 30x30 m excavation can be seen in Appendix A.12 and Appendix A.13 respectively.

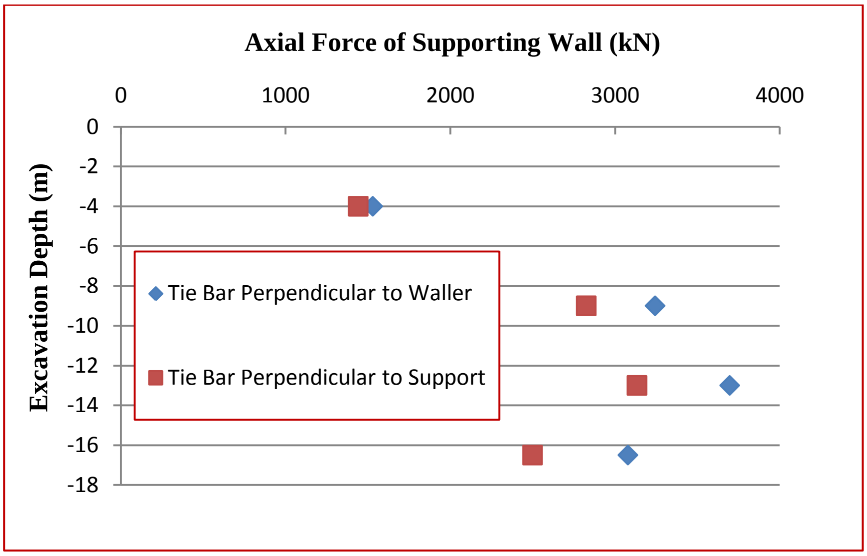

Figure 4.17 Maximum axial force of supports both for two tie bar connection alternatives for 20x20 m excavation with no surcharge in clay

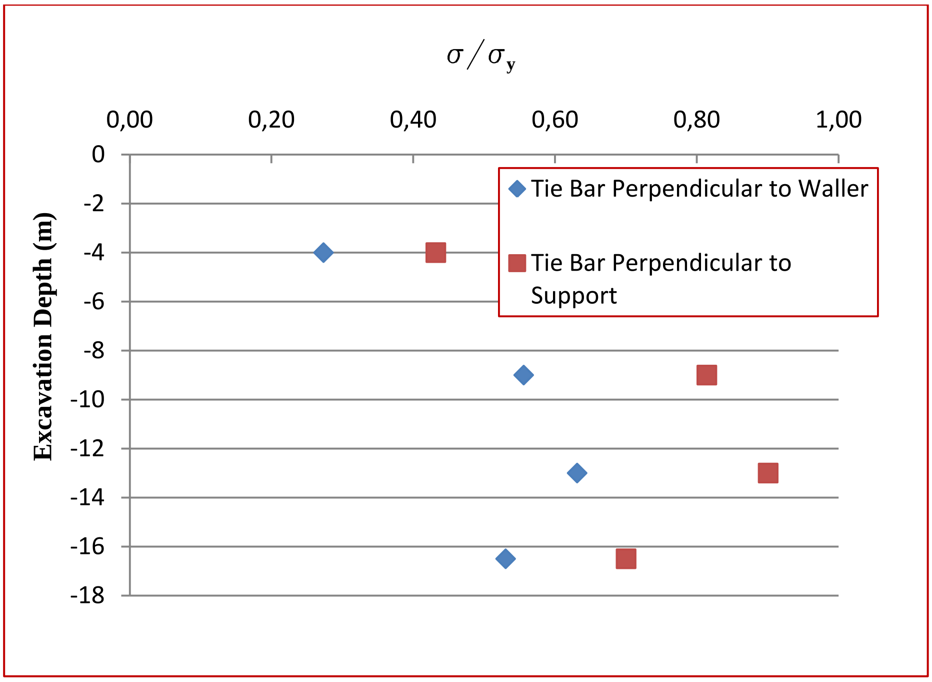

Figure 4.18 Normalized yield stress of supports vs. excavation depth both for two tie bar connection alternatives for 20x20 m excavation with no surcharge in clay

4.3 Comparison of Anchor-Supports with Other Supports in 3D

20 m wide square excavation with 20 m depth was intended to be retained both with anchored and braced supporting system. Lateral wall deflection and moment values of each three optimized retaining system were observed. Accordingly, anchor-supported walls exhibits considerably higher wall moment and lateral wall deformation values than braced supporting systems.(Figure 4.19) Just like analysis performed in clay, anchored supporting systems designated larger lateral wall deformation and moment values along excavation depth. (Appendix A.14)

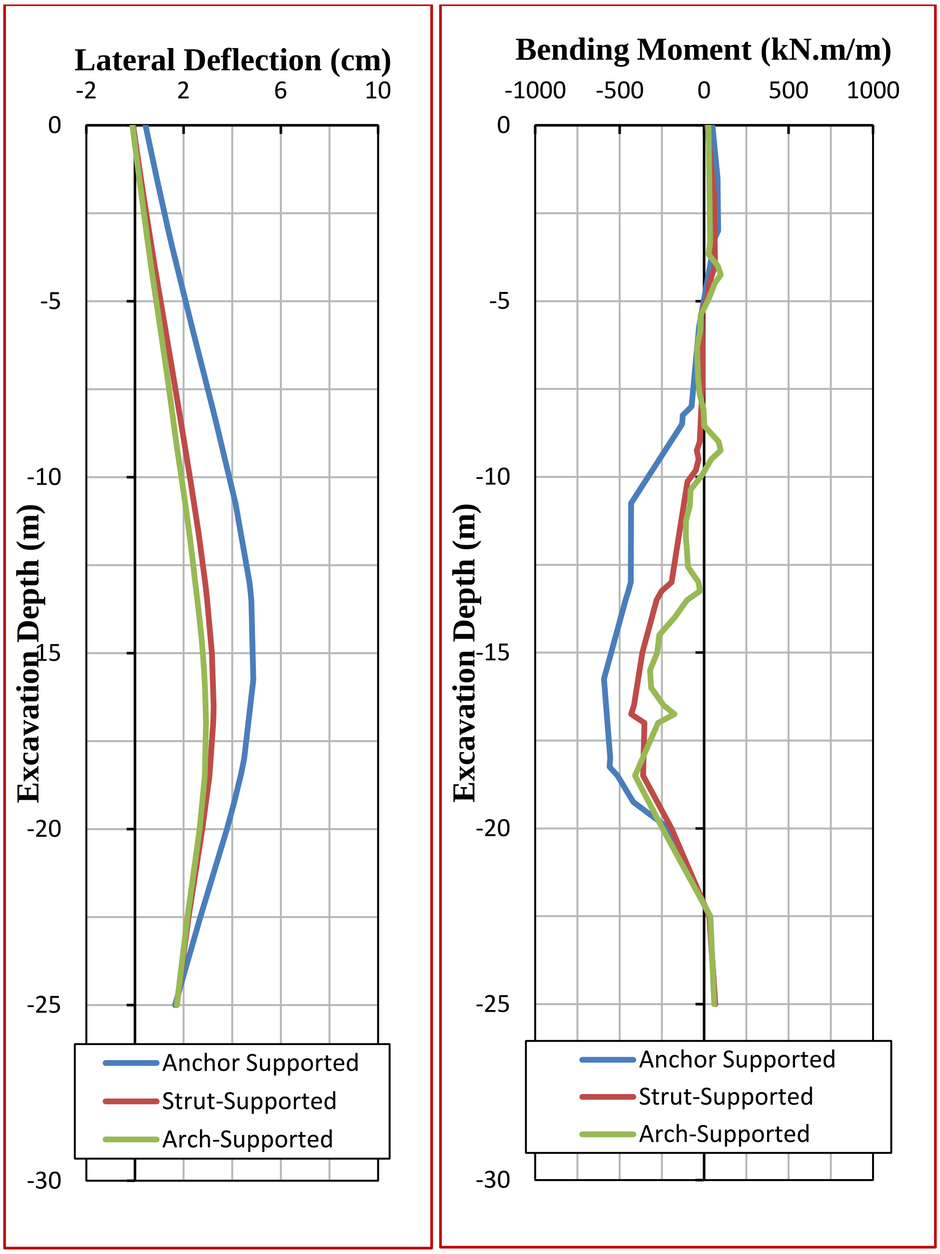

Figure 4.19 Wall deformation and moment vs. depth diagram of anchor-supported vs. strut-supported and arch-supported 20x20 m wide excavation in clay

4.4 Comparison of Arch-Supported and Strut-Supported Analyses in 3D

Upon the completion of comparison of lateral wall deflection between anchor-supported and strut supported excavations, it was concluded that strut system is superior to anchor-supported system. Thus, it was decided to perform comparative analyses of proposed arch-supported system with respect to strut-supported system.

In comparison, it was remarkably arranged to use supporting beams with same cross sections. Firstly, strut-supported 20x20 m wide excavation without surcharge was compared to parabolic-arch supported excavation (Figure 4.19). Smaller lateral wall deformation and moment values were observed in arch-supporting excavation along the excavation depth with respect to strut supported excavation. Same observation were taken from the analyses performed in sand.(Appendix A.14)

On the other hand, strut supports resulted in better results than arch-supports in terms of normalized yield stress. (Figure 4.20) Analyses performed in sand also give very similar results to clay and that findings can be visualized in Appendix A.15.

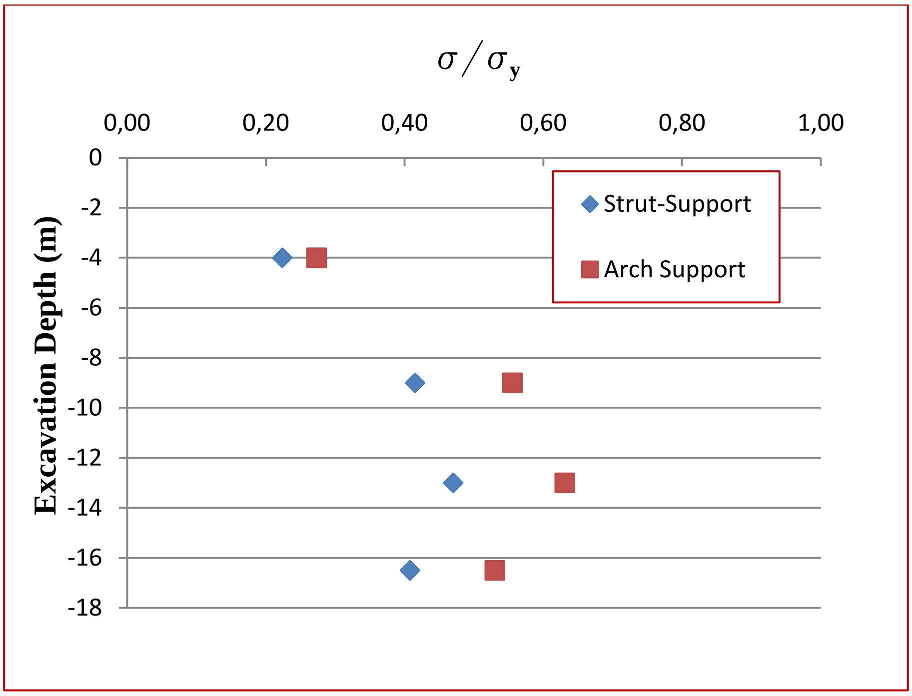

Figure 4.20 Normalized yield stress values for strut and arch supported 20x20 m wide excavation without surcharge in clay

After performing analysis without surface loading, the performance of arch supported system with respect to strut supported excavation was questioned. 100kPa and 200 kPa surface loading were applied on 20x20 m wide excavation case. It was observed that 20x20 m wide excavation with 200 kPa surcharge in clay exhibited similar deformation behavior compared to the ones without surcharge.(Figure 4.21) Both deformation and moment values increased, but still arch-supported walls exhibit smaller deformation and moment values than strut supported walls. Lateral wall deformation and moment profiles of 20x20 m wide excavation with 200 kPa surcharge in sand resulted in similar behavior projected in clay. (Appendix A.16)

However, similar to 20x20 m wide excavations without surface loading, normalized yield stress of arch-supports were higher with respect to strut supports, which increases cross-sectional requirement of supporting beam. (Figure 4.22) Higher normalized yield stress was observed in arch-supported excavations performed in sand with respect to strut supported systems. (Appendix A.17)

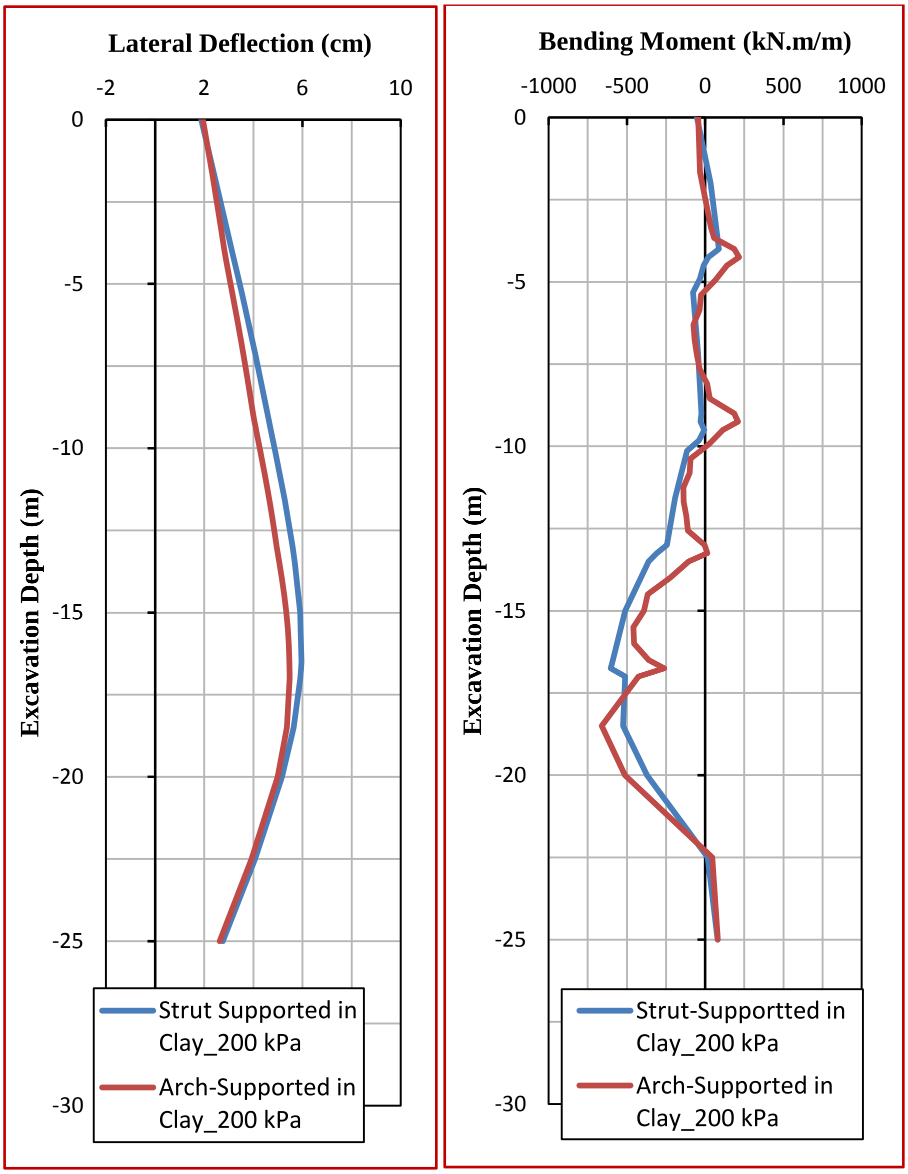

Figure 4.21 Wall deformation and moment vs. depth diagram of strut-supported vs. arch-supported excavation with 200 kPa surcharge in clay

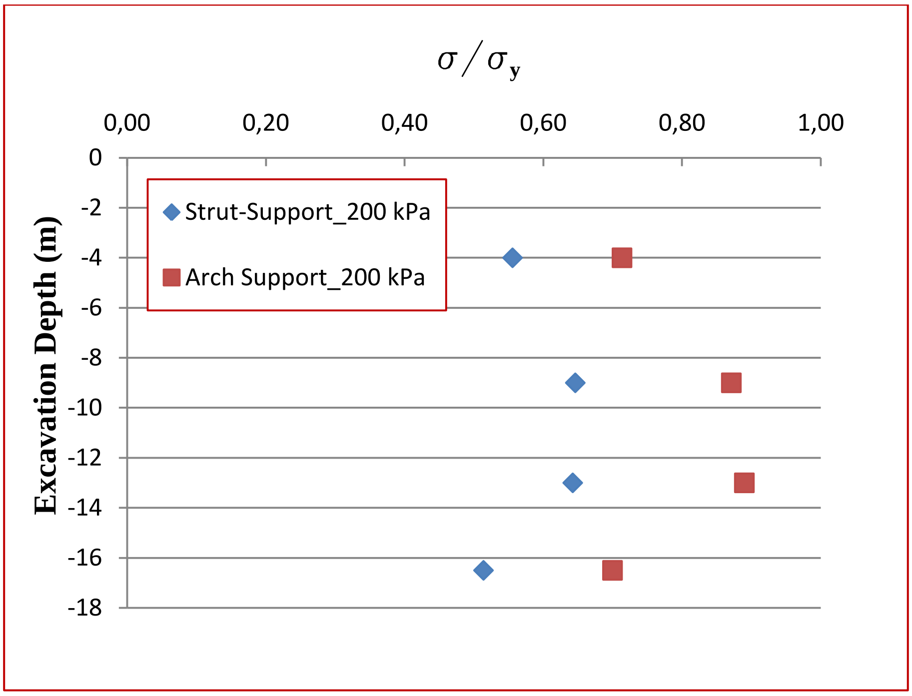

Figure 4.22 Normalized yield stress values for strut and arch supports in 20x20 m wide excavation with 200 kPa surcharge in clay

After performing several trials in 20x20 m wide excavation with variable surface loading in clay and sand, it was decided to increase excavation area. Initially, support levels were kept same. Following the study performed on output data of 30 m models, in order to decrease the tributary area of each support which is directly related with the load taken by an individual support, number of support location was increased from four to five (B). And two different support spacing alternatives (B and C) were experienced for five support level in order to monitor the effect of support spacing on stress values constituted on supporting beams. Lateral wall deflection and moment in the arch supported case relative to the strut supported case were shown in Figure 4.23.Just like 30x30 m wide excavation with (A) type support spacing, arch supported excavation gives smaller lateral wall deflection and moment values than strut supported excavation. However, as shown in Figure 4.24 precisely, increasing support points improved the result of normalized yield stress of supporting beams in 30x30 m width excavation cases and support spacing alternative (B) governs alternative (C). But there still exits less stress on strut supports than arch-supports. Similar lateral wall deformation and wall vs. excavation depth and normalized beam stress values occurred in 30x30 m wide excavations performed in sand with no surcharge. (Appendix 18 and Appendix 19)

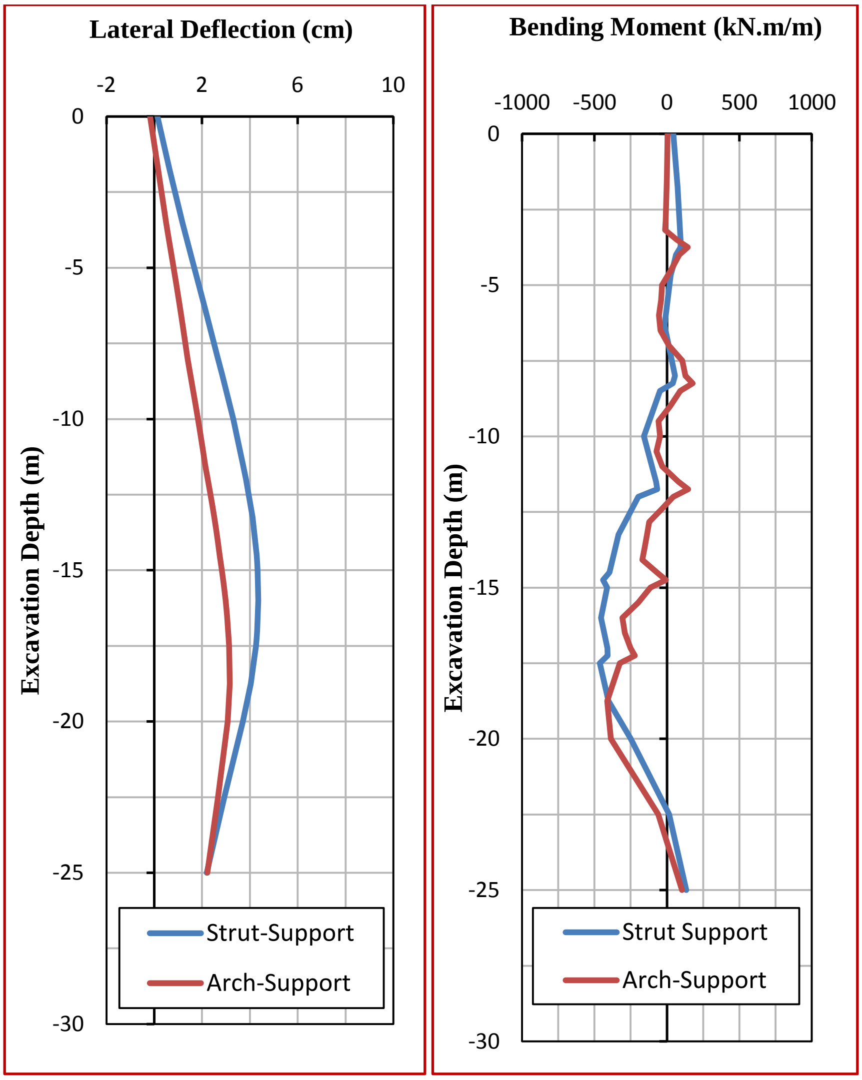

Figure 4.23 Wall deformation and moment vs. depth diagram of strut-supported vs. arch-supported 30x30 m wide excavation without surcharge in clay for (B) support spacing

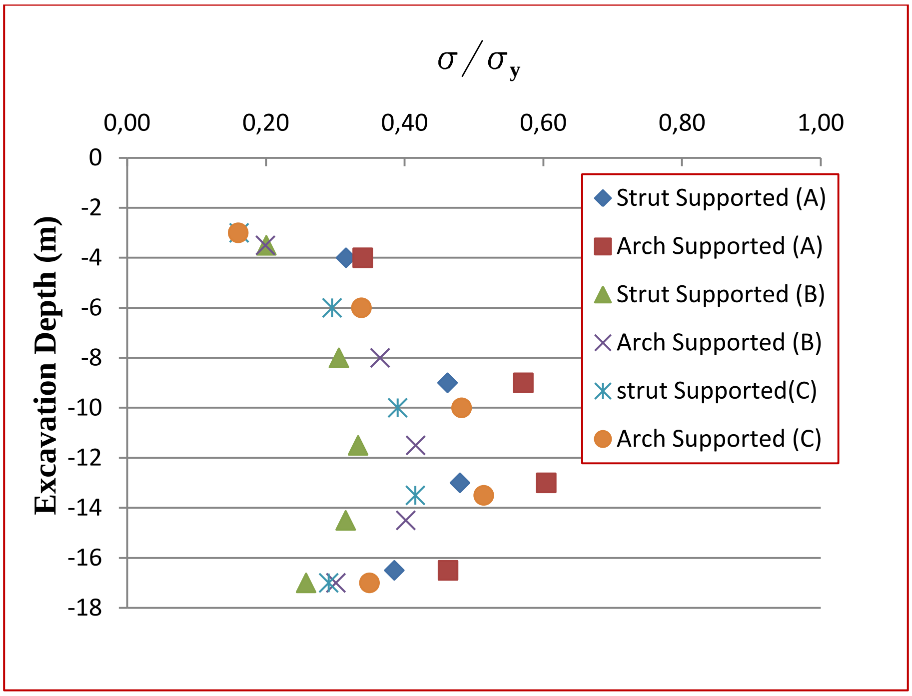

Figure 4.24 Normalized yield stress values for strut and arch supports in 30 x30 m wide excavation without surcharge for two support spacing combinations (A, B and C) in clay

After finishing comperative study between arch-supported and strut supported 30x30 m wide excavation, the analyses performed in 50x50 m wide excavation with surcharge variable was investigated. Since excavation width increased excessively, plan ratio of arch-supported construction area is increased with respect to strut-supported excavation (two bench of corner struts used in each support level.) Similar to analyses performed in 20x20 m wide excavation, lateral wall deflection and moment values of arch-supported excavation governs the results of strut supported excavations.(Figure 4.25) And, as the excavation width increases and with the presence of surface loads, difference in the lateral wall deformation values between strut and arch supported excavation increases. Similar results were observed for 50x50 m wide excavations in sand. (Appendix A.20)

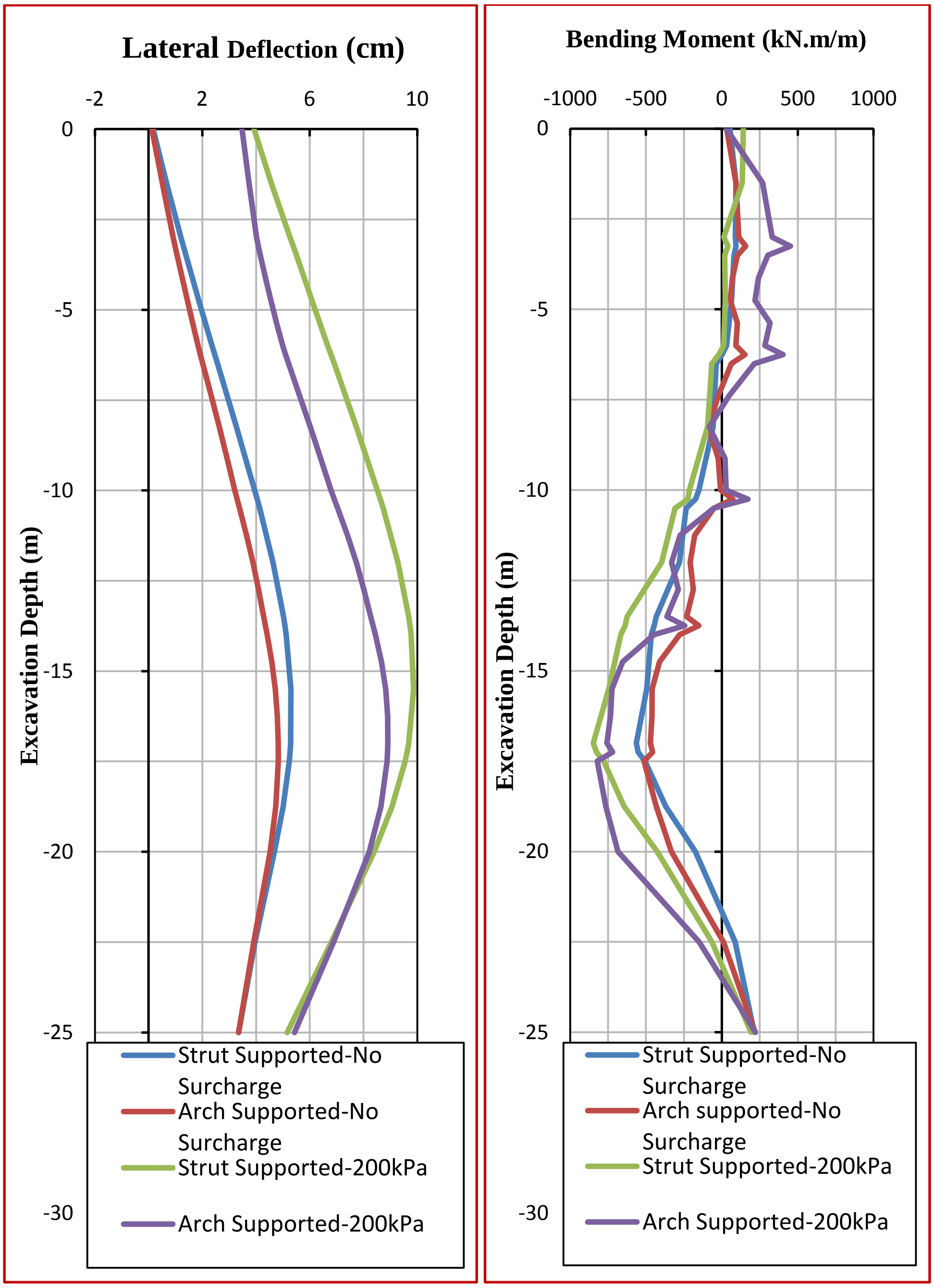

Figure 4.25 Wall deformation and moment vs. depth diagram of strut-supported vs. arch-supported 50x50 m wide excavation in clay with and without surcharge load

4.5 Cost Estimation and Feasibility Study

Cost analyses were performed for arch-supported and strut-supported retaining systems in order to compare two systems in terms of economy. 20x20 m excavation plan area without surface loading and 50x50 m excavation plan area with 200 kPa surcharge were selected as model excavations in clay. The two support systems were designed once more for each case such that the maximum horizontal deflection of the retaining wall is equal in the strut-supported and arch-supported options. The costs of the two options were compared for these two final designs that allow the same horizontal deflection, even though the strut supports hinder the construction area more.

In 50x50 m excavation analysis, other than parametric study, the number of strut beams was changed from two corner struts to three at each support level.(Figure 4.26) The reason for this change is that the system with two corner support beams was not capable to decrease the lateral wall deflection to that of arch-supported excavation. It should be noted that adding a third strut results in further hindrance of the construction space.

For same lateral wall deflection values, pile moment values were very close to each other, therefore pile reinforcement cost were estimated same both for strut and arch supported cases. Consequently, total weight of supporting beams and welding are the only factors affecting relative cost of the two systems. Material price of circular pipe section were taken as 1260 TL/ton, and 270 TL/ton were taken for welding, in the cost calculations.

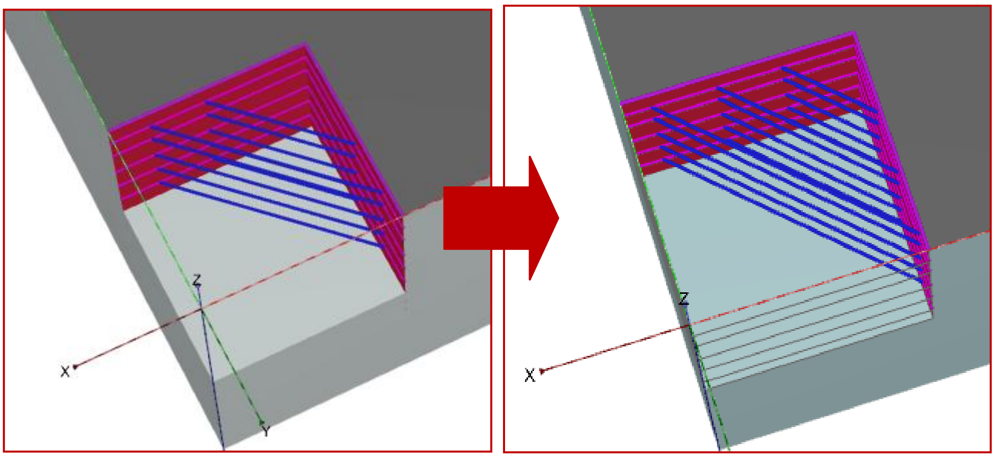

Figure 4.26 Geometry change of supporting beams in 50x50 m excavation in clay for cost estimation

The results of cost estimation is tabulated in Table 4.4 below. The total weight of arch-supported excavations were higher than strut supported excavations. Moreover, welding workmanship of arch supported excavations were more than strut-supported systems. As a result, arch supported excavations were more expensive systems than strut-supported ones.

Table 4.4 Total weight and estimated cost values of 20x20 m excavation without surcharge and 50x50 m excavation with 200kPa surface loading in clay

	SUPPORTING SYSTEM	TOTAL WEIGHT OF SUPPORTING BEAMS (tons)	COST (TL)
20x20 m	STRUT	7	8820
	ARCH	11	16830
50x50 m with 200kPa surcharge	STRUT	47	59220
	ARCH	79	120870

CHAPTER 5

CONCLUSION AND RECOMMENDATIONS

The aim of this study is to develop a new supporting system for deep excavations and then to compare the performance of conventional anchor and strut supporting systems. To simulate the behavior, several plane-strain and three dimensional analyses were conducted.

5.1 Summary of Observations

While making analysis to observe the fundamental points of the study, following secondary observations were made:

- Horizontal wall deflection, wall bending moment and axial forces in support members were larger in plane-strain analysis, compared to three dimensional analysis.

- Modeling pile cap in 3D decreases the wall deflection in the upper 10 m depth from ground level for the cases with surface loading.

- Retaining wall deflection and bending moment values increase as excavation width and applied surcharge load is increased around the excavation.

Following trends were observed during the studies performed related to anchor supported retaining systems:

- Greater lateral wall deflection values were obtained in anchor supported excavation compared to both strut and arch supported systems.

- Due to the stabilizing effect of the excavation corner, removing the anchors closest to the corner results in almost no change in wall deflection and moment values.

Findings received from comparison of arch-supported excavation with respect to strut-supported systems are listed below:

- If the arch-supports and the struts have the same cross section, lateral deflection observed in arch-supported excavation cases are slightly smaller (up to 13%) compared to strut supported cases, for all excavation width, and surcharge load, around excavation.

- Arch supports take larger stress and axial load values than strut-supported cases. In order to decrease that stress, larger sections should be selected for arch-supports which is not economical.

- Throughout the results taken from the analysis it was observed that the bending moment values in the piles of arch supported retaining systems were smaller than those of anchor and strut supported excavation cases.

- Arch segments were connected to walers by secondary beams called tie bars. It was seen that portion of the arch closest to the corner of the excavation takes high axial loads when tie bars were connected to walers with ninety degrees angle. In order to decrease the axial load on beams, the connection angle of tie bars were changed such that, tie bars are connected with an angle perpendicular to the adjacent arch segment. The change of tie bar connection angle decreases the axial load, but moment values on the arch increased and therefore higher stress values were observed on the arch segments.

- As the excavation width increase, the ratio of useable construction area of arch-supported excavation with respect to strut-supported excavation increase. For example, in 50x50 m width excavation case, the useable construction area of arch-supported excavation is 14.5% larger than strut-supported excavation with the same support cross-sections, and as illustrated in Figure 5.1, 27.0% larger than a strut-support system that allows the same horizontal deflection.

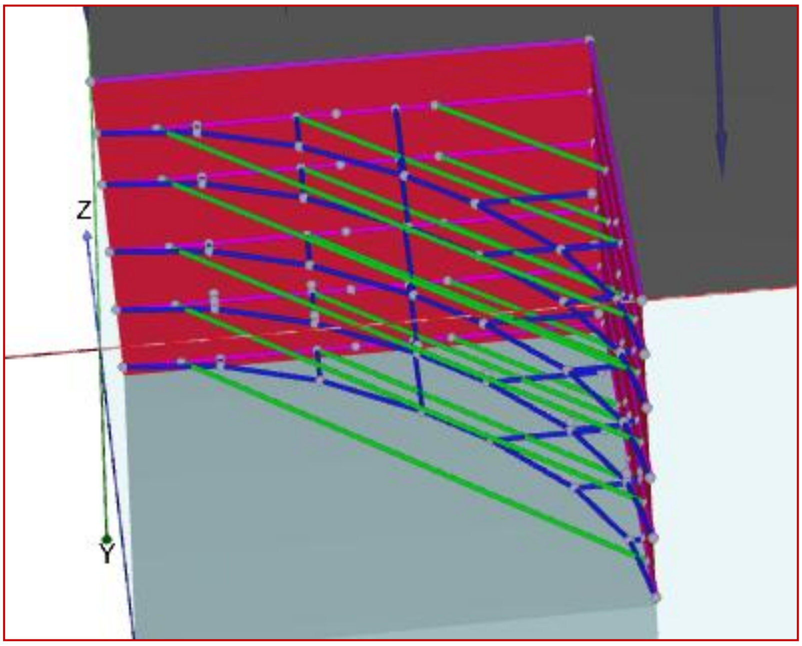

Figure 5.1 Two support systems that give the same maximum horizontal deflection for 50x50 m excavation with 200 kPa surcharge.

- Cost estimation study in arch and strut supported excavations in 20x20 m plan area without surface loading and 50x50 m plan area with 200 kPa surface loading show that arch supported systems are much more expensive than strut supported excavations.

5.2 Conclusion

Arch shape retaining system occupies less construction space and gives slightly smaller deflection and wall moment values than conventional supporting systems. But, except for specific cases, there was not any significant improvement. Thus, as the width of excavation increases or surface loading applied, the arch support results in smaller deflections compared to strut support. For instance, wall deflection reduced up to 18 percent in 50 m width with 200 kPa surface loading. However, larger axial load and stress values were observed in arch-supported beams, which increases cross-sectional requirement of arch supports.

5.3 Recommendations for Future Study

In this study, the primary focus was on structural and geotechnical performance of arch-supported systems on square shaped excavations. However, more detailed investigation may be conducted in terms of following issues;

- Performance of the arch-supported system in rectangular excavation with varying aspect ratios may be studied. Moreover, structural optimization of arch-supported bracing may be studied in detail in terms of parabolic equation of the geometry of bracing beam.

- Economical comparative analysis between strut-supported and arch-supported bracings may be performed in order to come up with the most feasible solution.

- Three dimensional finite element analysis program furnishes to model the geotechnical problems in detail, as was performed in pile cap and corner anchor examples. In several geotechnical problems the advantage of 3D analysis can be used in the future studies.

BIBLIOGRAPHY

Clough, G.W., and O’Rouke, T.D., *Construction Induced Movements of Insitu Walls, Design and Performance of Earth Retaining Structures*, ASCE, 439-470, 1990

Çalışan, O., *Design and Measurements of 30 m Deep Excavation*, Proc. Prof. İsmet Ordemir’i Anma Toplantısı ve 3. ODTÜ Geoteknik Mühendisliği Sempozyumu, 74-81, 2005

European Norm (BS EN 1997-1:2004) Eurocode 7:Geotechnical Design –Part 1:General Rules,European Committee for Standardization, Brussels, 2008

Goldberg, D.T., Jaworski, W.E., Gordon, M.D., *Lateral Support Systems and Underpinning:Volume 1, Design and Construction*, Federal Highway Administration Report FHWA RD-75-128, 1976

Katsura Y. et.al., *Lateral Pressures Acting On Earth Retaining Systems – A Survey On Japanese Literature*, Proceedings of the International Symposium on Underground Construction in Soft Ground, New Delhi, 283-291, 1994

Lambe TW, Turner EK, *Braced Excavations*, Proceedings of the speciality conference on lateral stresses in ground and design of earth retaining structures, ASCE, Cornell University, Ithaca, NY, pp 149-218, 1970

Mana, I.A., and Clough, G.W., *Predictions of Movements For Braced Cuts in Clay*, Journal of Geotechnical Engineering Division, ASCE, Vol. 107, No. GT6, 759-777, 1981

O’Rourke, T. D., *Ground Movements Caused by Braced Excavations*, J. Geotech. Engrg., ASCE, 107(9), 1159-1178, 1981

Ou, C. Y., Hsien. P. G., and Chiou, D. C., *Characteristics of Ground Surface Settlement During Excavation*, Can. Geotech. J., Ottawa, 30, 758-767, 1993

Ou, C.Y., Chiou, D.C., Wu, T.S., *Three-Dimensional Finite Element Analysis of Deep Excavations*, Journal of Geotechnical Engineering, ASCE, Vol. 122, No. 5, 337-345, 1996

Ou. C.Y.,Shiau, B.Y., Wang, I.W., *Three-Dimensional Deformation Behavior of the Taipei National Enterprise Center (TNEC) Excavation Case History*, Canadian Geotechnical Journal, 438-448, 2000

Peck , R.B., *Deep Excavations and Tunneling in Soft Ground*, Proceedings, Seventh I.C.S.M.F.E. State of Art Volume, Mexico, 225-290, 1969

PLAXIS 3D, *Manual*, 2010

Terzaghi, K. and Peck, P.B., *Soil Mechanics in Engineering Practice, 2nd Edition*, John Wiley & Sons, New York, 1967

BS EN 1537:2000 European Standard for Execution of special geotechnical work-Ground Anchors

The Turkish Standard TS EN 1997-1

U.S. Army Corps of Engineers, *Desıgn of Sheet Pıle Walls*, 1994

Ünlü, G., "*Analysis of Corner Effects on In-Situ Walls Supporting Deep Excavations: Comparison of Plane-strain and Three Dimensional Analysis"*, Master of Science Dissertation in Civil Engineering, METU, Ankara, 2008

Watanabe, T., *Lecture-Earth Retaining Design (in JSCE)*, JSSMFE, Vol.28, No.9, pp.61-66, 1980

Whittle, A.J., Hashash, Y. M. A., *Analysis of Behaviour of Propped Diaphragm Walls in Deep Clay Deposit*, Retaining Structures, Thomas Telford, London, 1993

Wong, I. H., Poh, T. Y., and Chuah H. L., *Performance of Excavation For Depressed Expressway in Singapore,* J. Geotech. And Geoenvir. Engrg., ASCE, 123(7), 617-625, 1997

Wong, K.S.,and Broms, B.B., Lateral Wall Deflections of Braced Excavations in Clay, Journal of Geotechnical Engineering, ASCE, 115(6), 853-870, 1989

APPENDIX A

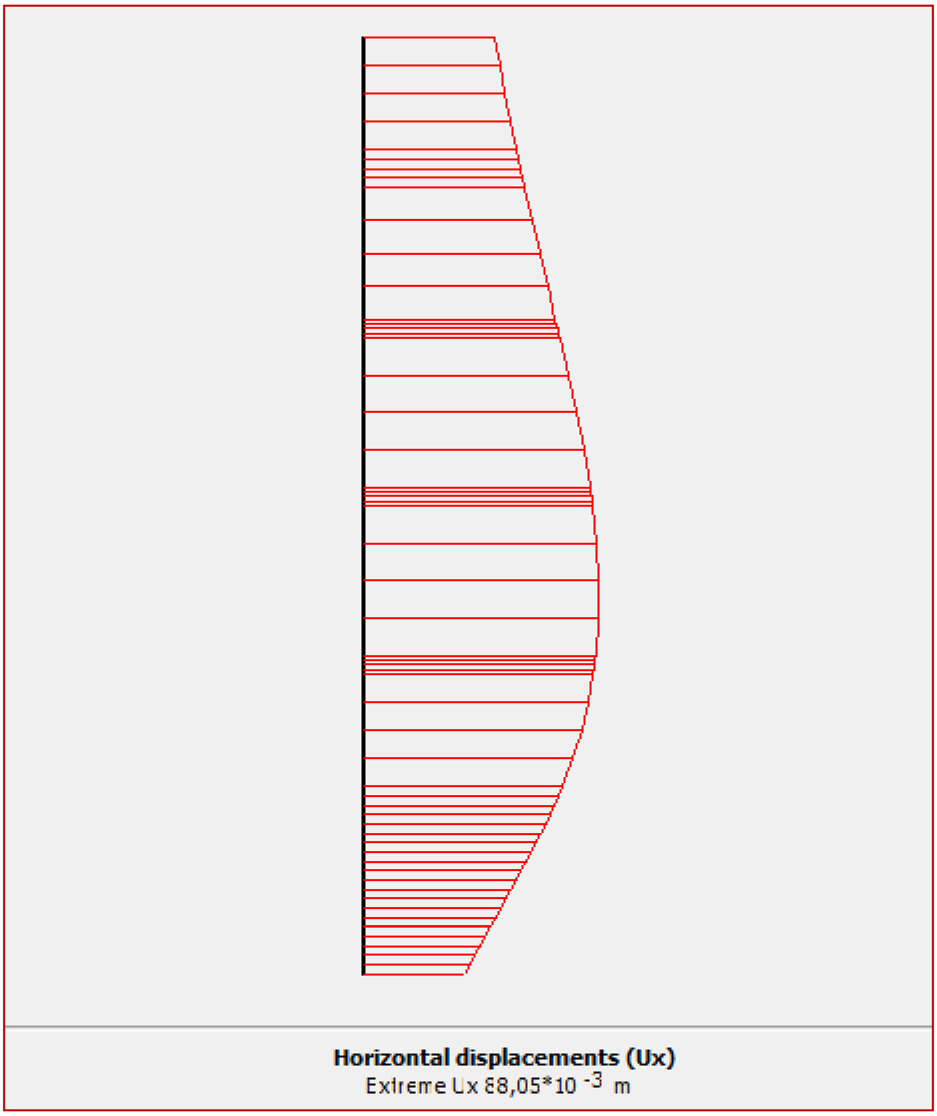

Figure A.1 Deflected Shape of supporting wall with anchors in sand

Figure A.2 Deflected shape of supporting wall with struts in sand.

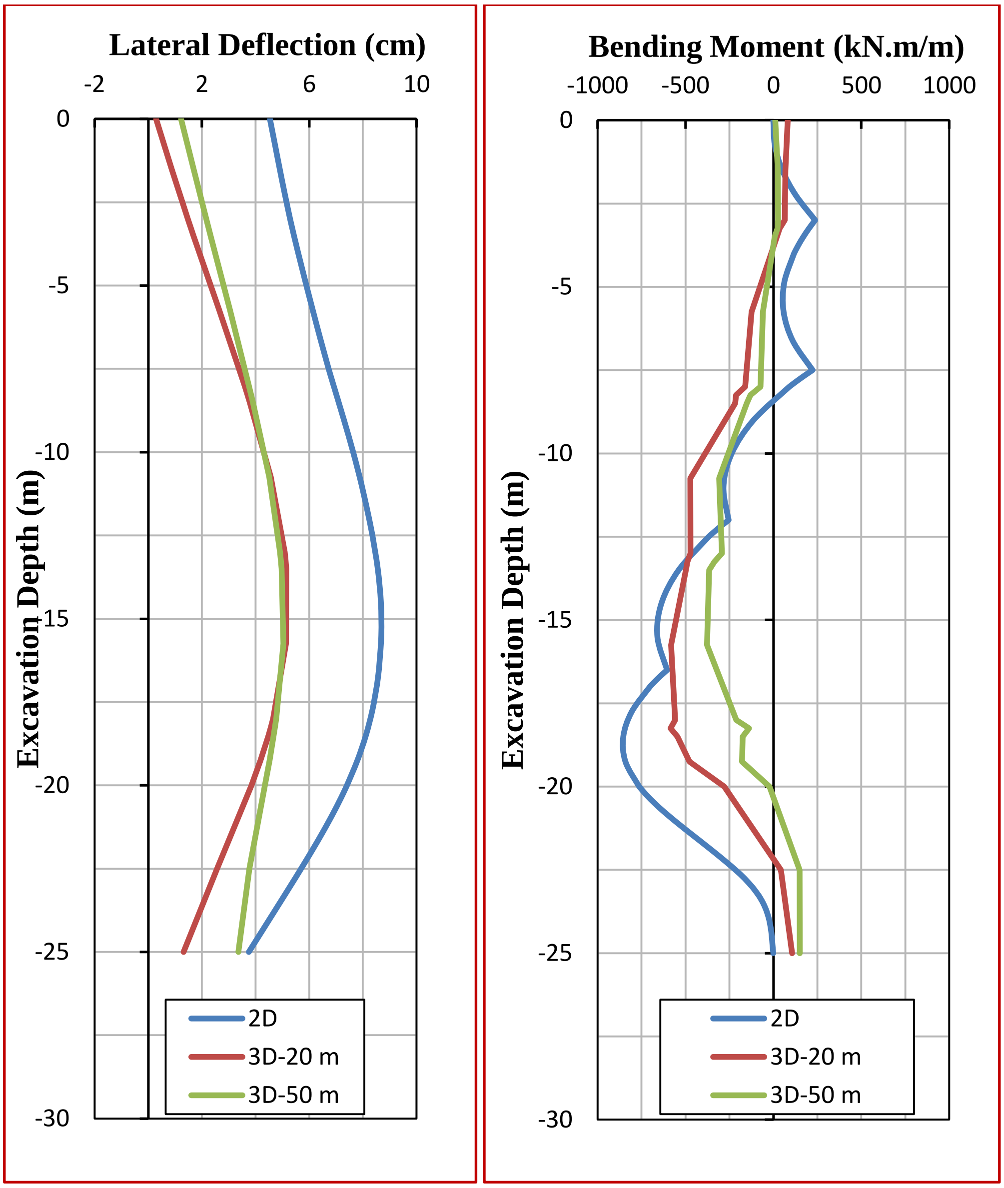

Figure A.3 Deformation and moment vs. depth for 20x20 m width in 2D and 20x20 m and 50x50 m width in 3D anchor-supported excavation cases in sand

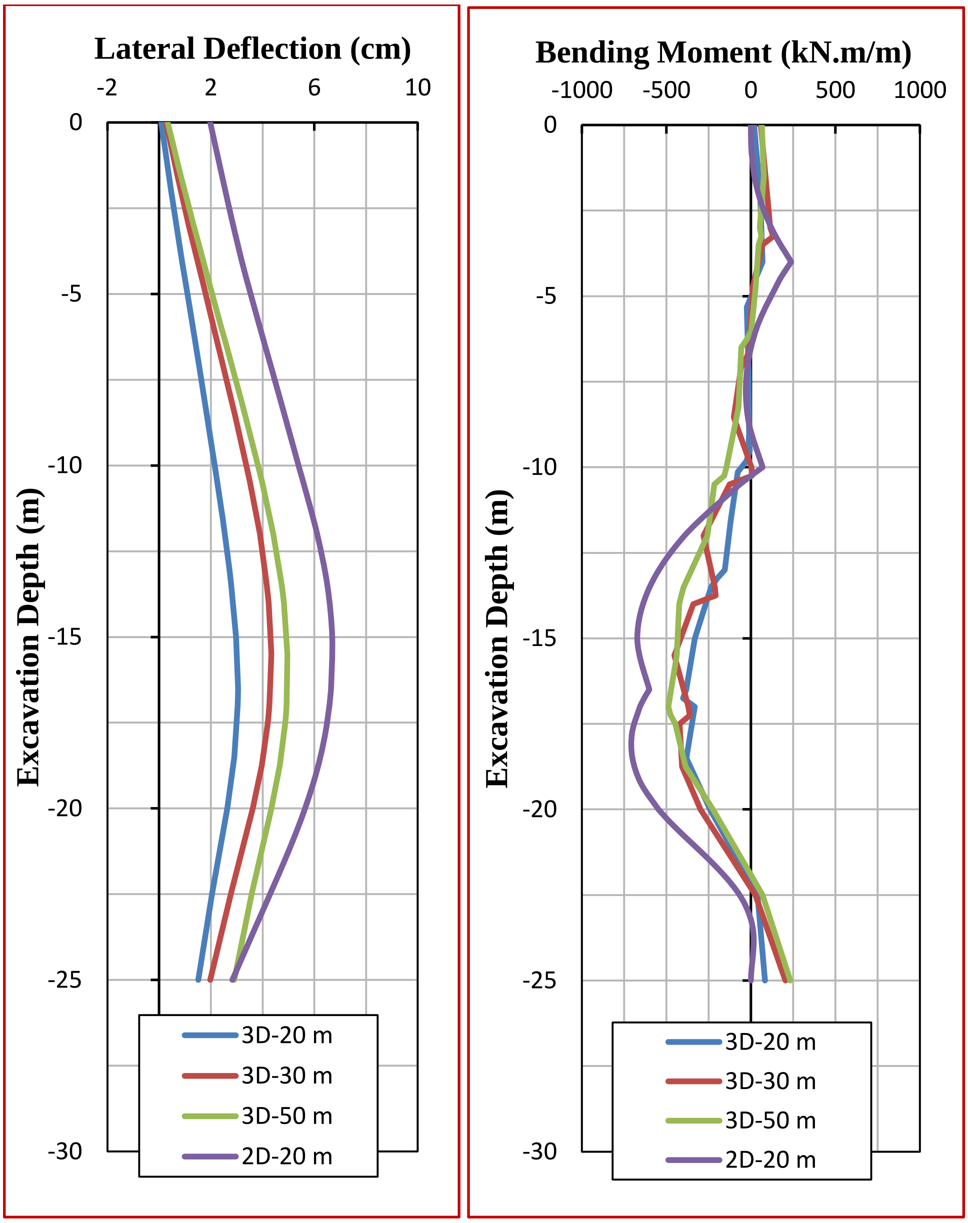

Figure A.4 Wall deformation and moment vs. depth diagram of 20x20 m strut-supported excavation in plane strain and 20x20 m,30x30 m and 50x50 m in 3D analysis results in sand

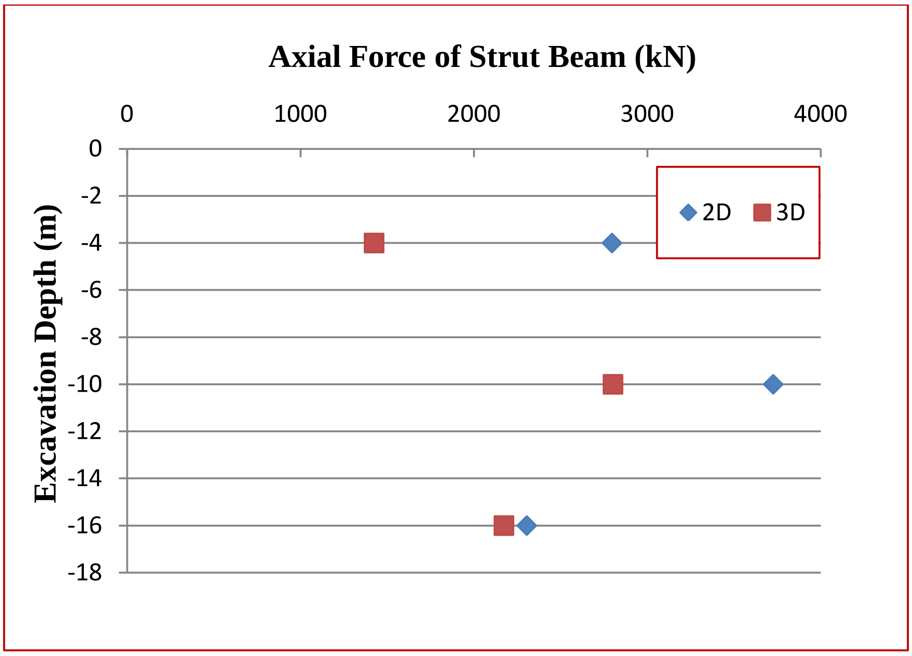

Figure A.5 Results of axial force of strut-supported beam in plane strain and 3D analysis for 20x20 m excavation in sand

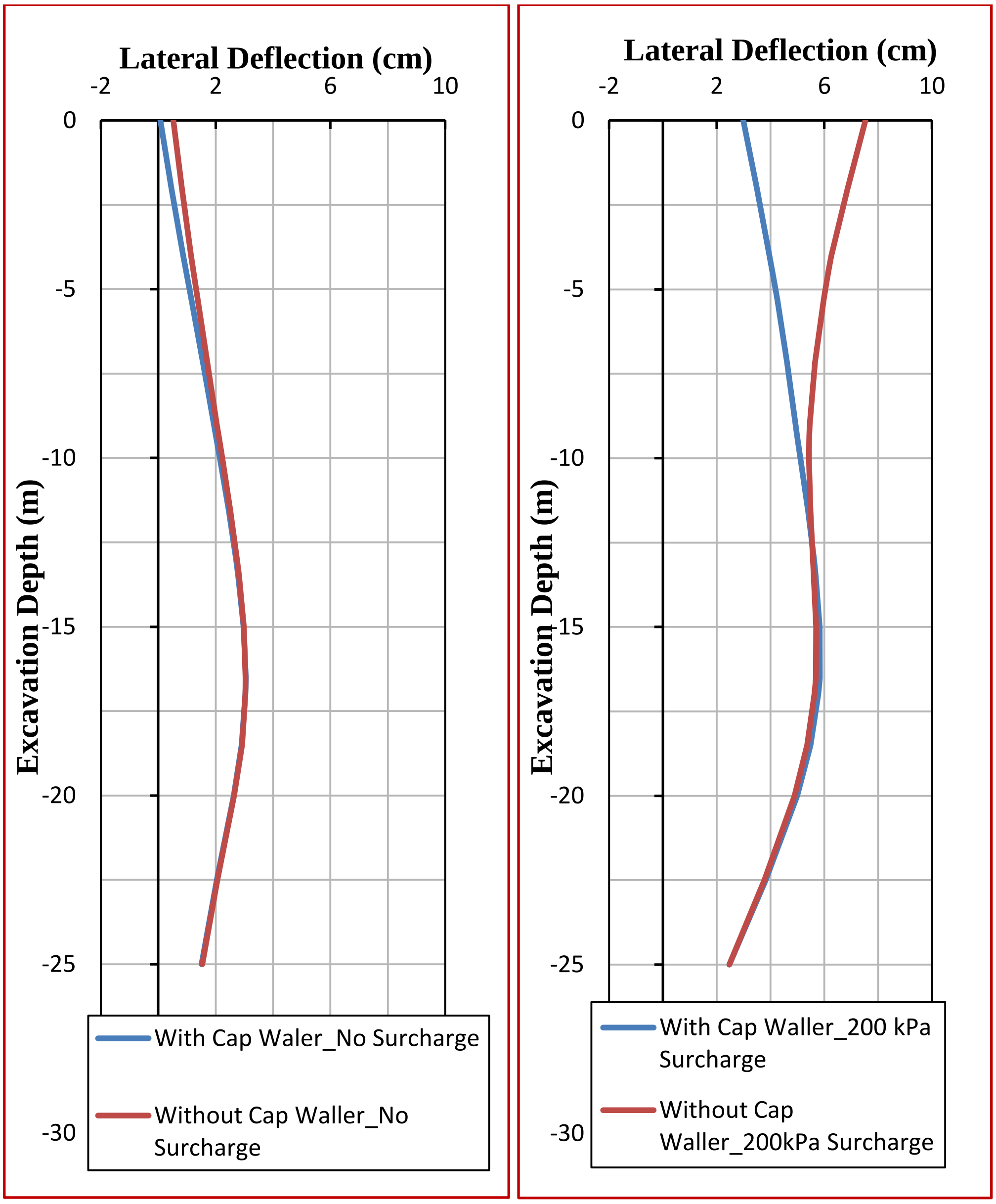

Figure A.6 The effect of presence of pile cap on strut-supported excavation with no surcharge and 200kPa Surcharge for 20x20 m excavation in sand

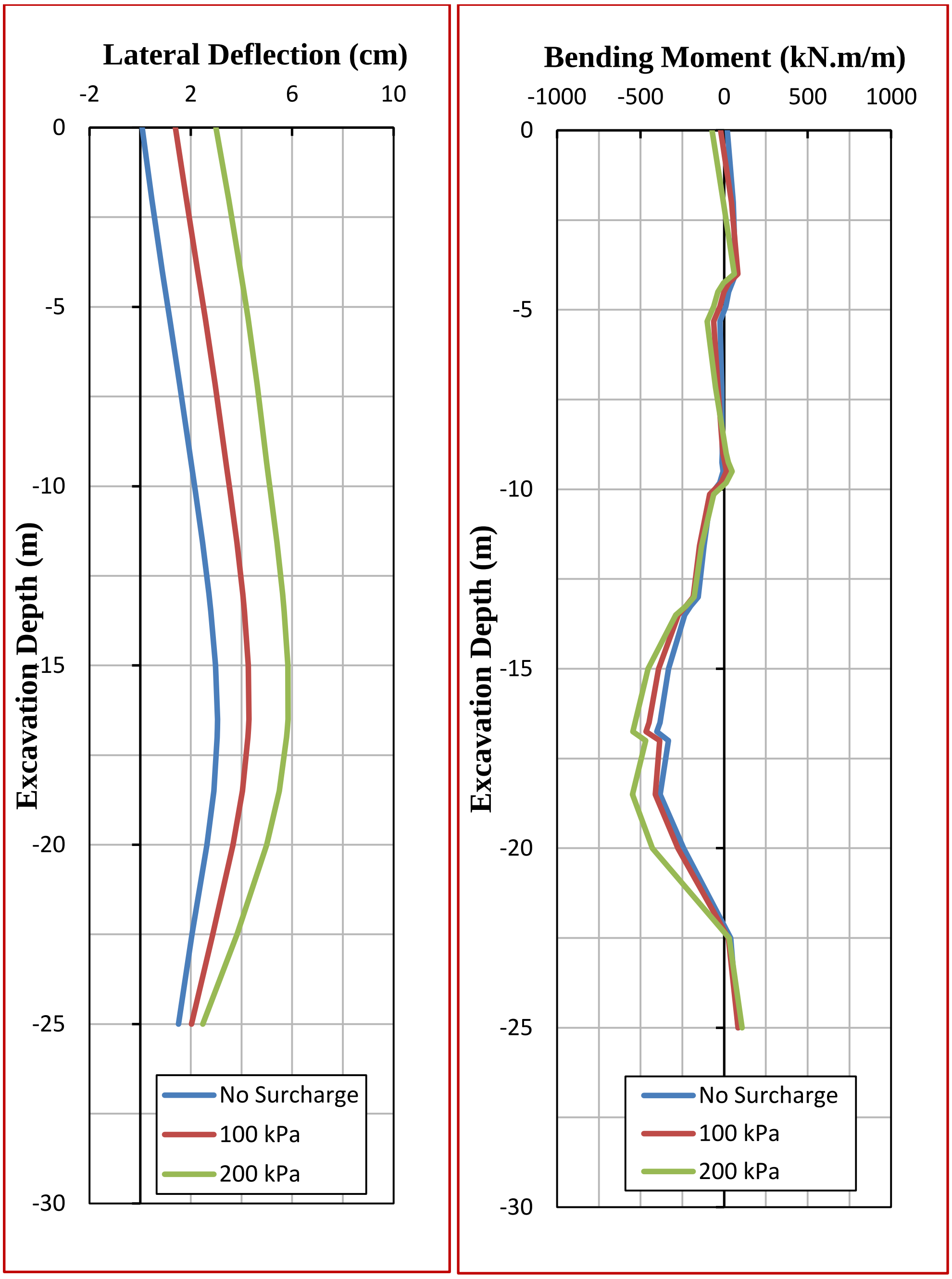

Figure A.7 Wall deformation and moment vs. depth diagram of 30x30 m (B) strut-supported excavation with surcharge variable in sand

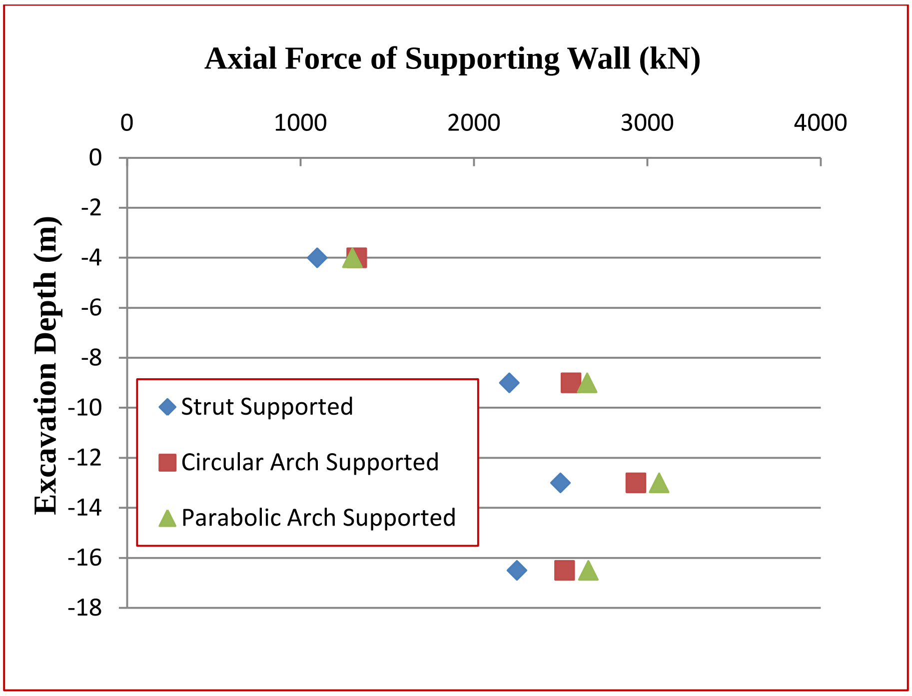

Figure A.8 Axial support load vs. depth diagram of strut-supported, circular arch-supported and parabolic arch-supported 20x20 m excavation with no surcharge in sand.

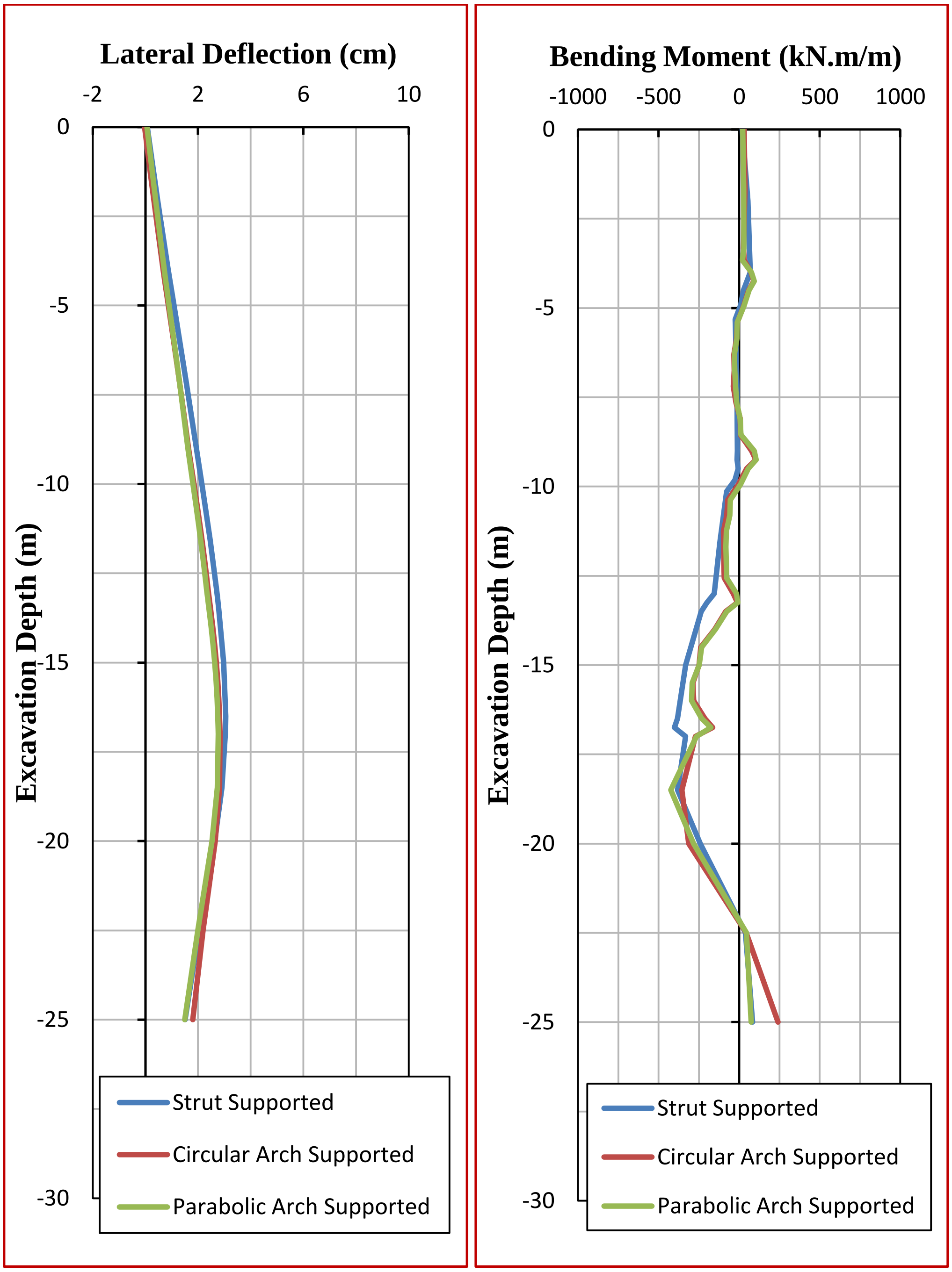

Figure A.9 Wall deformation and moment vs. depth diagram of strut-supported, arch-supported and parabolic arch-supported 20x20 m excavation without surcharge in sand

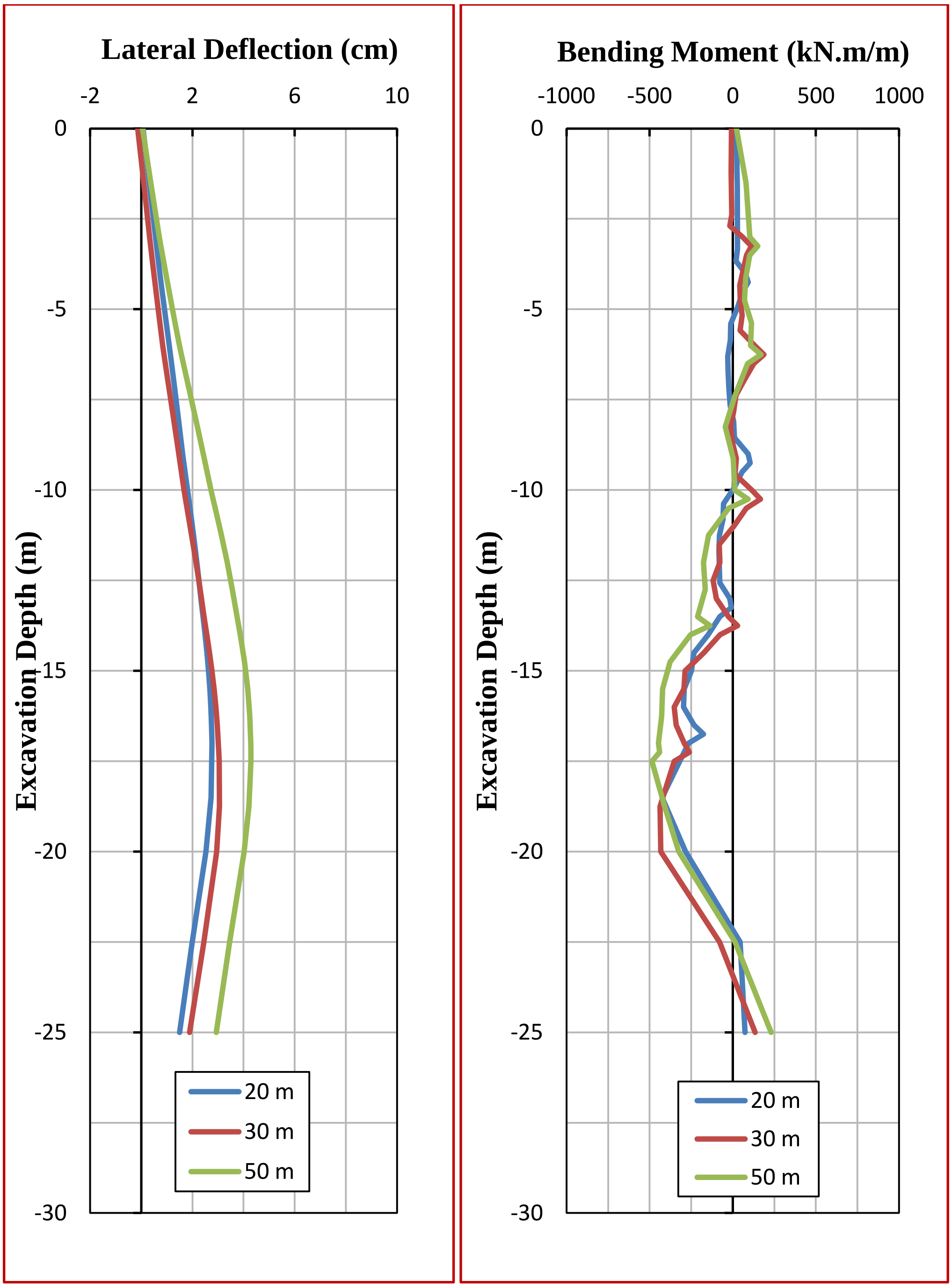

Figure A.10 Wall deformation and moment vs. depth diagram of arch-supported excavation with varying width and no surcharge in sand

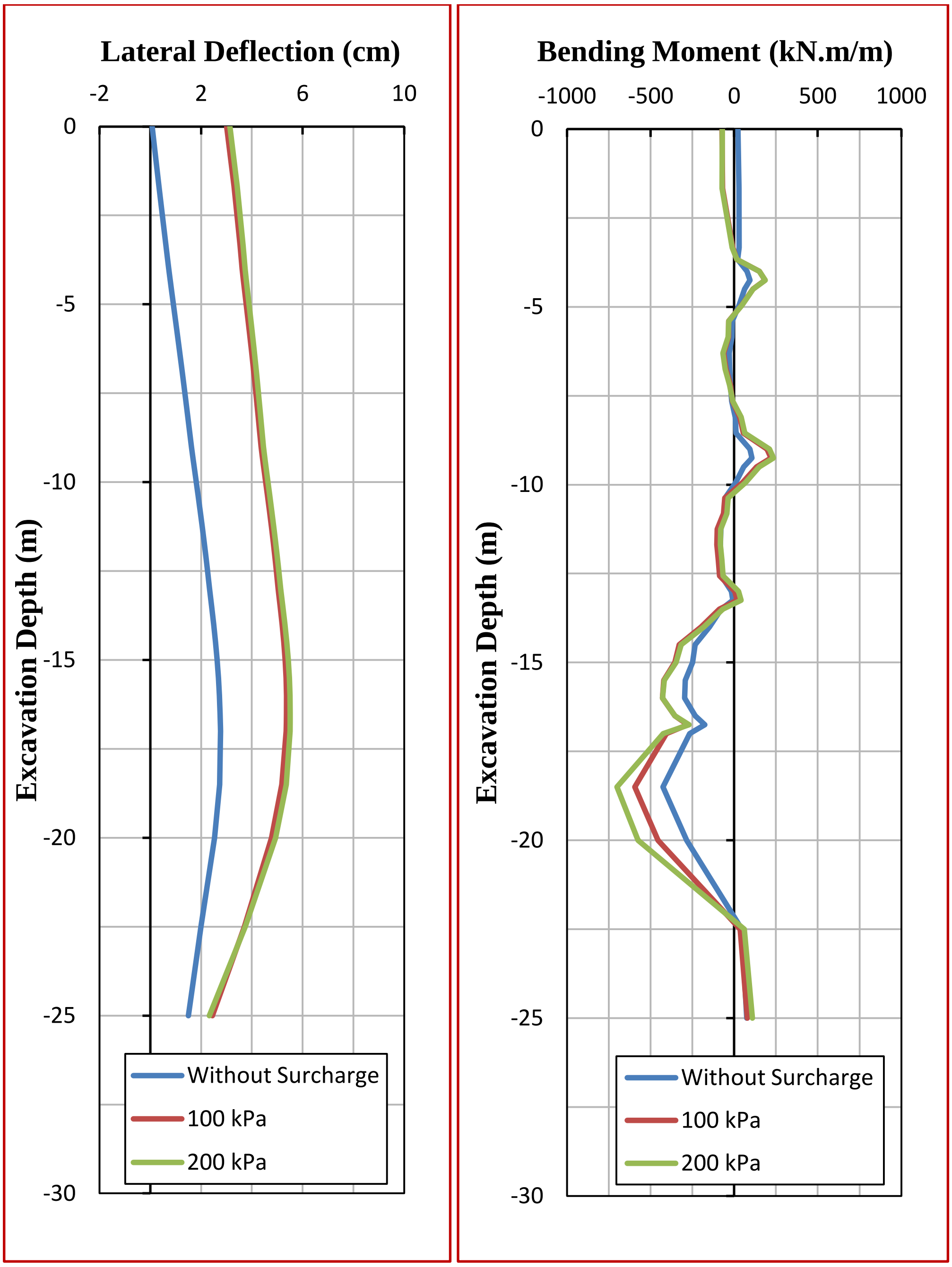

Figure A.11 Wall deformation and moment vs. depth diagram of arch-supported 30x30 m excavation with surcharge variable in sand

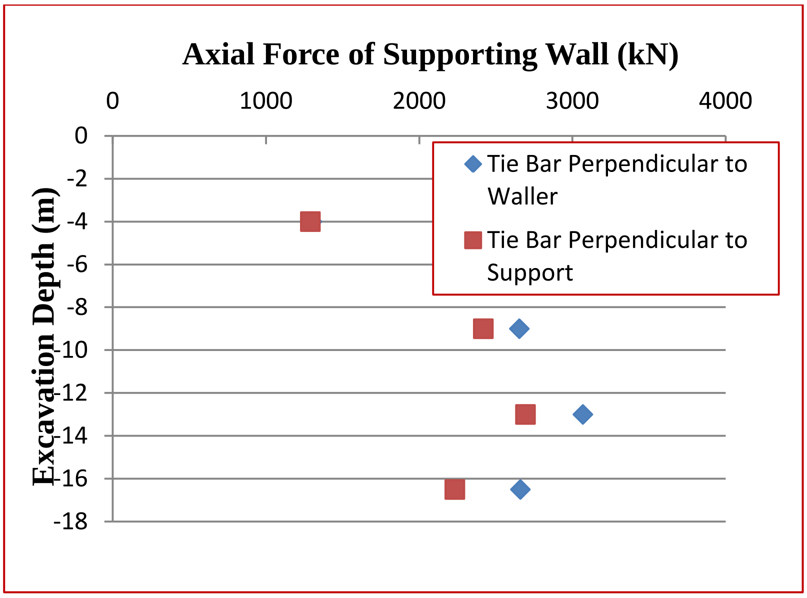

Figure A.12 Maximum axial force of supports both for two tie bar connection alternatives for 20x20 m excavation with no surcharge in sand

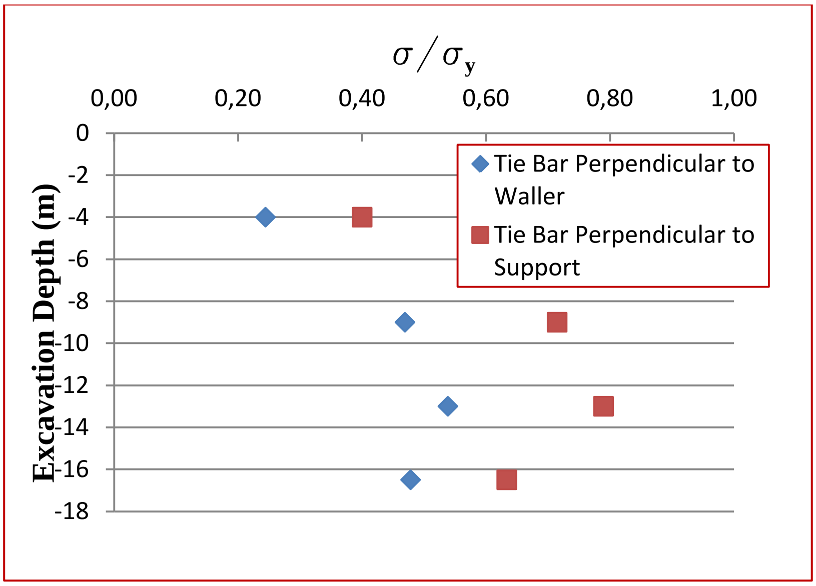

Figure A.13 Normalized yield stress of supports vs. excavation depth both for two tie bar connection alternatives for 20x20 m excavation with no surcharge in sand

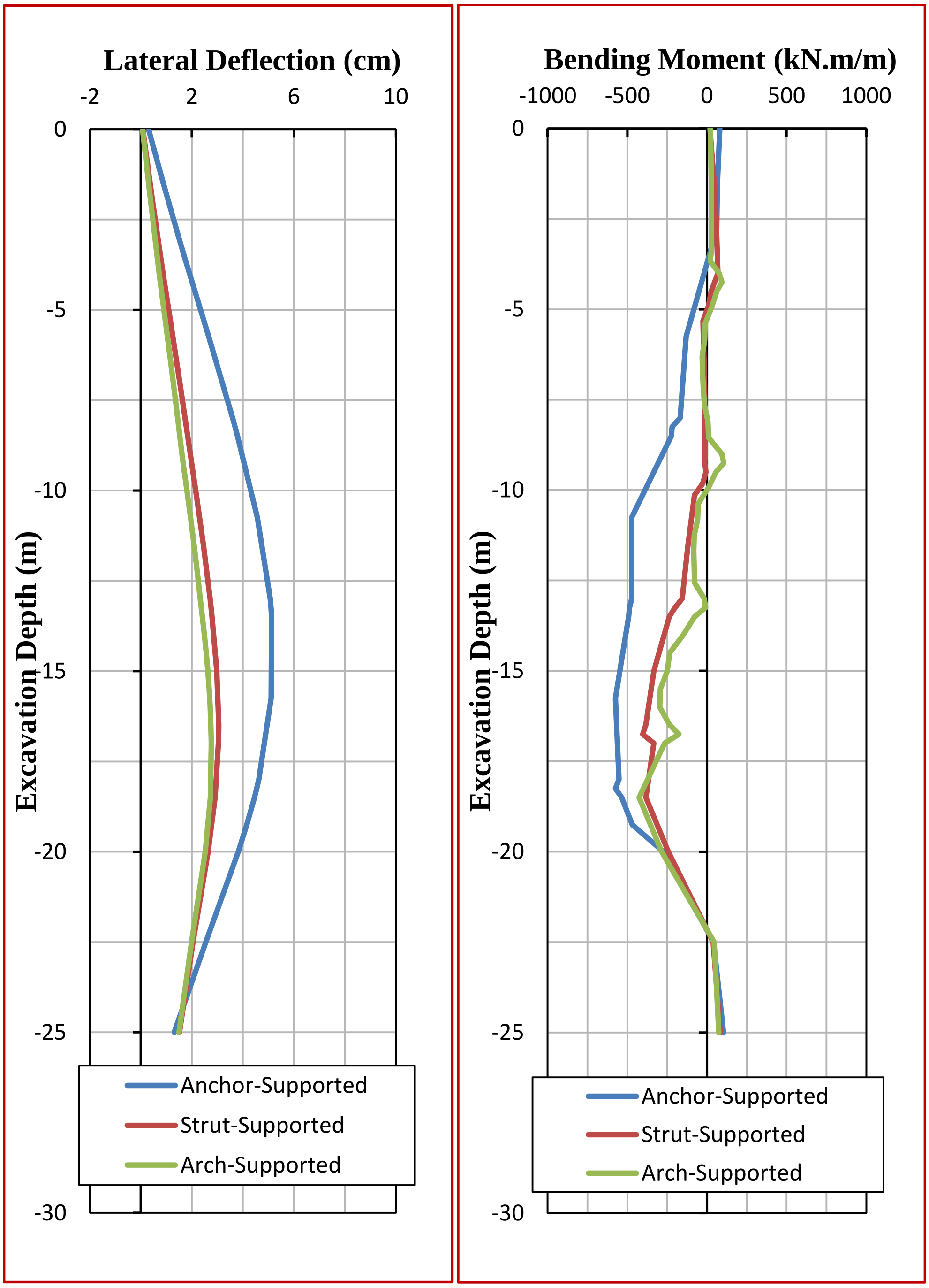

Figure A.14 Wall deformation and moment vs. depth diagram of anchor-supported vs. strut-supported and arch-supported 20x20 m wide excavation in sand

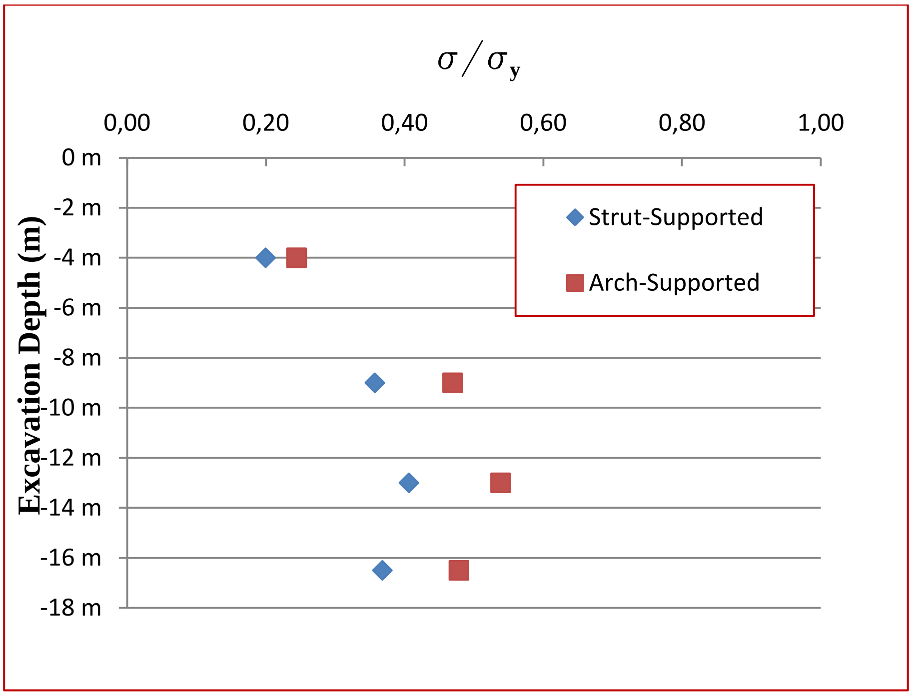

Figure A.15 Normalized yield stress values for strut and arch supported 20x20 m wide excavation without surcharge in sand

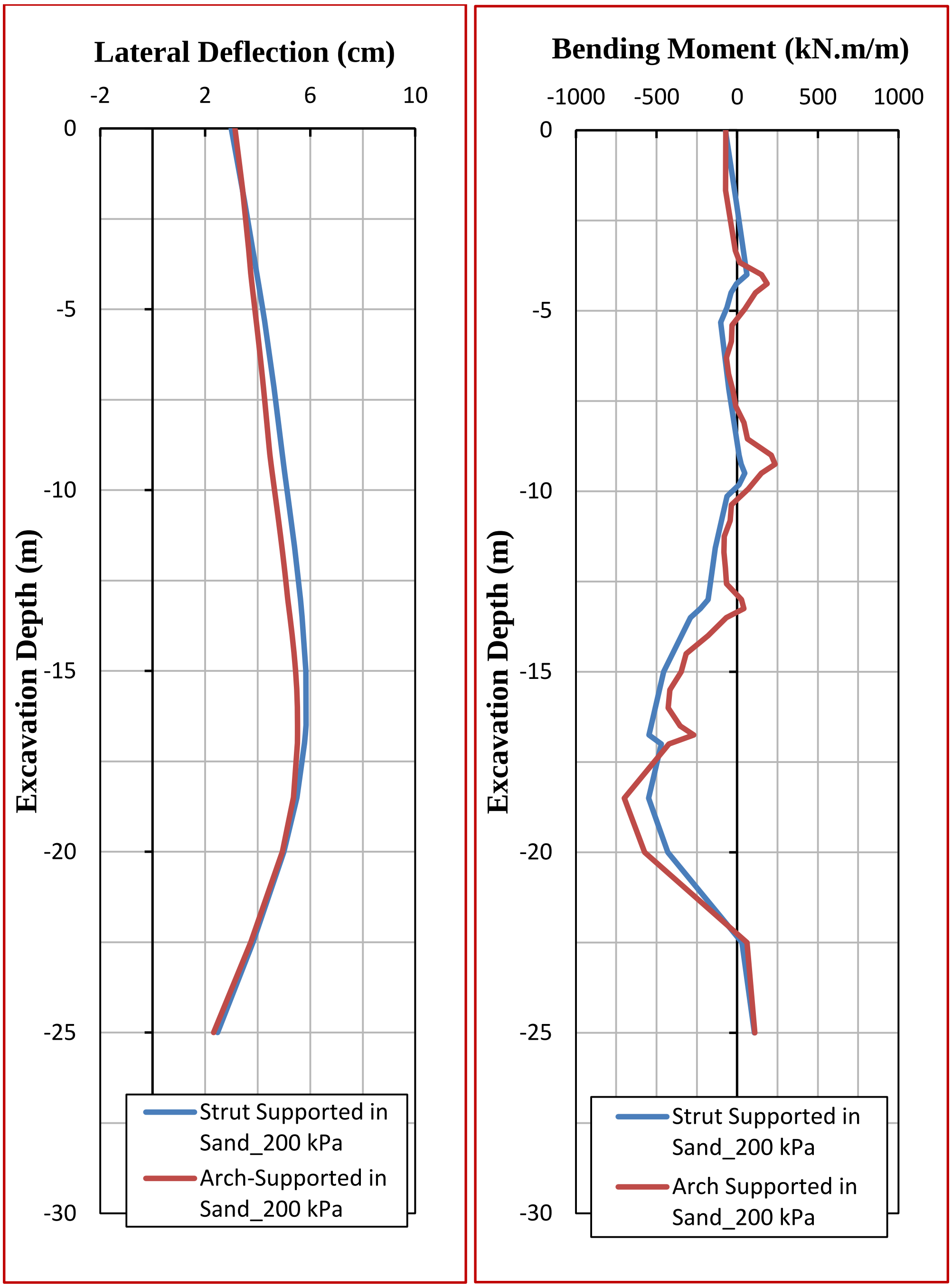

Figure A.16 Wall deformation and moment vs. depth diagram of strut-supported vs. arch-supported excavation with 200 kPa surcharge in sand

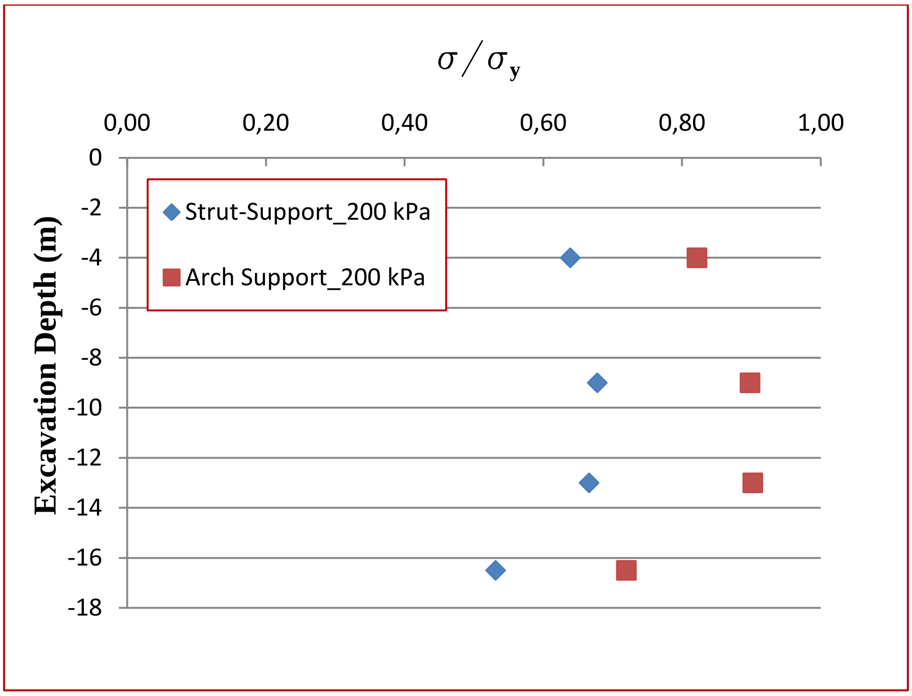

Figure A.17 Normalized yield stress values for strut and arch supports in 20x20 m wide excavation with 200 kPa surcharge in sand

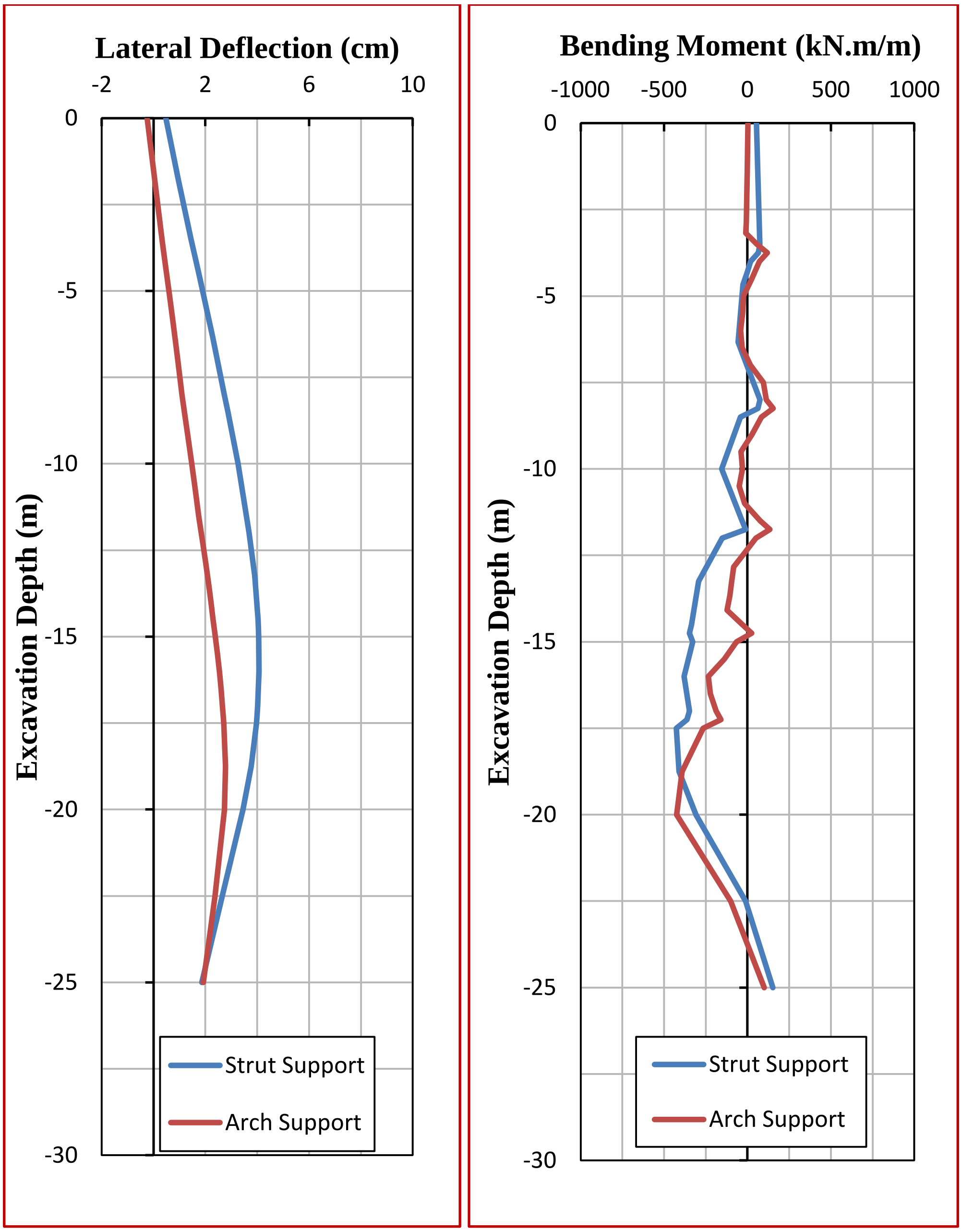

Figure A.18 Wall deformation and moment vs. depth diagram of strut-supported vs. arch-supported 30x30 m wide excavation without surcharge in sand for (B) support spacing

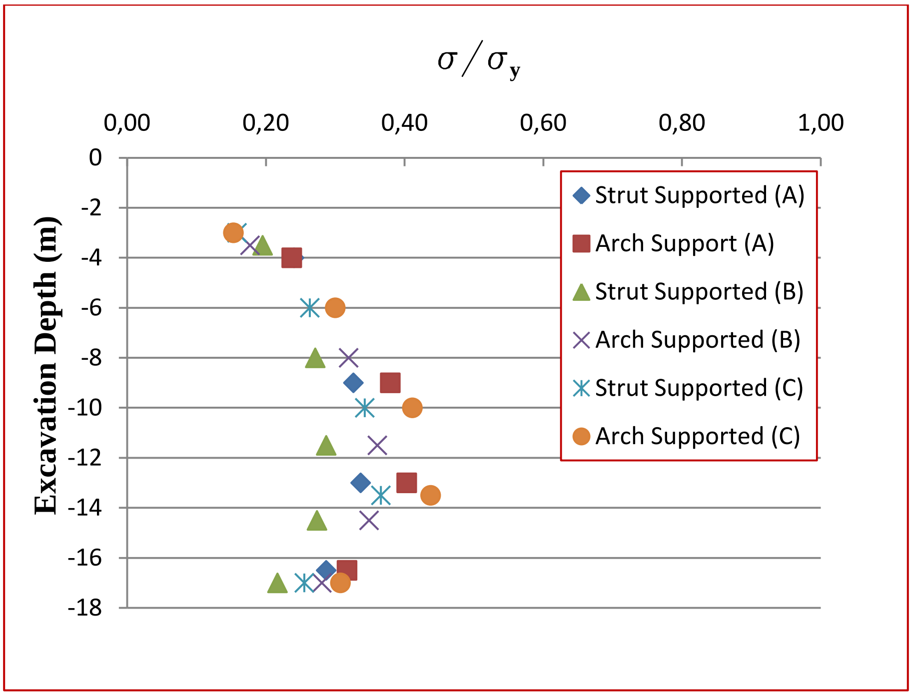

Figure A.19 Normalized yield stress values for strut and arch supports in 30x30m wide excavation without surcharge for two support spacing combinations (A, B and C) in sand

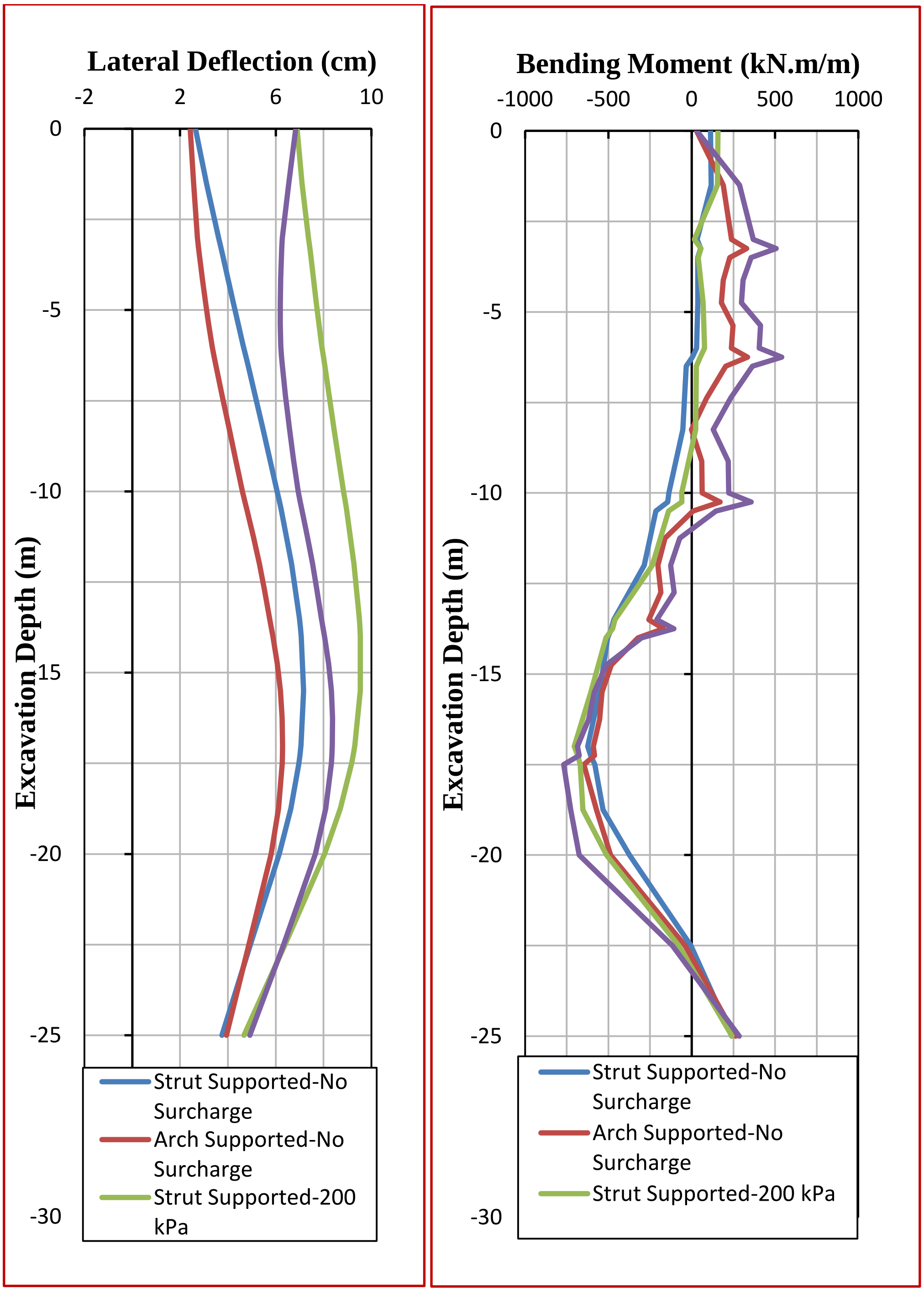

Figure A.20 Wall deformation and moment vs. depth diagram of strut-supported vs. arch-supported 50x50 m wide excavation in sand with and without surcharge load